A METHOD OF MEASURING EARTH RESISTIVITY

By Frank Wenner

1. INTRODUCTION

A knowledge of earth resistivity[1] (or specific resistance) may be of value in determining something of the composition of earth, such for example, as moisture content, whether it contains oil, ore of high conductivity, etc., or in the calculation or mitigation of damages to pipe systems by electrolysis caused by the return current of street-railway systems. For some of these or other reasons we may wish to determine the resistivity of limited portions of the earth.

For those cases in which we desire the resistivity of a fairly large portion of earth, extending to a considerable depth, or where there are reasons why we should not disturb the portion of earth to be measured, the following method is suggested: Four holes are made in the earth approximately uniformly spaced in a straight line. The diameter of the holes is not more than 10 per cent of the distance between them, and all extend to approximately the same depth, which is usually that at which we are most concerned with the resistivity. In each hole is placed an electrode, which makes electrical contact with the earth only near the bottom, as shown in Fig. 1.

This constitutes a four-terminal conductor[2] the resistance of which depends upon the distance between the electrodes and the

[1] Here we are concerned with the volume resistivity, which is the resistance of a portion of a conductor having unit length and unit cross section. It is usually expressed as the resistance in ohms of a centimeter cube.

[2] A four-terminal conductor is a conductor provided with two terminals to which currect leads may be connected and two terminals to which potential leads may be connected. The resistance of such a conductor is the difference in potential between the potential terminals divided by the current entering and leaving through the current terminals. For a more complete discussion of the four-terminal conductor see this Bulletin, 8, p. 360, 1912, Reprint No. 181.

resistivity, mainly in a region whose linear dimensions are of the same order as the distance between the outside electrodes, but does not depend appreciably upon the size of the electrodes nor the kind of electrical connection they make with the earth.

Therefore, if the depth of the holes, the distance between them, and the resistance (using 1 and 4 as current and 2 and 3 as potential terminals, or 2 and 3 as current and 1 and 4 as potential terminals) are measured, we have data from which the effective resistivity in the vicinity can be calculated.

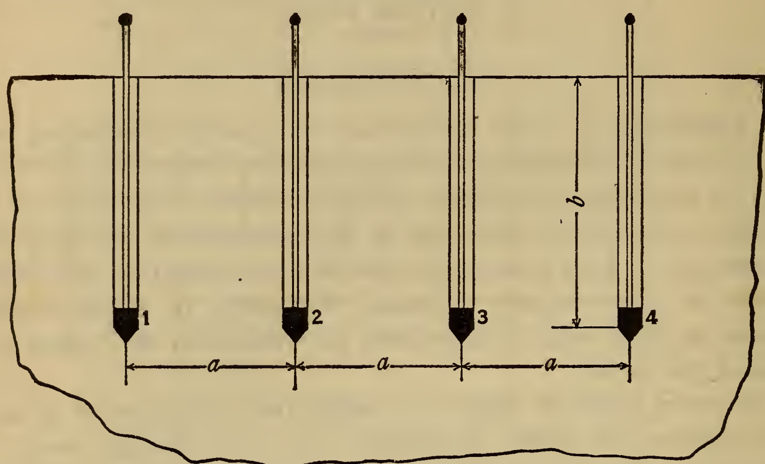

FIG. 1.—*Diagram showing four electrodes in earth constituting four-terminal conductor as used in measuring earth resistivity*

In case a is the distance between the holes (1 to 2, 2 to 3, and 3 to 4), b the depth of the holes, ρ the resistivity, and R the measured resistance, then

$$\rho = \frac{4\pi aR}{1 + \frac{2a}{\sqrt{a^2+4b^2}} - \frac{2a}{\sqrt{4a^2+4b^2}}} = \frac{4\pi aR}{n} \qquad (1)$$

where n has a value between 1 and 2 depending upon the ratio of (b to a) the depth of the electrodes to the distance between them. Where $b=a$, $n=1.187$; $b=2a$, $n=1.038$; and $b=4a$, $n=1.003$.

In case b is large in comparison with a,

$$\rho = 4\pi a\ R \qquad (2)$$

and in case b is small in comparison with a,

$$\rho = 2\pi a\ R \qquad (3)$$

If the holes are not in a straight line, or are not of a uniform depth or spacing, the resistivity is easily calculated when the depth of each of the holes and the distances of each from each of the other three are known.

2. DERIVATION OF EQUATIONS

To derive equation (1) and the more general relation we may proceed as follows:

Referring to Fig. 2, which is intended to represent a part of an infinite conductor of uniform resistivity, let a unit current enter

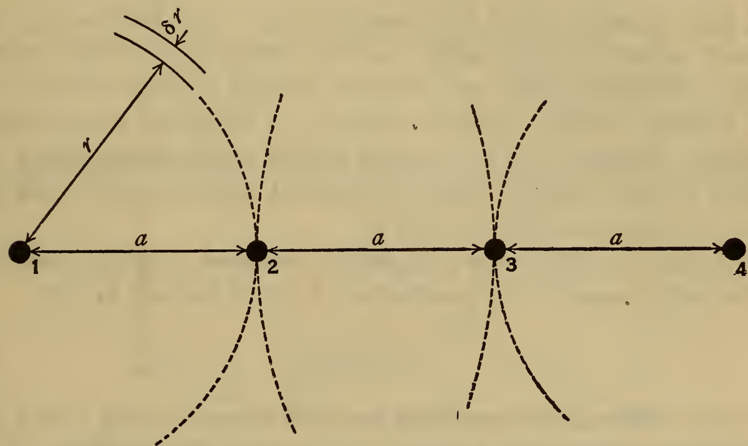

FIG. 2.—*Diagram used in showing the relation between the resistivity, resistance, and distances between terminals in an infinite conductor*

at the point designated 1. This current flows radially away from 1 and at a distance r its density is $1/4\pi r^2$. This follows from the fact that at any distance r from 1 the current density is uniform over the surface of a sphere whose center is at 1 and whose area is $4\pi r^2$. Since the potential gradient is the current-density times the resistivity,

$$-\frac{\delta e}{\delta r}=\frac{\rho}{4\pi r^2} \tag{4}$$

where e is the potential at the distance r from 1.

To get the drop in potential, $e'-e''$ between two points distant r' and r'' from 1 we must integrate the potential gradient from $r=r'$ to $r=r''$ or

$$e'-e''=\frac{\rho}{4\pi}\int_{r'}^{r''} r^{-2}\delta r=\frac{\rho}{4\pi}\left[\frac{1}{r'}-\frac{1}{r''}\right] \tag{5}$$

If e_x is the drop in potential between the points 2 and 3, distant a and $2a$ from 1, caused by unit current flowing radially from 1, equation (5) gives

$$e_x = \frac{\rho}{8\pi a} \tag{6}$$

Also if e_y represents the drop in potential between 2 and 3 caused by unit current flowing radially toward 4

$$e_y = \frac{\rho}{8\pi a} \tag{7}$$

If unit current enters the conductor at 1 and leaves at 4, the current density at any point[3] is the vector sum of the current density resulting from unit current flowing radially from 1 and unit current flowing radially toward 4. Likewise, the potential difference between any two points is that which results from unit current flowing radially from 1 plus that which results from unit current flowing radially toward 4.

Therefore the difference in potential between 2 and 3 caused by unit current entering the conductor at 1 and leaving at 4 is

$$e_x + e_y = \frac{\rho}{4\pi a} \tag{8}$$

Since the difference in potential for unit current, using 1 and 4 as current terminals and 2 and 3 as potential terminals, is the resistance R,

$$R = \frac{\rho}{4\pi a} \tag{9}$$

R is the resistance of the earth between the equipotential surfaces on which the potential electrodes are placed. It is equal to the resistance of a cylinder of the earth of radius $2a$ and length a.

However, in the measurement of earth resistivity, unless the distance between the electrodes is small in comparison with their distance below the surface, we can not assume that we have an infinite conductor, so equation (9) does not apply.

Referring to Fig. 3, which again represents a part of an infinite conductor, if we let e_1 be the drop in potential between the points

[3] The current distribution and equipotential surfaces are the same as the "lines of force" and equipotential surfaces in the field about two spheres with equal opposite charges.

2 and 3, caused by unit current entering the conductor at 1, from equation (5) we have

$$e_1 = \frac{\rho}{4\pi}\left[\frac{1}{r_{12}} - \frac{1}{r_{13}}\right] \tag{10}$$

Likewise, if we designate the drop in potential between 2 and 3, caused by unit current leaving at 4, by e_4; that caused by unit

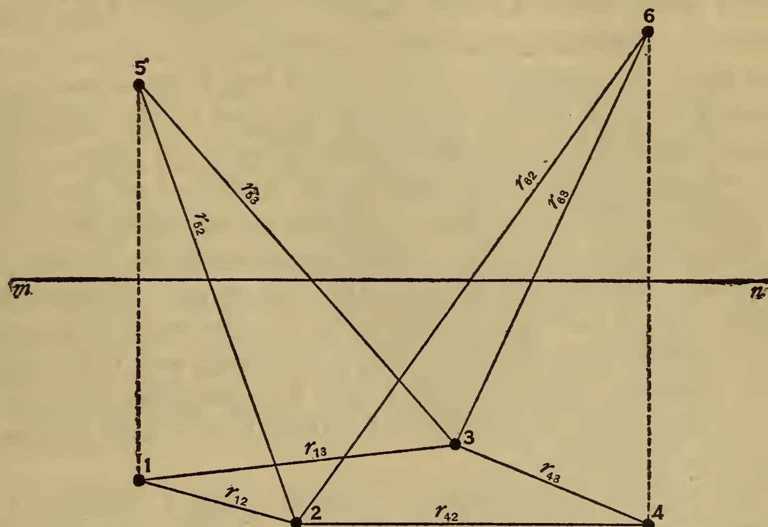

FIG. 3.—*Diagram used in showing relation between the resistivity, resistance, and distances between terminals or electrodes in a semiinfinite conductor*

current entering at 5, by e_5; and that caused by unit current leaving at 6, by e_6; we have

$$\begin{aligned} e_4 &= \frac{\rho}{4\pi}\left[\frac{1}{r_{43}} - \frac{1}{r_{42}}\right] \\ e_5 &= \frac{\rho}{4\pi}\left[\frac{1}{r_{52}} - \frac{1}{r_{53}}\right] \\ e_6 &= \frac{\rho}{4\pi}\left[\frac{1}{r_{63}} - \frac{1}{r_{62}}\right] \end{aligned} \tag{11}$$

Now, if a current I enters at 1 and leaves at 4 and at the same time an equal current enters at 5 and leaves at 6, the drop in potential, E, between 2 and 3 is I $(e_1 + e_4 + e_5 + e_6)$ or

$$E = \frac{I\rho}{4\pi}\left[\frac{1}{r_{12}} - \frac{1}{r_{13}} + \frac{1}{r_{43}} - \frac{1}{r_{42}} + \frac{1}{r_{52}} - \frac{1}{r_{53}} + \frac{1}{r_{63}} - \frac{1}{r_{62}}\right] \tag{12}$$

In the derivation of this equation it has been assumed that 1, 2, 3, 4, 5, and 6 represent points. However, the equation can be used without appreciable error where 1, 2, 3, 4, 5, and 6 represent metallic electrodes or terminals in a conductor of relatively high resistivity, providing the dimensions of the electrodes are small in comparison with the distances between them.

If 5 and 6 are so located that we can choose a plane (represented by the line *m n* of Fig. 3) through the conductor, such that the lines connecting 1 and 5 and 4 and 6 are normal to and bisected by it, it will be evident, on account of the symmetrical arrangement, that no current passes through this plane. Therefore we may remove that part of the conductor on one side of the plane without disturbing conditions on the other side. That is, the equation applies to a semi-infinite conductor having four terminals, providing we consider that the current terminals have images and we take into consideration the distances of the potential terminals both from the current terminals and their images. This, however, does not require that the potential terminals be in the same plane as the current terminals and their images, as shown in the Fig. 3.

Since the drop in potential E between 2 and 3 divided by the current I entering at 1 and leaving at 4 is the resistance R, it follows from equation (12) that

$$R=\frac{\rho}{4\pi}\left[\frac{1}{r_{12}}-\frac{1}{r_{13}}+\frac{1}{r_{43}}-\frac{1}{r_{42}}+\frac{1}{r_{52}}-\frac{1}{r_{53}}+\frac{1}{r_{63}}-\frac{1}{r_{62}}\right] \tag{13}$$

It will, therefore, be evident that the equation gives the relation between the resistivity, resistance, depth, and distance between small electrodes in the earth, as shown in Fig. 1, or in the more general case where the electrodes are not in a straight line.

If the electrodes are all at a uniform depth b and at a uniform distance apart a in a straight line, then $r_{12}=a$, $r_{13}=2a$, $r_{43}=a$, $r_{42}=2a$, $r_{52}=\sqrt{4b^2+a^2}$, $r_{53}=\sqrt{4b^2+4a^2}$, $r_{63}=\sqrt{4b^2+a^2}$, and $r_{62}=\sqrt{4b^2+4a^2}$. Therefore,

$$R=\frac{\rho}{4\pi}\left[\frac{2}{a}-\frac{1}{a}+\frac{2}{\sqrt{a^2+4b^2}}-\frac{2}{\sqrt{4a^2+4b^2}}\right] \tag{14}$$

which, when solved for ρ, gives equation (1).

In the derivation of these equations we have assumed a uniform resistivity. If the resistivity is not uniform, a solution (except in special cases) is not possible. However, the measured resistance, and consequently the value found for the resistivity, using the equations, depends mainly on the resistivity of the portion of earth between the inner electrodes having a cross section equal to the square of half the distance between the outer electrodes.

3. MEASUREMENT OF THE RESISTANCE

Since the electrodes are small, the resistance between the current electrodes and earth, or between any of the electrodes and earth, is large in comparison with the resistance R of the four-terminal conductor, and usually not very constant. Also, since earth acts as an electrolyte there is, in general, an electromotive force in any circuit containing two of the electrodes and polarization at any electrode through which appreciable current passes, even though the current may be alternating. For these reasons none of the usual methods for measuring the resistance of a four-terminal conductor, such as the Thomson bridge and Matthiessen and Hockin bridge methods, seem to meet the conditions very well.

Fortunately there is, in general, no need to measure the resistance to a high accuracy. There is, therefore, no reason why we may not use an ammeter for measuring the current and a voltmeter for measuring the resulting difference in potential between the potential terminals, providing the voltmeter is so used that its readings are not affected by the high resistance between each of these terminals and earth.

The potentiometer arrangement shown in Fig. 4 (using alternating current to obviate the more serious difficulties which might arise on account of polarization with direct current) seems to meet conditions fairly well. The current terminals or electrodes are connected to a source of alternating voltage of suitable value (50 to 150 volts for electrodes about 3 or 4 cm in diameter and 30 to 50 cm apart). Across the line is connected a transformer stepping down, usually to one-tenth or one-twentieth of the voltage across the current terminals. The low-voltage side of the transformer is connected to the ends of a slide wire, one end

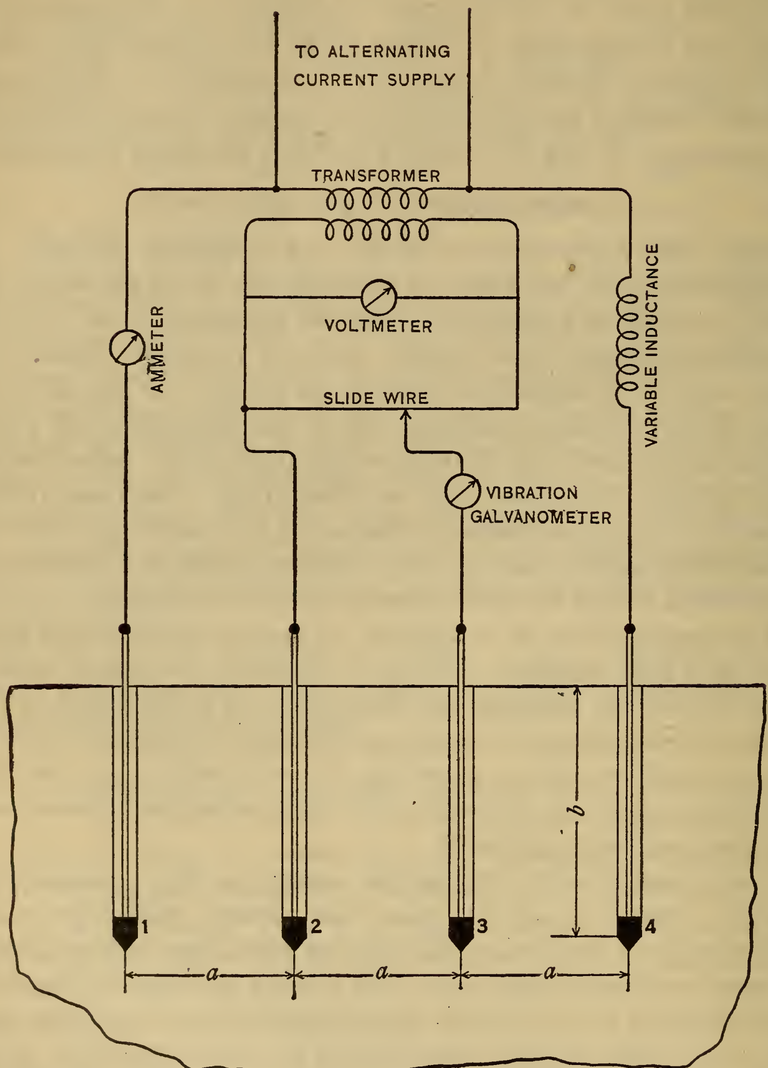

FIG. 4.—*Diagram showing arrangement for measuring four-terminal earth resistance by potentiometer-voltmeter-ammeter method*

of which is also connected to one of the potential terminals. The other potential terminal is connected through a vibration galvanometer [4] (tuned to the frequency of the test current) to the adjustable contact on the slide wire. An ammeter is connected into a lead to one of the current terminals and a voltmeter across the ends of the slide wire, or, if the ratio of the transformer is known when connected to the terminals of the slide wire, the voltmeter may be connected across the line. If the resistance per division of the slide wire is known, we may use an ammeter in series with it instead of the voltmeter.

On account of phase displacement resulting from polarization at the current electrodes, a variable inductance (or inductance with variable resistance in parallel) is connected into one of the leads so that the test current may be brought in phase with the voltage of the low side of the transformer. This is one of the conditions necessary for a zero current through the galvanometer. The other condition is that the magnitude of the *ri* drop in that part of the slide wire between the adjustable contact and the end connected to one of the potential terminals be equal to the voltage drop across the potential terminals.

If, then, adjustments [5] are made so that no current flows through the galvanometer, and the position of the sliding contact, the value of the test current, and the voltage across (or current in) the slide wire are read, we have data from which the resistance R is readily calculated.

From the measured resistance and the depth and distance between electrodes the effective resistivity may be calculated as explained above. The result obtained depends mainly upon the resistivity near and between the inner or potential electrodes, and very little upon the resistivity at distances from them equal to or more than the distance between the outer or current electrodes, providing the four electrodes are approximately uniformly spaced.

---

[4] If alternating current of from 300 to 1000 cycles is available, a telephone receiver could be used to advantage in place of the vibration galvanometer.

[5] As the accuracy required is not high it is not necessary to take special precautions in regard to induced currents, distributed capacity, etc.

4. USE OF THE METHOD

The method has been tried out by the author using approximately the arrangement shown in Fig. 4. It has also been used by McCollum and Logan in their investigation of earth resistivity, the results of which, it is expected, will be published soon in one of the Bureau's Technological Papers.

In a particular measurement the electrodes were placed at a depth of approximately 125 cm and so spaced that (referring to Fig. 3) $r_{12}=25$, $r_{13}=58$, $r_{43}=31$, and $r_{42}=64$ cm. This gives 251 cm for r_{52} and r_{63}, and 255 cm for r_{53} and r_{62}. These values substituted in equation (14) give

$$R=\frac{\rho}{4\pi}\ .0397 \text{ or } \rho=316\ R$$

The measured value of R, the mean of several ratios of potential difference to current, was found to be 25.3, which give 8000 for ρ, the resistivity expressed as the mean resistance in ohms of a centimeter cube.

So far the method has been used only for determining resistivities in a region a few meters or less in radius and very close to the surface. To measure the effective resistance of a much larger portion of earth, extending to a considerable depth, the electrodes would be placed much farther apart. By using large electrodes a considerable distance apart, a large test current and a very sensitive detector (either of the vibration galvanometer or the separately excited dynamometer type) it should be possible to get some idea of the effective resistivity from the surface to a considerable depth, even though the electrodes are placed practically on the surface. The result obtained would depend to a considerable extent upon the resistivity of a surface layer should it be low, as is usually the case. The effect of the surface layer could be estimated roughly from the results obtained from measurements with the electrodes closer together, and thus some idea obtained as to the resistivity at different depths. Such a measurement might be of assistance in locating deposits of ore of high conductivity.

WASHINGTON, JULY 15, 1915.

IEEE Guide for Measuring Earth Resistivity, Ground Impedance, and Earth Surface Potentials of a Grounding System

IEEE Power and Energy Society

Sponsored by the
Substations Committee

IEEE
3 Park Avenue
New York, NY 10016-5997
USA

28 December 2012

IEEE Std 81™-2012
(Revision of
IEEE Std 81-1983)

IEEE Std 81™-2012
(Revision of
IEEE Std 81-1983)

IEEE Guide for Measuring Earth Resistivity, Ground Impedance, and Earth Surface Potentials of a Grounding System

Sponsor

Substations Committee
of the
IEEE Power and Energy Society

Approved 5 December 2012

IEEE-SA Standards Board

Approved 3 October 2014

American National Standards Institute

measurements, the test devices are operated at a test frequency that is slightly above or below the power system frequency to obtain more accurate measurements.

6.6 Coupling between test leads

Inductive coupling can occur between components of two or more ac circuits by means of the mutual inductance that associates the two circuits. The coupling effect between test leads becomes important when measuring low values of ground impedance. Any voltage produced in the potential lead due to coupling from current flowing in the current lead is directly added to the true voltage and produces a measurement error. The 50 Hz or 60 Hz inductive coupling between two parallel test leads might be as high as 0.1 Ω/100 m. As a result, the error can be appreciable because low ground impedance usually occurs in ground grids that cover large areas, and long test leads are typically required to reach remote earth. Thus, the coupling between test leads can introduce large errors when a ground grid covering a large area has a relatively low impedance.

Conversely, a ground grid that covers a small area usually has a relatively high ground impedance, which allows shorter test leads to reach remote earth. Thus, the effects of coupling can be expected to be worse on measurements of large-area, low-impedance grounds. As a rule of thumb, test lead coupling is usually negligible on measurements of grounds that are 10 Ω or greater, is almost always important on measurements of 1 Ω or less, and can be significant in the range between 1 Ω and 10 Ω.

Test lead coupling can be minimized by appropriately routing the potential and current leads. When test lead coupling is anticipated, appropriate routing may include separating the leads or crossing the leads at 90°.

6.7 Buried metallic objects

Partially or completely buried objects, such as rails and metallic pipelines, located in the vicinity of the ground being tested, will have considerable influence on test results (Dawalibi and Mukhedkar [B23], Rudenberg [B55]). Earth potential contours are distorted and gradients are increased when measured above buried metallic objects.

Whenever the presence of buried metallic structures is suspected in the area where soil resistivity measurements are to be performed and the location of these structures is known, the influence of these structures on the soil resistivity measurement results can be minimized by aligning the test probes in a direction perpendicular to the routing of these structures. Locate test probes as far as possible from buried structures.

7. Earth resistivity

7.1 General

The techniques for measuring soil resistivity are essentially the same for most measurements. However, the interpretation of the recorded data can vary considerably, especially where soils with nonuniform resistivities are encountered. The added complexity caused by nonuniform soils is common, and in only a few cases, the soil resistivities are constant with increasing depth.

Earth resistivity varies not only with the type of soil but also with temperature, moisture, mineral content, and compactness (Figure 1). The literature indicates that the values of earth resistivity vary from less than 1 Ω-m for sea water up to 10^9 Ω-m for sandstone. The resistivity of the earth increases slowly with decreasing temperatures from 25 °C to 0 °C. Below 0 °C, the resistivity increases rapidly. In frozen soil, as in the surface layer of soil in winter, the resistivity can be exceptionally high.

Table 1 shows the resistivity values for various soils and rocks. More detailed tables are available in IEEE Std 80[6] (Rudenberg [B55], Thug [B60]).

Usually there are several layers of soil, each having a different resistivity. Lateral changes can also occur, but in general, these changes are gradual and negligible in the vicinity of the sites concerned.

In most cases, the measurement will show that the resistivity ρ_a is mainly a function of depth z. For purposes of illustration, we will assume that this function can be written as follows:

$$\rho_a = \phi(z) \tag{1}$$

The nature of the function ϕ is in general not simple, and consequently, the interpretation of the measurements will consist of establishing a simple equivalent function ϕ_e, which will give the best approximation. In the case of power and communication circuits, a two horizontal layer configuration (IEEE Std 80, Dawalibi and Mukhedkar [B21], Endrenyi [B26], Giao and Sarma [B30], Sunde [B57], Thug [B60]) and an exponential earth (Sunde [B57], Thug [B60]) have proven to be good approximations that can be useful in determining system designs.

Some publications (IEEE Std 80, Dawalibi and Mukhedkar [B23], Dawalibi and Mukhedkar [B21], Endrenyi [B26], Giao and Sarma [B30], Rudenberg [B55], Sunde [B57], Thapar and Gross [B59], Thug [B60]) have shown that earth surface potential gradients inside or adjacent to an electrode are mainly a function of topsoil resistivity. In contrast, the ground electrode resistance is primarily a function of deep soil resistivity. In this case, deep soil resistivity refers to depths roughly the diameter of a horizontal electrode system or up to ten times the depth of vertical electrodes. This definition of deep soil resistivity is not valid in those extreme cases where the electrode is buried in extremely high-resistivity topsoil.

[6] Information on references can be found in Clause 2.

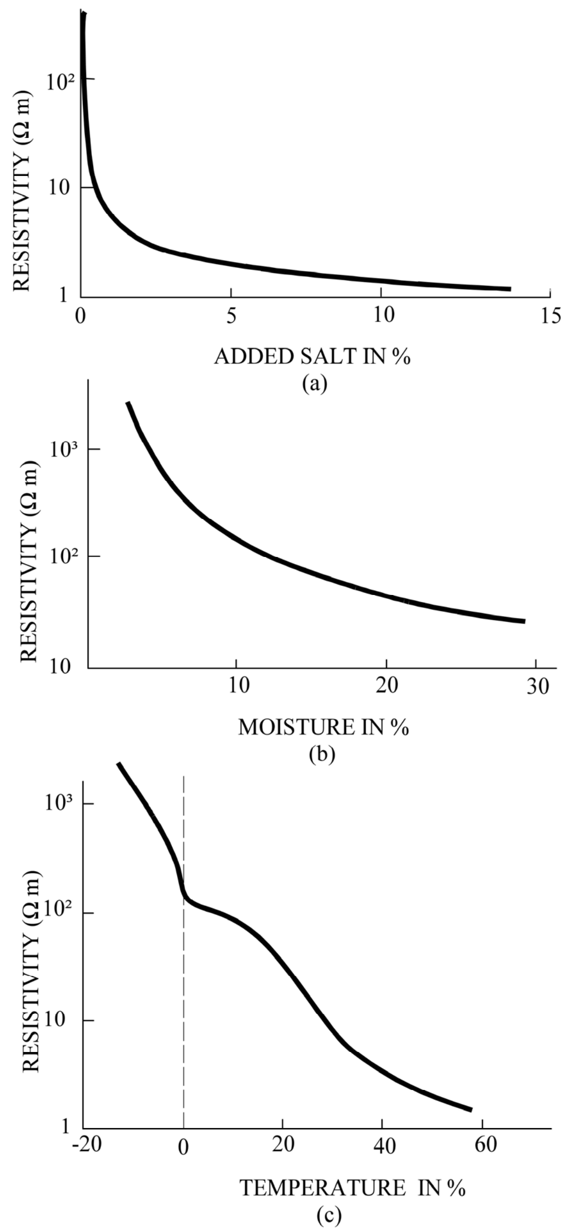

Figure 1 —Earth resistivity variations (Rudenberg [B55]): (a) salt, (b) moisture, and (c) temperature

When measuring soil resistivity to determine the earth return (zero sequence) impedance of an ac transmission line, it is important to understand that the earth return impedance is a function of the log of the distance between a conductor and its equivalent return path. This equivalent earth return depth De is assumed to be 658.5 × $(\rho\ /\ f)^{0.5}$ (Carson [B17]) based on uniform soil resistivity and relatively low frequency. For 50 and 60 cycle power frequencies, the equivalent earth return depth approaches 1000 m. For higher frequencies such as power line carrier (~150 kHZ), radio, or surge impedance calculations, the equivalent earth return depth is roughly 20 m or less. It is therefore important to perform both shallow and deep resistivity measurements along transmission lines to provide adequate information for determining the earth return impedance.

Table 1—Geological period and formation [B57]

<table>
<tr><th>Earth resistivity ohm-meters</th><th>Quarternary</th><th>Cretaceous tertiary quarternary</th><th>Carboniferous triassic</th><th>Cambrian Ordovician Devonian</th><th>Precambrian and combination with Cambrian</th></tr>
<tr><td>1 Sea water</td><td rowspan="6"></td><td></td><td rowspan="2"></td><td rowspan="4"></td><td rowspan="6"></td></tr>
<tr><td>10 Unusually low</td><td rowspan="2">Loam
Clay
Chalk</td></tr>
<tr><td>30 Very low</td><td rowspan="4">Chalk
Trap
Diabase
Shale
Limestone
Sandstone</td></tr>
<tr><td>100 Low</td><td rowspan="5"></td></tr>
<tr><td>300 Medium</td><td rowspan="3">Shale
Limestone
Sandstone
Dolomite</td></tr>
<tr><td>1000 High</td></tr>
<tr><td>3000 Very high</td><td rowspan="2">Coarse sand and gravel in surface layers</td><td rowspan="2"></td><td rowspan="2">Sandstone
Quartzite
Slate
Granite
Gneisses</td></tr>
<tr><td>10 000 Unusually high</td><td></td></tr>
</table>

7.2 Methods of measuring earth resistivity

7.2.1 Geological information and soil samples

Often, at the site where a grounding system is to be installed, extensive geotechnical work will be performed. This work usually involves geological prospecting, which can provide a considerable amount of information on the nature and configuration of the soil. Such data could be of considerable assistance to the design engineer, who should try to obtain at least the following information:

— Type of soil in each layer
— Moisture content
— Soil pH
— Depth of groundwater

The determination of soil resistivity from the values of resistance measured between opposite faces of a soil sample of known dimensions is not recommended, as the unknown interfacial resistances of the soil sample and the electrodes are included in the measured value.

Obtaining a useful approximation of soil resistivity from resistivity measurements on samples is difficult, and in some cases impossible. This is due to the difficulty of obtaining representative homogeneous soil samples and in duplicating the original soil compaction and moisture content in the test cell.

7.2.2 Variation of depth method or three-point method

In this method, the ground resistance measurements are repeated several times in correlation with the ground rod incremental increase in depth. The purpose of this method is to force more test current through the deep soil. The measured resistance value will then reflect the apparent resistivity for each depth of the rod. Ground rods are preferred for this measurement because they offer two important advantages:

a) The theoretical value of ground rod resistance is simple to calculate with adequate accuracy.
b) Driving ground rods also gives confirmation of how deep the rods can be driven during installation.

A disadvantage of this method is that the rod might vibrate as it is driven, resulting in poor contact with the soil along its length, thus, making a conversion to true apparent resistivity difficult.

The variation of depth method gives useful information about the nature of soil in the vicinity of the rod (five to ten times the rod length). For additional details regarding this method, refer to 8.2. For large areas, several rod locations can give an indication of significant lateral changes in soil resistivity. If a large volume (large area and depth) of soil is tested, then it might be preferable to use the four-point method because driving long rods might not be practical in some soils.

7.2.3 Four-point method

A good method for measuring the apparent resistivity of large volumes of undisturbed earth is the four-point method (Wenner [B62]). Four auxiliary probes are installed in the earth, all at depth *b* and spaced (in a straight line) at intervals *a*. A test current *I* is passed between the two outer probes, and the potential *V* between the two inner probes is measured with a potentiometer or high-impedance voltmeter. Then, the *V/I* ratio gives the resistance *R* in ohms.

Two different variations of the four-point method are often used, as follows:

a) *Equally Spaced or Wenner Arrangement.* With this arrangement, the probes are equally spaced, as shown in Figure 2(a). Let *a* be the distance between two adjacent probes. Then, the apparent resistivity ρ in the terms of the length units in which *a* and *b* are measured is

$$\rho = \frac{4\pi aR}{1 + \frac{2a}{\sqrt{a^2 + 4b^2}} - \frac{a}{\sqrt{a^2 + b^2}}} \tag{2}$$

Theoretically, the electrodes should be point contacts or hemispherical electrodes of radius *b*. However, in practice, four rods are usually placed in a straight line at intervals *a*, driven to a depth not exceeding 0.1 *a*. Then, the user can assume $b = 0$ and the equation becomes

$$\rho = 2\pi aR \tag{3}$$

and gives the approximate apparent soil resistivity to the depth *a*.

A set of readings taken with various probe spacings gives a set of resistivities that, when plotted against spacing, indicates whether there are distinct layers of different soil or rock and gives an idea of their respective resistivities and depth (Figure 3).

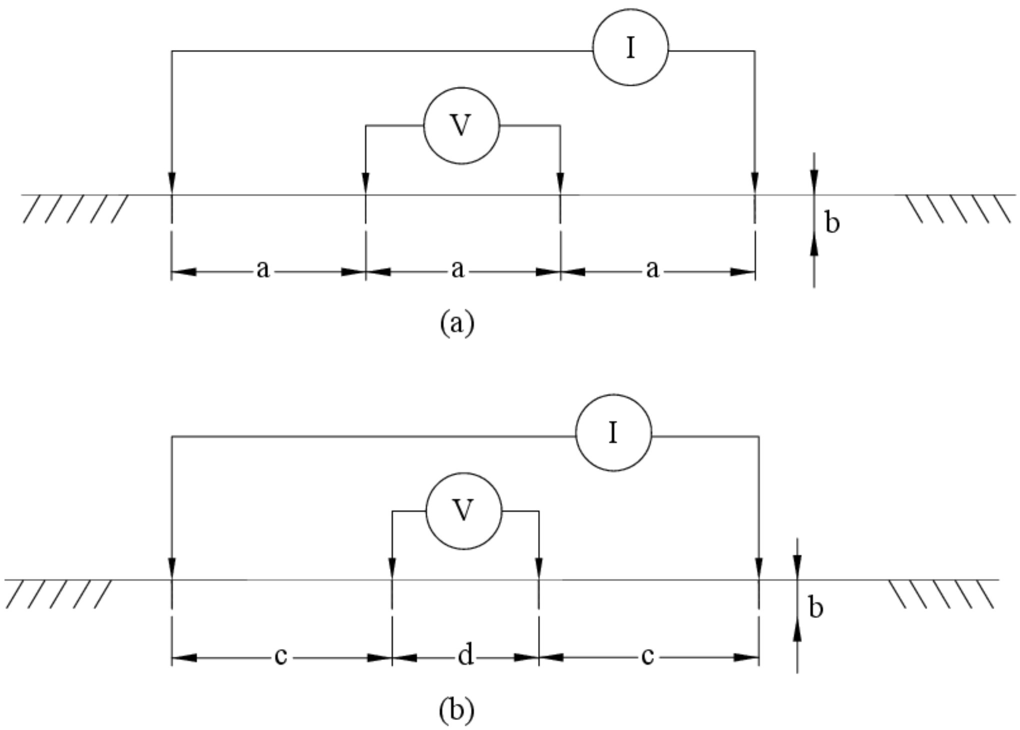

Figure 2 —Four point method: (a) equally spaced test probes and (b) unequally spaced test probes

b) *Unequally Spaced or Schlumberger–Palmer Arrangement.* One shortcoming of the Wenner method is the rapid decrease in magnitude of potential between the two inner electrodes when their spacing is increased to relatively large values. Historically, instruments were inadequate for measuring such low potential values, although improved sensitivity in modern testers mitigates this disadvantage to some extent. Another disadvantage with the Wenner method is the requirement to reposition all four probes for each depth to be measured. The arrangement shown in Figure 2(b) can be used to measure soil resistivity successfully when current probes are separated by a large distance or to expedite testing for multiple current probe locations.

With the Schlumberger method, the inner probes are placed closer together and the outer probes are placed farther apart. Unlike the Wenner method, which requires all probes to be moved to calculate soil resistivity at different depths, the Schlumberger method only required the outer probes to be repositioned for subsequent measurements. Reducing the number of probes to be repositioned for each test makes the Schlumberger method a faster choice for testing at different depths.

The equation to be used in this case can be easily determined (Palmer [B50]). If the depth of burial of the electrodes b is small compared to their separation d and c, and $c > 2d$, then the measured apparent resistivity can be calculated as follows:

$$\rho = \pi c(c+d)R/d \tag{4}$$

The resistivity calculated by Equation (4) is the apparent resistivity to the approximate depth [2*c* +*d*]/2, which is the distance from the center of the test to the outer current probes [Figure 2(b)].

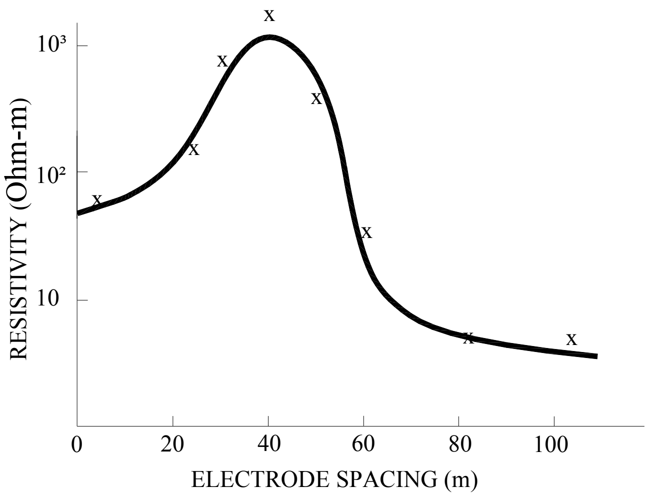

Figure 3 —Typical resistivity curve

Like the variation of depth method, the four-point method gives the apparent resistivity for a specific, although broader, volume of soil. It is advantageous to take measurements along several profiles around the area of concern to detect lateral changes in soil resistivity, as well as to determine any possible interference effects on the measurements due to nearby conductive objects. Another way to gain confidence that conductive objects in the earth do not affect the measurements is to repeat the same measurement in the same location, but 90° relative to the first one. The measured values should correlate.

7.3 Interpretation of measurements

The interpretation of the results obtained in the field is perhaps the most difficult part of the measurement process. As mentioned in 7.1, the earth resistivity variation is large and complex because of the heterogeneity of earth. Except for very few cases, it is essential to establish a simple equivalent to the earth structure. This equivalent depends on the following factors:

a) The accuracy and extent of the measurements
b) The method used
c) The complexity of the mathematics involved
d) The purpose of the measurements

For applications in power engineering, the two-layer equivalent model is accurate enough in many cases without being mathematically too involved. However, there are computer solutions available that can effectively estimate multilayer soil models for various measurement techniques.

7.3.1 Geological information and soil samples

Special tools or mathematical equations are not necessary to interpret such information, which are mainly given in the figures and tables provided by geological explorations. As shown in Table 1, determining an accurate soil model from simple classifications of types of soil is difficult. The classifications simply give a crude estimation of the resistivity of different types of soils.

7.3.2 Variation of depth method (see Annex B)

The following interpretations assume that the tested ground is a rod driven to various depths l_l through l_n. Table 2 shows a sample set of measured values. Assuming the rod radius r is small compared to l, Equation (7) can be used to compute an apparent resistivity for each measured value. The user should note that Equation (7) is derived based on the assumption of uniform soil resistivity, so the apparent resistivity is approximate, at best.

The ground resistance of the rod buried in a uniform soil is given by Thug [B60]:

$$R = \frac{\rho}{2\pi l} \ln \frac{2l}{r} \tag{5}$$

or

$$R = \frac{\rho}{2\pi l} \left[\ln\left(\frac{4l}{r}\right) - 1 \right] \tag{6}$$

depending on the approximations used.

Rearranging for apparent resistivity gives:

$$\rho_a = \frac{R 2\pi l}{\ln\left(\frac{4l}{r}\right) - 1} \tag{7}$$

For each length l of the rod, the measured resistance value R determines the apparent resistivity value ρ_α, which, when plotted against l, provides a visual aid for determining earth resistivity variation with depth. For more clarity, suppose that the field tests of Table 2 gave the curve shown in Figure 4(a) and Figure 4(b). These curves were mathematically derived to fit perfect two-layer soil models. By inspection of the curve, it can be concluded that the soil structure for Figure 4(a) is at least two distinct layers. For small values of l (0 m to 6 m), the soil has a resistivity value of nearly 300 Ω-m. The lower layer is more conductive. Its resistivity value approaches 100 Ω-m. Thus, an adequate two-layer soil model can be obtained by visual inspection for this case. Now consider the curve of Figure 4(b). For this case, the upper layer soil is approximately 100 Ω-m to a depth of approximately 6 m. However, the exact value of the lower layer cannot be obtained through visual inspection. The value appears to approach 250 Ω-m, but the correct value is 300 Ω-m. The following two solutions are then possible:

a) Continue measurements with rods driven deeper into the soil
b) Use analytical techniques to compute, from the measured data, an equivalent earth resistivity model

Table 2—Expected three-point field measurements for mathematically derived two-layer soil models

Rod depth m (ft)	ρ_1= 300, ρ_2= 100, h = 6. 1 m (20 ft)		ρ_1 = 100, ρ_2 = 300, h = 6.1 m (20 ft)	
	Resistance (Ω)	Apparent resistivity (Ω-m)	Resistance (Ω)	Apparent resistivity (Ω-m)
0.3 (1.0)	647.60	299.3	218.30	100.9
0.9 (3.0)	270.60	296.5	92.68	101. 6
1.5 (5.0)	177.10	294.7	61.52	102.4
3.0 (10.0)	97.63	290.0	35.13	104.4
4.5 (15.0)	67.85	284. 5	25.43	106.6
6.1 (20.0)	50.82	272.6	20.63	110. 7
9.1 (30.0)	21.77	165.8	18.22	138.7
15.2 (50.0)	10.91	129.7	14.58	173.3
21.3 (70.0)	7.41	118.4	12.16	194.2
27.4 (90.0)	5.64	112.5	10.42	207.8
33.5 (110.0)	4.57	108.9	9.13	217.5
39.6 (130.0)	3.84	106.1	8.12	224.3
45.7 (150.0)	3.32	104.2	7.31	229.4

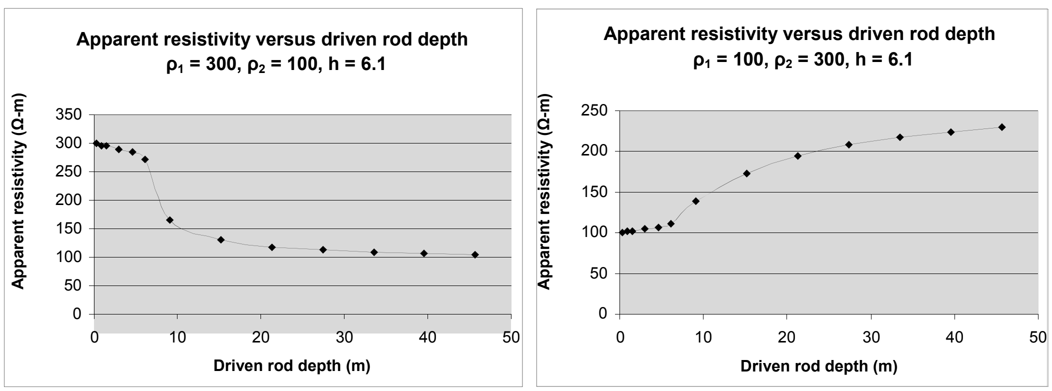

(a) (b)

Figure 4 —Variation of depth mathematically derived field measurements

When using analytical methods (computer software) to determine the soil parameters, it is appropriate to replace the simple Equation (5) or Equation (6), which assume uniform soil resistivity, with more exact equations based on layered soil models. Then, the soil parameters for each layer can be determined to obtain the best fit with the measured driven-rod resistances.

Additional measurements will certainly help in obtaining the resistivity of each layer. However, the thicknesses of each layer are not always easy to determine. Moreover, driving rods to great depth can be difficult and expensive.

The resistance of a rod in such earth models is known or can be easily calculated (see Annex A). Using a simple computer program or simply by a cut-and-try method, the best fit to the experimental results can be obtained (see Annex B).

As mentioned, the variation of depth method fails to predict earth resistivity at large distances from the area where the test rod is embedded (distances larger than five to ten times the driven rod length). For large areas, several rod locations can give an indication of significant lateral changes in soil resistivity.

7.3.3 Four-point method

The interpretation of the four-point method is similar to that of the method described in 7.3.2. For example, in the case of the Wenner arrangement, the measured apparent resistivity is plotted against the electrode spacing *a*. The resulting curve then indicates the soil structure. Again the depths of various layers might not be easy to determine by visual inspection of the curve. Many authors (Gish and Rooney [B32], Lancaster-Jones [B43], Thug [B60], Wenner [B62]) gave quick empirical rules to help in establishing the layer thickness. The following are examples:

a) The Gish and Rooney method [B32]: From the resistivity curve, a change in formation, for example, another layer is reached at a depth equal to any electrode separation at which a break or change in curvature occurs.
b) The Lancaster–Jones method [B43]: The depth to the lower layer is taken as two thirds the electrode separation at which the point of inflexion occurs.
c) Zohdy [B63] stated there are five axioms that hold true about soil resistivity sounding curves (plots of apparent resistivity vs. probe separation):
    1) The computed apparent resistivities are always positive.
    2) As the actual resistivity increases or decreases with greater depth, the apparent resistivities also increase or decrease with greater probe spacings.
    3) The maximum change in apparent resistivity occurs at a probe spacing larger than the depth at which the corresponding change in actual resistivity occurs. Thus, the changes in apparent resistivity are always plotted to the right of the probe spacing corresponding to the change in actual resistivity.
    4) The amplitude of the curve is always less than or equal to the amplitude of the actual resistivity versus depth curve.
    5) In a multilayer model, a change in the actual resistivity of a thick layer results in a similar change in the apparent resistivity curve.

Using these axioms as guidance, one can estimate the appropriate multilayer model that best represents a particular soil structure, realizing that the probe spacings from the sounding curves *do not* correspond to the actual depth of change in resistivity, and that the magnitudes of the apparent resistivities *do not* correspond to the actual resistivity. Typically, one of the following earth models is used:

— Uniform resistivity
— Horizontal layers of uniform resistivities (see Annex A)
— Exponential variation of the resistivity (see Annex A)

For each model, the mathematical relation between the apparent resistivity and the various earth parameters needs to be known or to be easy to calculate.

The best model to use depends on the purpose of the measurements. Often, a two-layer earth model gives excellent results (Thug [B60]).

Figure 5 shows a mathematically derived set of values representing equally spaced field measurements (Table 3) for two perfect two-layer earth soil models. In Figure 5(a), the first few readings appear to indicate a changing soil resistivity at shallow depth, then subsequent readings approach the correct value of 300 Ω-m, and finally the readings approach the correct lower layer soil resistivity of 100 Ω-m. From this curve, a clear indication of the depth of the upper layer cannot be easily determined, although it appears to be something less than 5 m. None of the approximate methods mentioned above correctly predicts the depth of 6.1 m. In Figure 5(b), the depth of the upper layer is even more difficult to predict. In fact, it is not clear from Figure 5(b) that there is a distinct change in soil resistivities; it appears to be continuously changing to a value near 300 Ω-m.

The methods discussed in Annex A and Annex B can be used to determine the best-fit soil parameters for uniform or two-layer soil models. Alternatively, software is available that can interpret the measurements into an appropriate soil model consisting of uniform soil or several layers of soil.

Table 3—Expected four-point, equally spaced field measurements for mathematically derived two-layer soil models

Spacing m (ft)	$\rho_1 = 300$, $\rho_2 = 100$, h = 6.1 m (20 ft)		$\rho_1 = 100$, $\rho_2 = 300$, h = 6.1 m (20 ft)	
	Resistance (Ω)	Apparent resistivity (Ω-m)	Resistance (Ω)	Apparent resistivity (Ω-m)
0.3 (1.0)	159.15	300.0	53.05	100.0
0.9 (3.0)	52.99	299.7	17.71	100.1
1.5 (5.0)	31.67	298.5	10.67	100.6
3.0 (10.0)	15.38	289.8	5.51	103.9
4.5 (15.0)	9.64	272.6	3.92	110.9
6.1 (20.0)	6.49	248.7	3. 16	121.0
9.10 (30.0)	3.56	203.3	2.50	142.8
15.2 (50.0)	1.51	144.5	1.90	181.4
21.3 (70.0)	0.90	120.4	1.56	208.6
27.4 (90.0)	0.64	110.8	1.32	227.8
33.5 (110.0)	0.51	106.5	1.15	241.4
39.6 (130.0)	0.42	104.3	1.01	251.7
45.7 (150.0)	0.36	103.1	0.90	259.6

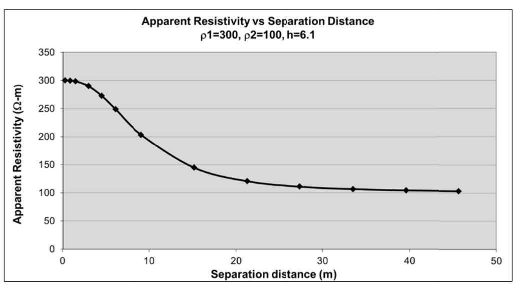

(a)

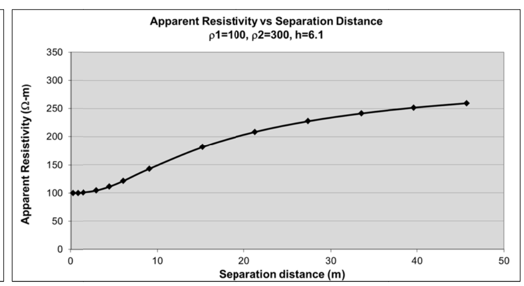

(b)

Figure 5—Four-point, equally spaced method mathematically derived field measurements

7.4 Guidance on performing field measurements

7.4.1 Interferences

When making measurements using the variation-of-depth or four-point methods, be careful to avoid interferences from nearby structures or circuits. These interferences might be passive or active. Passive interferences include, but are not limited to, metallic fences, transmission or distribution line pole grounds, large building foundations, buried conductive objects, and metallic pipes. These passive interferences can act as a short circuit to distort the potentials created in the soil from the injected test current. Active interferences include, but are not limited to, parallel transmission or distribution lines, parallel communication circuits and stray dc currents. Use test probes made of a material that will minimize galvanic voltages between the probes. These active interferences can be a source of current that is added to or subtracted from the injected test current, again, distorting the potentials at the potential probes.

MONOGRAFÍA

ESTACIÓN DE REFERENCIA DE OPERACIÓN CONTÍNUA
C.O.R.S. GEO-9 (Municipio de Tarija)

1.- FORMULARIO

PROPIETARIOS: COTOBOL / GeoBolivia SRL
Preparado Por: COLEGIO DE TOPÓGRAFOS DE BOLIVIA
Nombre Punto CORS: GEO-9
Fecha de instalación: 25/11/2021
Fecha de actualización: 25/11/2021

2.- IDENTIFICACION DE LA ESTACIÓN G.N.S.S.

Nombre de la Estación: GEO-9
Identificación de la Estación: GEO-9
Inscripción del Monumento: Sin inscripción
Informaciones Adicionales: ---

3.- INFORMACIÓN SOBRE LA UBICACION

Municipio: Tarija
Provincia: Cercado
Información Adicional: Antena instalada en una estructura metálica en el 2do. Piso, empotrada en una columna de concreto cerca del tanque de agua en el domicilio ubicado en la Av. José J Pérez, calle Ambrosio Catoira No.227, Zona Senac, Barrio Andalucía.
Enlace RED MARGEN: Punto enlazado al "Marco de Referencia Geodésico Nacional" MARGEN – SIRGAS, mediante las Estaciones Permanentes del Instituto Geográfico Militar TJA(Tarija), VMON(Villamontes) y YCBA (Yacuiba).

4.- COORDENADAS OFICIALES

Coordenadas Oficiales			
Coordenadas Geodésicas			
Latitud:	-21°32´25,86143"	Sigma:	0.0011
Longitud:	-64°45´09,69598"	Sigma:	0.0011
Altura Elipsoidal:	1965,4023m	Sigma:	0.0011
Coordenadas Cartesianas			
X:	2532364,27679	Sigma:	0.0011
Y:	-5370034,83330	Sigma:	0.0011
Z:	-2327886,02685	Sigma:	0.0011
Coordenadas UTM			
UTM (Norte):	7617010,3987		
UTM (Este):	318487,7002		
Meridiano Central:	-63		
ZONA UTM:	20		

5.- INFORMACIÓN DEL RECEPTOR G.N.S.S.

INFORMACIÓN DEL RECEPTOR

Tipo do Receptor: SOUTH NET S9
Número de Serie: S490A5117341500
Versión del Firmware: 1.8.1245
Fecha de Instalación: 25/11/2021 16:02 UTC

INFORMACIÓN DE LA ANTENA

Tipo de Antena (Nombre IGS): STHCR3-G3 SOUTH
Número de Serie: **C**2016001896
Altura de la Antena (m): 0.000 m
Fecha de instalación: 25/11/2021
URL imagen: https://www.ngs.noaa.gov/ANTCAL/LoadImage?name=STHCR3-G3%26STHC.gif

Nota: La Estación de Referencia de Operación Continua C.O.R.S. GEO9 registra información con intervalos de 15" Segundos y envía señales de corrección N.T.R.I.P. en los diferentes formatos RTCM, CMR y 15° en la máscara de elevación.

Informaciones
https://www.geoboliviasrl.com

PROYECTO **TIERRA LINDA**
ESPACIAMIENTO **10 METROS**
FECHA **04/06/2024**
LONGITUD TOTAL **800 METROS**
SISTEMA **WGS-84 UTM 20 K**

	ESTACA	PROGRESIVA	ESTE	NORTE	ALTURA
Carrete 1-1	1-1	0	316070.31	7615748.88	2037.47
Carrete 1-3	1-3	20	316086.00	7615759.86	2038.85
Carrete 1-5	1-5	40	316102.60	7615772.40	2038.29
Carrete 1-7	1-7	60	316118.80	7615785.32	2036.17
Carrete 1-9	1-9	80	316135.41	7615798.17	2034.56
Carrete 1-11	1-11	100	316151.54	7615811.18	2035.78
Carrete 1-13	1-13	120	316167.56	7615824.03	2036.16
Carrete 1-15	1-15	140	316183.12	7615837.16	2035.46
Carrete 1-17	1-17	160	316198.16	7615851.01	2034.64
Carrete 1-19	1-19	180	316212.95	7615864.50	2033.63
Carrete 1-21	1-21	200	316228.61	7615878.37	2033.42
Carrete 2-2	2-2	210	316236.29	7615884.72	2033.44
Carrete 2-3	2-3	220	316243.32	7615891.68	2033.49
Carrete 2-4	2-4	230	316249.78	7615899.05	2033.76
Carrete 2-5	2-5	240	316256.98	7615905.32	2031.78
Carrete 2-6	2-6	250	316266.23	7615909.20	2031.35
Carrete 2-7	2-7	260	316273.76	7615915.57	2031.81
Carrete 2-8	2-8	270	316281.48	7615921.35	2032.30
Carrete 2-9	2-9	280	316288.46	7615927.63	2030.38
Carrete 2-10	2-10	290	316294.61	7615934.27	2027.78
Carrete 2-11	2-11	300	316300.85	7615942.48	2027.27
Carrete 2-12	2-12	310	316307.72	7615949.63	2026.87
Carrete 2-13	2-13	320	316314.88	7615956.50	2026.70
Carrete 2-14	2-14	330	316322.39	7615963.01	2026.32
Carrete 2-15	2-15	340	316329.56	7615969.79	2025.97
Carrete 2-16	2-16	350	316337.19	7615976.33	2025.44
Carrete 2-17	2-17	360	316344.72	7615982.82	2024.66
Carrete 2-18	2-18	370	316352.05	7615989.52	2023.40
Carrete 2-19	2-19	380	316360.07	7615995.45	2022.58
Carrete 2-20	2-20	390	316368.46	7615999.16	2021.91
CentroCarrete 2-21	2-21	400	316377.61	7616002.38	2021.49
Carrete 3-2	3-2	410	316385.19	7616007.22	2022.14
Carrete 3-3	3-3	420	316394.21	7616011.70	2021.19
Carrete 3-4	3-4	430	316403.39	7616015.55	2020.85
Carrete 3-5	3-5	440	316412.18	7616020.32	2020.06
Carrete 3-6	3-6	450	316421.19	7616024.34	2019.98
Carrete 3-7	3-7	460	316429.70	7616029.42	2020.07
Carrete 3-8	3-8	470	316438.70	7616033.61	2020.10
Carrete 3-9	3-9	480	316447.43	7616038.75	2019.93

Carrete 3-10	3-10	490	316455.73	7616044.19	2019.24
Carrete 3-11	3-11	500	316463.42	7616049.57	2018.66
Carrete 3-12	3-12	510	316471.57	7616055.36	2018.36
Carrete 3-13	3-13	520	316479.34	7616060.89	2018.03
Carrete 3-14	3-14	530	316487.28	7616066.99	2017.73
Carrete 3-15	3-15	540	316495.18	7616073.23	2017.53
Carrete 3-16	3-16	550	316502.84	7616079.66	2017.29
Carrete 3-17	3-17	560	316510.65	7616085.72	2017.02
Carrete 3-18	3-18	570	316518.38	7616091.96	2016.74
Carrete 3-19	3-19	580	316526.48	7616097.88	2016.69
Carrete 3-20	3-20	590	316534.78	7616103.50	2016.68
Carrete 3-21	3-21	600	316543.11	7616108.66	2016.64
Carrete 4-3	4-3	620	316558.13	7616121.32	2017.22
Carrete 4-5	4-5	640	316574.47	7616133.28	2017.16
Carrete 4-7	4-7	660	316591.49	7616143.41	2016.29
Carrete 4-9	4-9	680	316609.33	7616152.24	2015.56
Carrete 4-11	4-11	700	316625.54	7616163.50	2016.58
Carrete 4-13	4-13	720	316642.02	7616175.02	2016.97
Carrete 4-15	4-15	740	316658.66	7616186.08	2017.43
Carrete 4-17	4-17	760	316674.74	7616198.04	2017.71
Carrete 4-19	4-19	780	316690.55	7616210.12	2017.91
Carrete 4-21	4-21	800	316707.24	7616220.97	2017.62

Pozo Tierra Linda			316370.879	7616014.879	2022.479

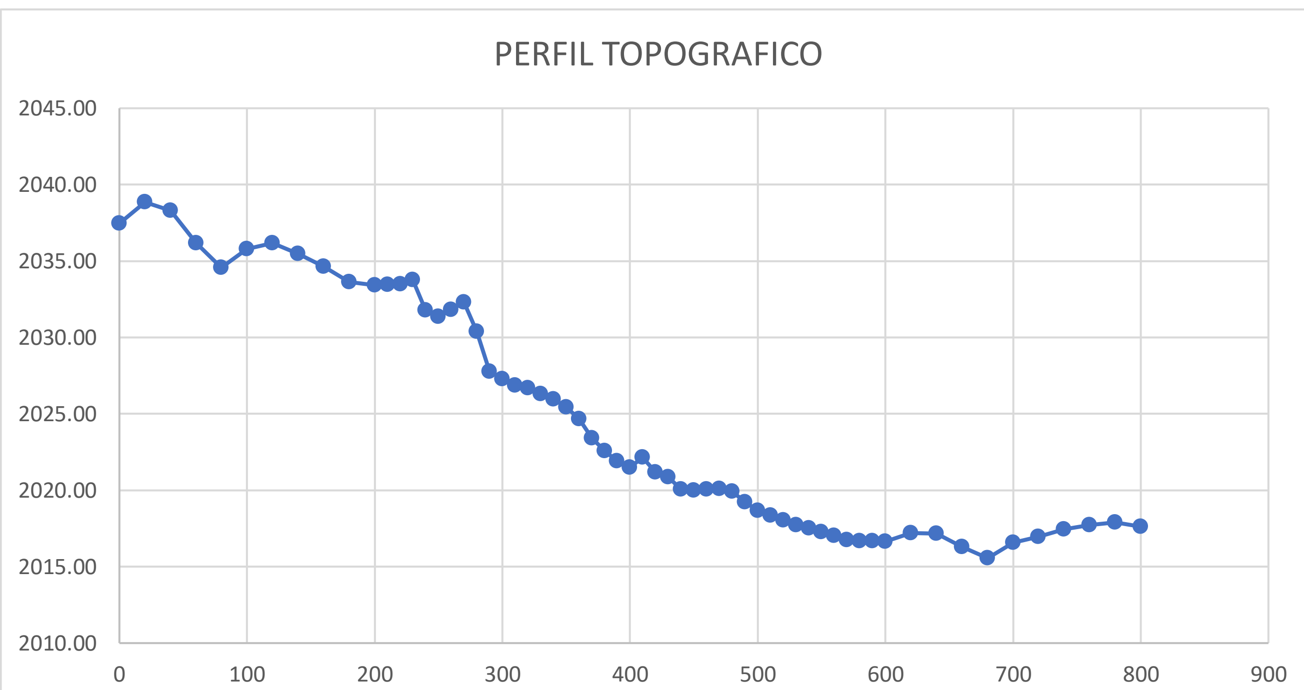

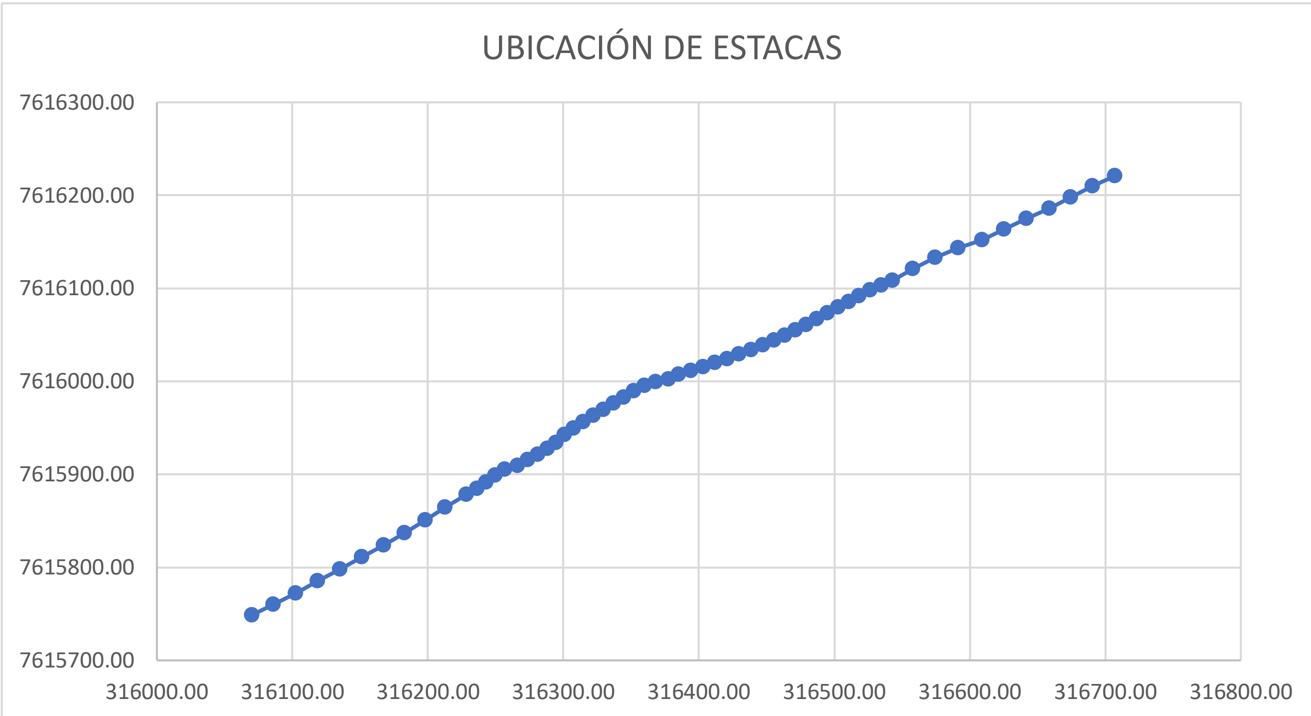
UBICACIÓN DE ESTACAS
7616300.00
7616200.00
7616100.00
7616000.00
7615900.00
7615800.00
7615700.00
316000.00
316100.00
316200.00
316300.00
316400.00
316500.00
316600.00
316700.00
316800.00

PROYECTO **FRAY QUEBRACHO**
ESPACIAMIENTO **10 METROS**
FECHA **05/06/2024**
LONGITUD TOTAL **800 METROS**
SISTEMA **WGS-84 UTM 20 K**

	ESTACA	PROGRESIVA	ESTE	NORTE	ALTURA
Carrete 1-1	1-1	0	320216.60	7621413.44	1996.96
Carrete 1-3	1-3	20	320220.99	7621433.14	1995.18
Carrete 1-5	1-5	40	320227.40	7621452.66	1994.27
Carrete 1-7	1-7	60	320235.80	7621471.58	1992.37
Carrete 1-9	1-9	80	320242.75	7621491.10	1990.37
Carrete 1-11	1-11	100	320251.19	7621509.50	1989.57
Carrete 1-13	1-13	120	320260.11	7621527.77	1989.06
Carrete 1-15	1-15	140	320269.80	7621545.96	1988.73
Carrete 1-17	1-17	160	320279.72	7621563.88	1988.60
Carrete 1-19	1-19	180	320287.97	7621582.25	1988.45
Carrete 1-21	1-21	200	320296.82	7621598.83	1988.08
Carrete 2-2	2-2	210	320300.99	7621608.21	1988.25
Carrete 2-3	2-3	220	320303.39	7621617.77	1987.66
Carrete 2-4	2-4	230	320306.72	7621627.05	1987.05
Carrete 2-5	2-5	240	320311.70	7621635.77	1986.44
Carrete 2-6	2-6	250	320315.41	7621644.91	1987.07
Carrete 2-7	2-7	260	320319.36	7621654.12	1986.27
Carrete 2-8	2-8	270	320323.77	7621663.66	1985.51
Carrete 2-9	2-9	280	320327.40	7621672.45	1985.13
Carrete 2-10	2-10	290	320331.71	7621681.45	1984.95
Carrete 2-11	2-11	300	320336.05	7621690.56	1984.95
Carrete 2-12	2-12	310	320340.49	7621699.46	1984.86
Carrete 2-13	2-13	320	320344.90	7621708.53	1984.79
Carrete 2-14	2-14	330	320349.27	7621717.44	1984.76
Carrete 2-15	2-15	340	320353.70	7621726.47	1984.69
Carrete 2-16	2-16	350	320357.99	7621735.45	1984.72
Carrete 2-17	2-17	360	320361.78	7621744.69	1984.69
Carrete 2-18	2-18	370	320365.69	7621754.01	1984.69
Carrete 2-19	2-19	380	320369.86	7621762.99	1984.09
Carrete 2-20	2-20	390	320375.23	7621771.44	1983.87
CentroCarrete 2-21	2-21	400	320381.34	7621779.33	1983.37
Carrete 3-2	3-2	410	320387.61	7621785.68	1983.03
Carrete 3-3	3-3	420	320393.55	7621793.78	1982.85
Carrete 3-4	3-4	430	320399.52	7621801.75	1982.51
Carrete 3-5	3-5	440	320405.45	7621809.82	1982.38
Carrete 3-6	3-6	450	320408.53	7621819.63	1982.25
Carrete 3-7	3-7	460	320407.07	7621829.10	1980.91
Carrete 3-8	3-8	470	320407.92	7621838.52	1979.78
Carrete 3-9	3-9	480	320407.37	7621847.81	1978.70
Carrete 3-10	3-10	490	320408.48	7621857.84	1978.74
Carrete 3-11	3-11	500	320411.71	7621867.34	1978.76

Carrete 3-12	3-12	510	320414.58	7621876.75	1978.97
Carrete 3-13	3-13	520	320417.66	7621886.14	1979.33
Carrete 3-14	3-14	530	320420.01	7621895.85	1979.57
Carrete 3-15	3-15	540	320423.19	7621905.35	1979.90
Carrete 3-16	3-16	550	320426.48	7621914.77	1980.07
Carrete 3-17	3-17	560	320429.36	7621924.35	1980.06
Carrete 3-18	3-18	570	320432.19	7621933.86	1979.91
Carrete 3-19	3-19	580	320435.22	7621943.30	1979.46
Carrete 3-20	3-20	590	320438.05	7621952.97	1979.07
Carrete 3-21	3-21	600	320441.23	7621962.30	1978.23
Carrete 4-3	4-3	620	320444.33	7621981.03	1977.47
Carrete 4-5	4-5	640	320448.40	7622000.82	1978.44
Carrete 4-7	4-7	660	320453.93	7622019.67	1979.85
Carrete 4-9	4-9	680	320460.17	7622038.64	1981.43
Carrete 4-11	4-11	700	320466.27	7622057.83	1982.45
Carrete 4-13	4-13	720	320472.46	7622076.79	1982.96
Carrete 4-15	4-15	740	320478.18	7622095.11	1983.67
Carrete 4-17	4-17	760	320484.39	7622113.96	1983.82
Carrete 4-19	4-19	780	320490.14	7622132.84	1984.10
Carrete 4-21	4-21	800	320496.70	7622151.83	1984.15

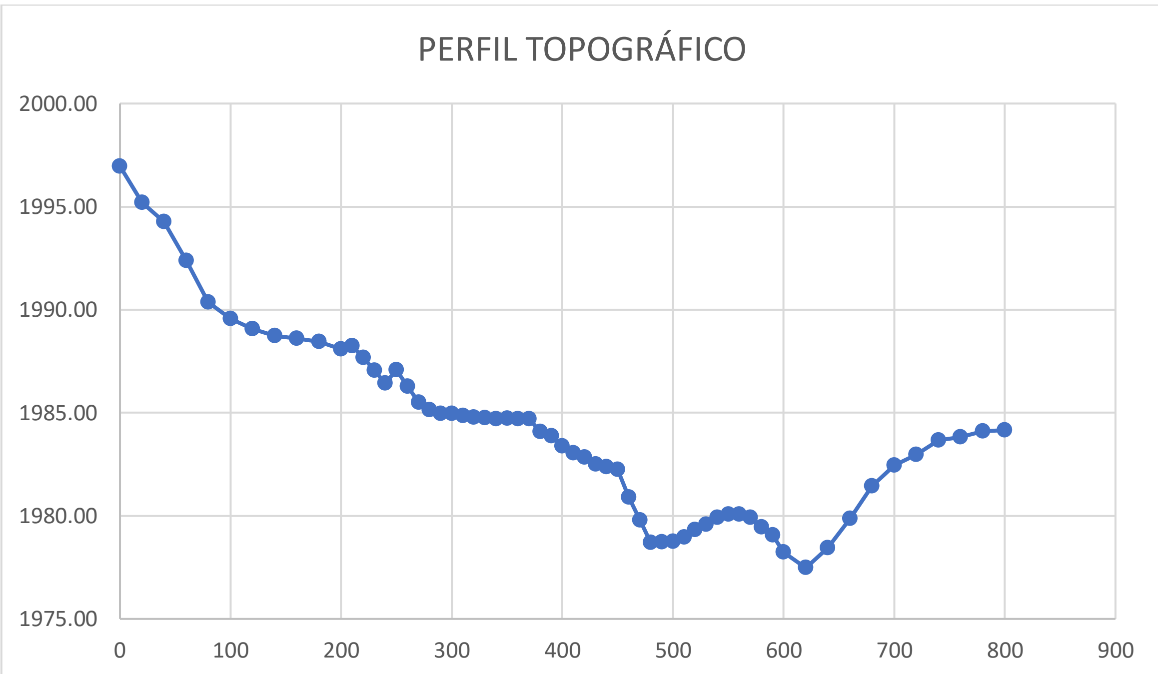

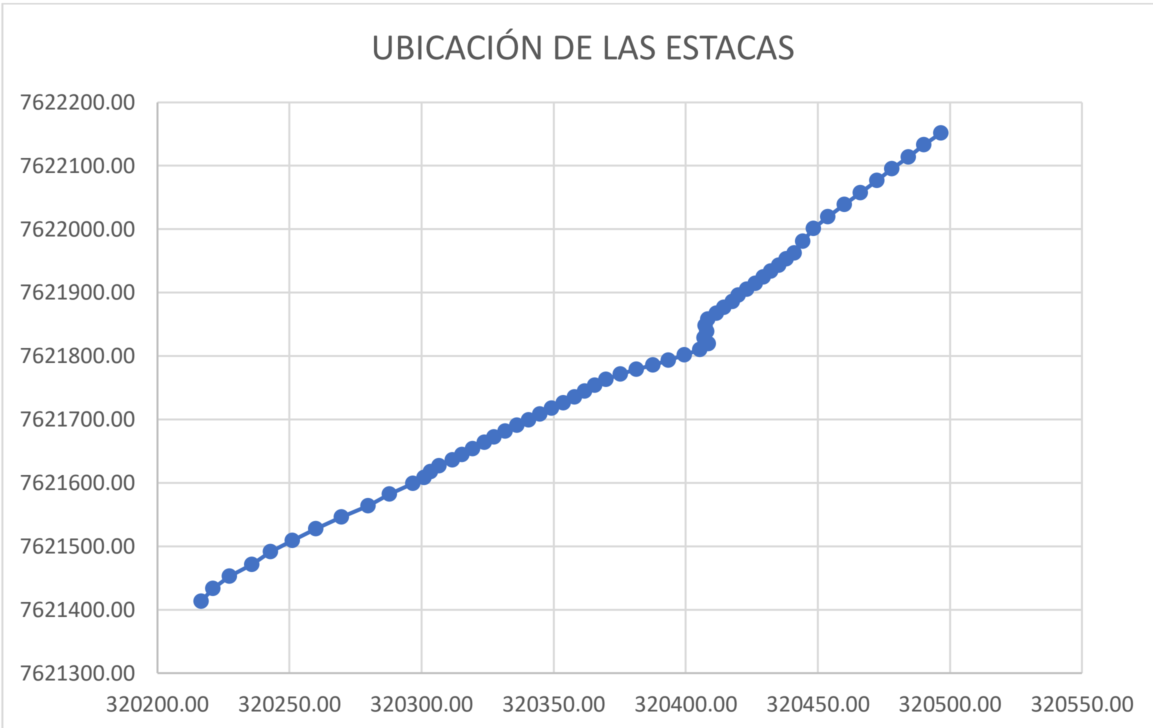
UBICACIÓN DE LAS ESTACAS
7622200.00
7622100.00
7622000.00
7621900.00
7621800.00
7621700.00
7621600.00
7621500.00
7621400.00
7621300.00
320200.00
320250.00
320300.00
320350.00
320400.00
320450.00
320500.00
320550.00

PROYECTO	**YESERA**
ESPACIAMIENTO	**10 METROS**
FECHA	**07/06/2024**
LONGITUD TOTAL	**800 METROS**
SISTEMA	**WGS-84 UTM 20 K**

	ESTACA	PROGRESIVA	ESTE	NORTE	ALTURA
Carrete 1-1	1-1	0	336698.441	7625190.561	2202.449
Carrete 1-3	1-3	20	336715.280	7625201.628	2201.514
Carrete 1-5	1-5	40	336732.968	7625212.568	2200.719
Carrete 1-7	1-7	60	336750.708	7625223.827	2200.207
Carrete 1-9	1-9	80	336767.942	7625235.943	2199.558
Carrete 1-11	1-11	100	336785.491	7625246.900	2199.191
Carrete 1-13	1-13	120	336802.319	7625258.623	2198.398
Carrete 1-15	1-15	140	336819.693	7625269.346	2197.272
Carrete 1-17	1-17	160	336834.974	7625282.917	2195.408
Carrete 1-19	1-19	180	336851.462	7625294.314	2193.710
Carrete 1-21	1-21	200	336866.477	7625307.584	2193.293
Carrete 2-2	2-2	210	336873.378	7625314.854	2193.326
Carrete 2-3	2-3	220	336880.619	7625321.925	2193.175
Carrete 2-4	2-4	230	336887.291	7625329.159	2192.844
Carrete 2-5	2-5	240	336894.464	7625336.079	2192.296
Carrete 2-6	2-6	250	336901.280	7625343.314	2191.708
Carrete 2-7	2-7	260	336907.961	7625351.225	2191.010
Carrete 2-8	2-8	270	336913.200	7625359.486	2190.392
Carrete 2-9	2-9	280	336920.436	7625366.273	2189.013
Carrete 2-10	2-10	290	336926.968	7625373.603	2188.812
Carrete 2-11	2-11	300	336933.766	7625381.341	2188.271
Carrete 2-12	2-12	310	336938.614	7625389.936	2187.521
Carrete 2-13	2-13	320	336943.068	7625398.903	2186.628
Carrete 2-14	2-14	330	336947.886	7625407.778	2185.842
Carrete 2-15	2-15	340	336952.618	7625416.232	2184.807
Carrete 2-16	2-16	350	336958.049	7625424.758	2184.374
Carrete 2-17	2-17	360	336964.565	7625432.224	2184.273
Carrete 2-18	2-18	370	336970.705	7625440.125	2183.744
Carrete 2-19	2-19	380	336978.311	7625446.623	2183.093
Carrete 2-20	2-20	390	336985.803	7625453.405	2182.462
CentroCarrete 2-21	2-21	400	336993.829	7625460.137	2181.808
Carrete 3-2	3-2	410	337001.848	7625466.933	2181.147
Carrete 3-3	3-3	420	337009.590	7625473.266	2180.416
Carrete 3-4	3-4	430	337017.291	7625479.612	2179.708
Carrete 3-5	3-5	440	337024.839	7625486.124	2178.993
Carrete 3-6	3-6	450	337032.257	7625493.137	2178.326
Carrete 3-7	3-7	460	337040.188	7625499.018	2177.727
Carrete 3-8	3-8	470	337047.525	7625505.763	2177.182

Carrete 3-9	3-9	480	337054.722	7625512.623	2176.596
Carrete 3-10	3-10	490	337062.255	7625519.195	2176.044
Carrete 3-11	3-11	500	337069.992	7625525.640	2175.539
Carrete 3-12	3-12	510	337077.883	7625531.672	2175.040
Carrete 3-13	3-13	520	337085.908	7625537.741	2174.492
Carrete 3-14	3-14	530	337093.821	7625543.648	2173.974
Carrete 3-15	3-15	540	337101.620	7625550.052	2173.433
Carrete 3-16	3-16	550	337109.449	7625556.283	2172.976
Carrete 3-17	3-17	560	337117.510	7625562.132	2172.377
Carrete 3-18	3-18	570	337125.320	7625568.206	2171.856
Carrete 3-19	3-19	580	337133.625	7625573.816	2171.344
Carrete 3-20	3-20	590	337141.679	7625579.744	2170.865
Carrete 3-21	3-21	600	337149.607	7625585.558	2170.344
Carrete 4-3	4-3	620	337165.117	7625598.134	2169.285
Carrete 4-5	4-5	640	337180.423	7625611.196	2168.248
Carrete 4-7	4-7	660	337196.044	7625623.489	2167.253
Carrete 4-9	4-9	680	337211.078	7625636.418	2166.032
Carrete 4-11	4-11	700	337226.514	7625649.376	2164.916
Carrete 4-13	4-13	720	337241.590	7625662.330	2164.026
Carrete 4-15	4-15	740	337256.646	7625675.455	2163.190
Carrete 4-17	4-17	760	337271.671	7625689.033	2162.693
Carrete 4-19	4-19	780	337288.099	7625700.428	2162.350
Carrete 4-21	4-21	800	337304.629	7625711.135	2161.659

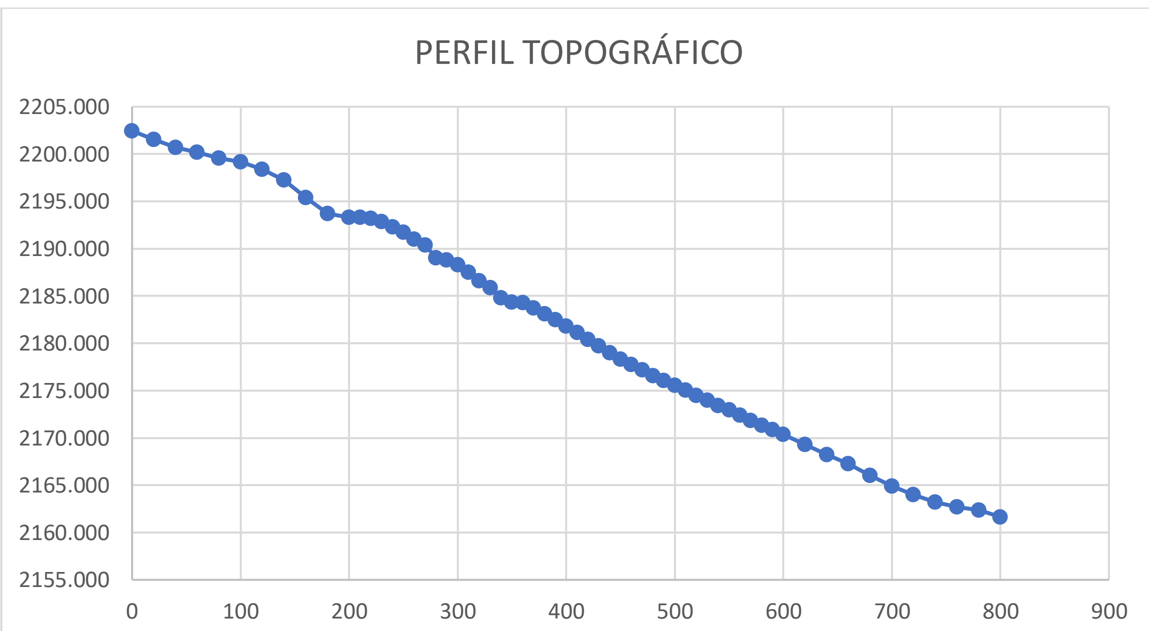

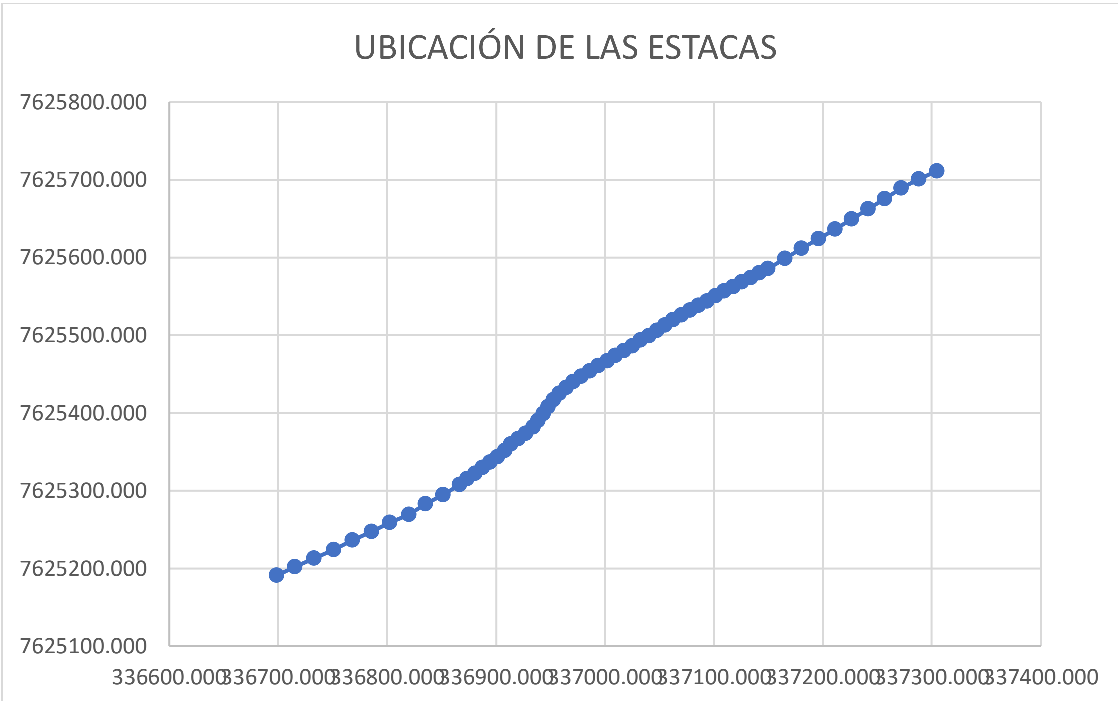
UBICACIÓN DE LAS ESTACAS
7625800.000
7625700.000
7625600.000
7625500.000
7625400.000
7625300.000
7625200.000
7625100.000
336600.000
336700.000
336800.000
336900.000
337000.000
337100.000
337200.000
337300.000
337400.000

ANEXO 5a

TIERRA LINDA

De acuerdo al proceso de datos tenemos lo siguiente:

ARREGLO: SCHLUMBERGER

CABLES: 4X21

TIEMPO DE IP: 0.5 SEGUNDOS

VENTANAS IP: 6

INTERVALOS IP

VENTANA	TIEMPO EN MS
1	0.02
2	0.04
3	0.06
4	0.08
5	0.12
6	0.18
Tiempo total	0.5 MS

```
Reading file D:\Oficina\Clientes Geofisica\Tarija OB\Inversion\Tierra Linda\Schlumberger\Sch 0.5\L1-TIERRA-LINDA-SCHLUMBERGER-05TF1edit.INV

Schlumberger_1
Minimum electrode spacing is    5.0.
General array
Wenner-Schlumberger array arrangement
Total number of data points is 690.
IP values given in terms of chargeability
Half-size model blocks used for general array data set.
Model with half the unit electrode spacing is used
Number of electrodes is 119
Number of data levels is 25.
Topography present 2.
Minimum electrode location is    0.0.
Maximum electrode location is  800.0.
Minimum electrode spacing is    5.0.
Reading inversion results.
The model has 14 layers and 1267 blocks.
Iteration  1 : Abs. error   5.64   15.02.
Iteration  2 : Abs. error   2.64   11.07.
Iteration  3 : Abs. error   1.73   11.02.
Iteration  4 : Abs. error   1.36   11.00.
Iteration  5 : Abs. error   1.17   10.99.

Topographical data present in inversion file.
Schwartz-Christoffel transformation topography modelling was used.
Blocks sensitivity information present.
Average sensitivity is 1.292.
Inversion constraints information present.
Reading of file has been completed.
```

ITERACIÓN 1

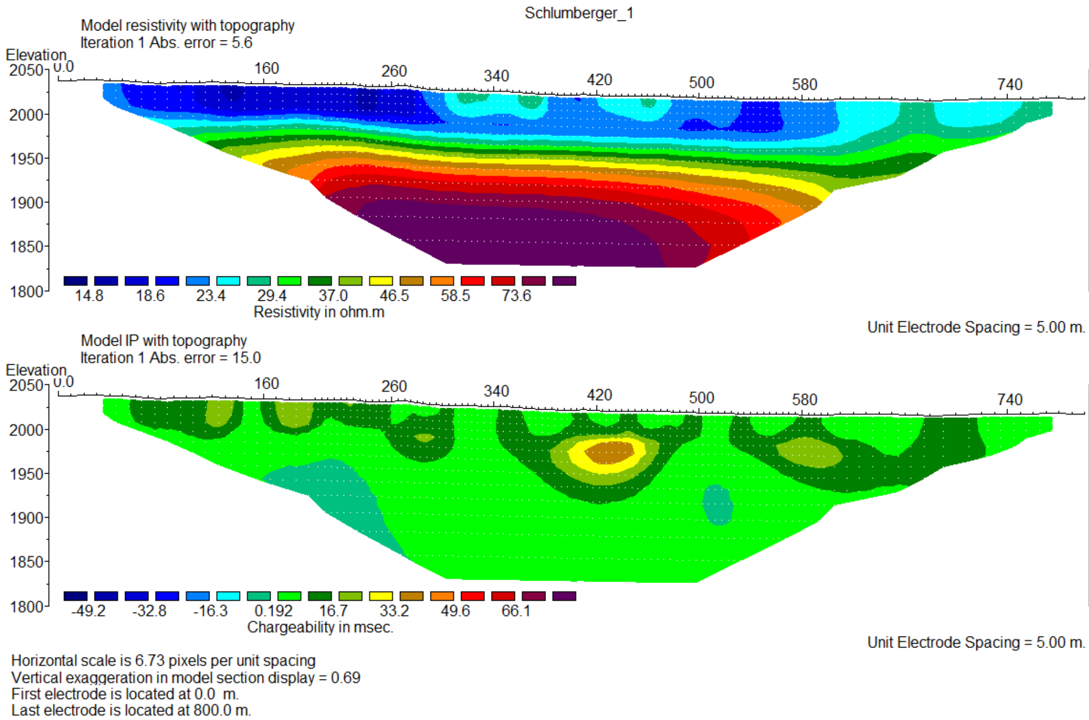

ITERACIÓN 3

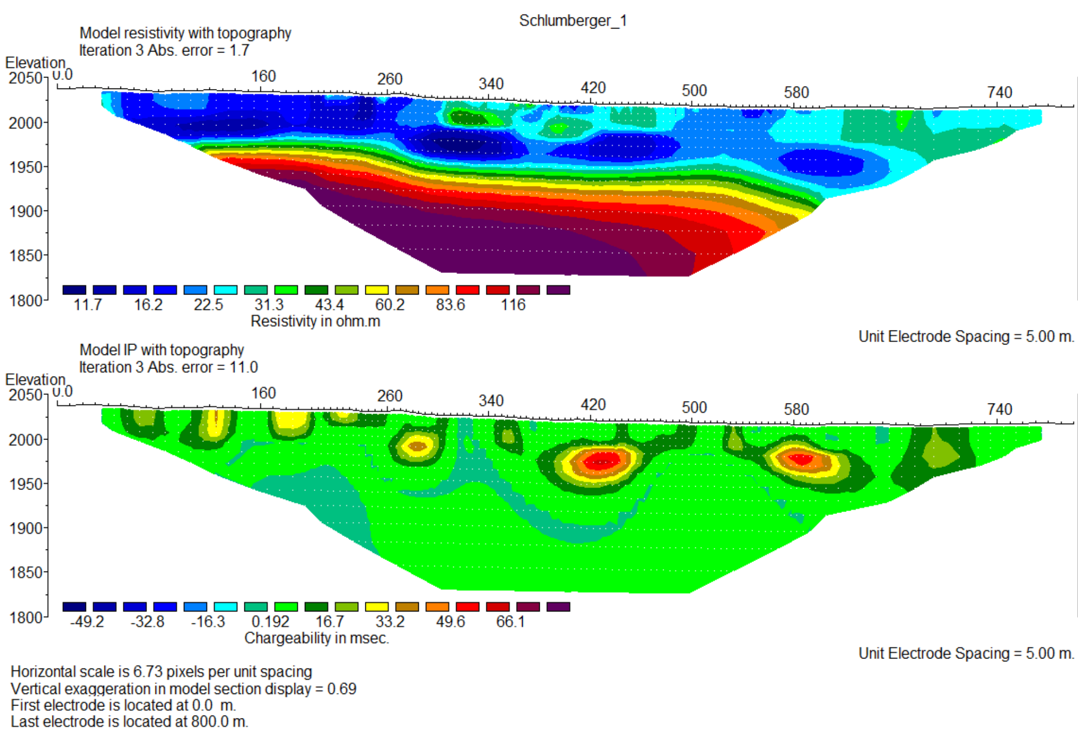

ITERACIÓN 5

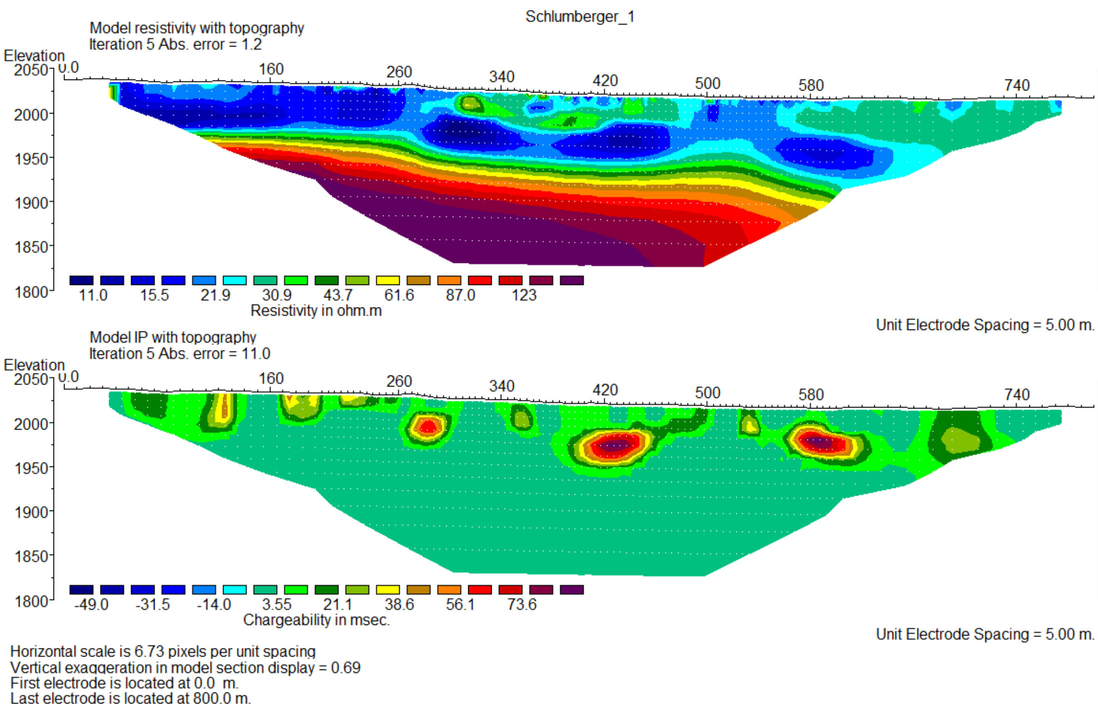

ITERACIÓN 5 BLANCO Y NEGRO

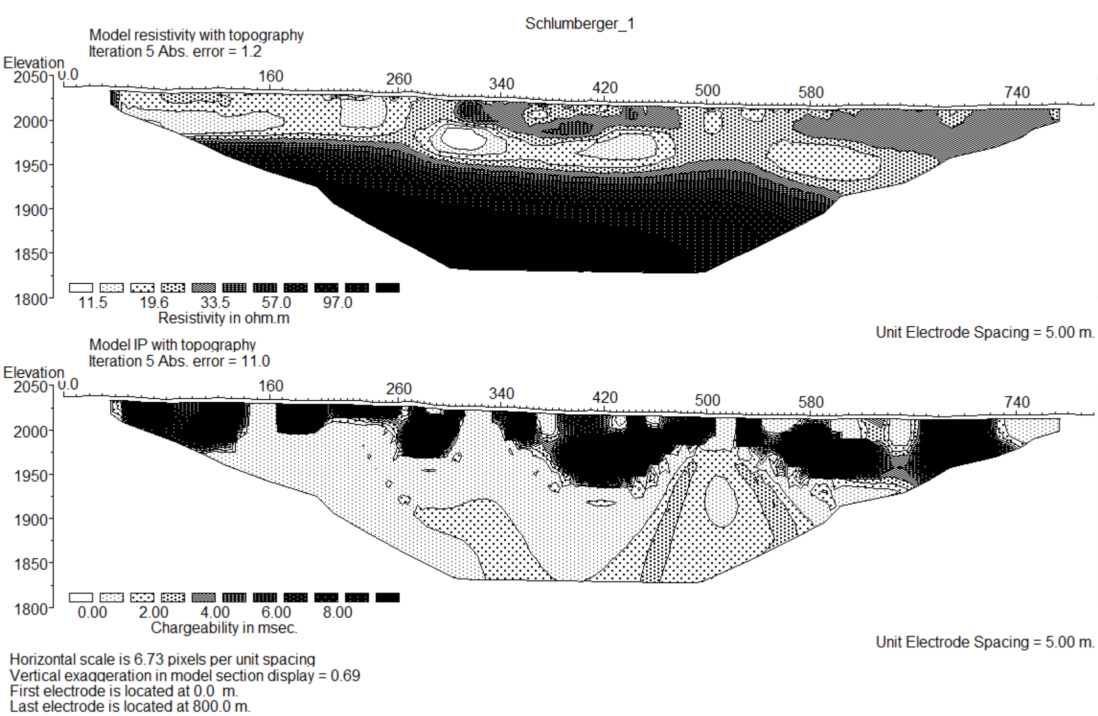

ARREGLO: SCHLUMBERGER

CABLES: 4X21

TIEMPO DE IP: 1.0 SEGUNDO

VENTANAS IP: 8

INTERVALOS IP

VENTANA	TIEMPO EN MS
1	0.02
2	0.04
3	0.06
4	0.08
5	0.12
6	0.16
7	0.22
8	0.3
Tiempo total	1.0 MS

```
Reading file D:\Oficina\Clientes Geofisica\Tarija OB\Inversion\Tierra Linda\Schlumberger\Sch 1\L1-TIERRA-LINDA-SCHLUMBERGER-1TF1edit.INV

Schlumberger_2
Minimum electrode spacing is    5.0.
General array
Wenner-Schlumberger array arrangement
Total number of data points is 694.
IP values given in terms of chargeability
Half-size model blocks used for general array data set.
Model with half the unit electrode spacing is used
Number of electrodes is 119
Number of data levels is 26.
Topography present 2.
Minimum electrode location is    0.0.
Maximum electrode location is  800.0.
Minimum electrode spacing is    5.0.
Reading inversion results.
The model has 15 layers and 1270 blocks.
Iteration  1 : Abs. error   5.88   18.49.
Iteration  2 : Abs. error   2.80   12.74.
Iteration  3 : Abs. error   1.88   12.69.
Iteration  4 : Abs. error   1.48   12.66.
Iteration  5 : Abs. error   1.29   12.65.

Topographical data present in inversion file.
Schwartz-Christoffel transformation topography modelling was used.
Blocks sensitivity information present.
Average sensitivity is 1.293.
Inversion constraints information present.
Reading of file has been completed.
```

ITERACIÓN 1

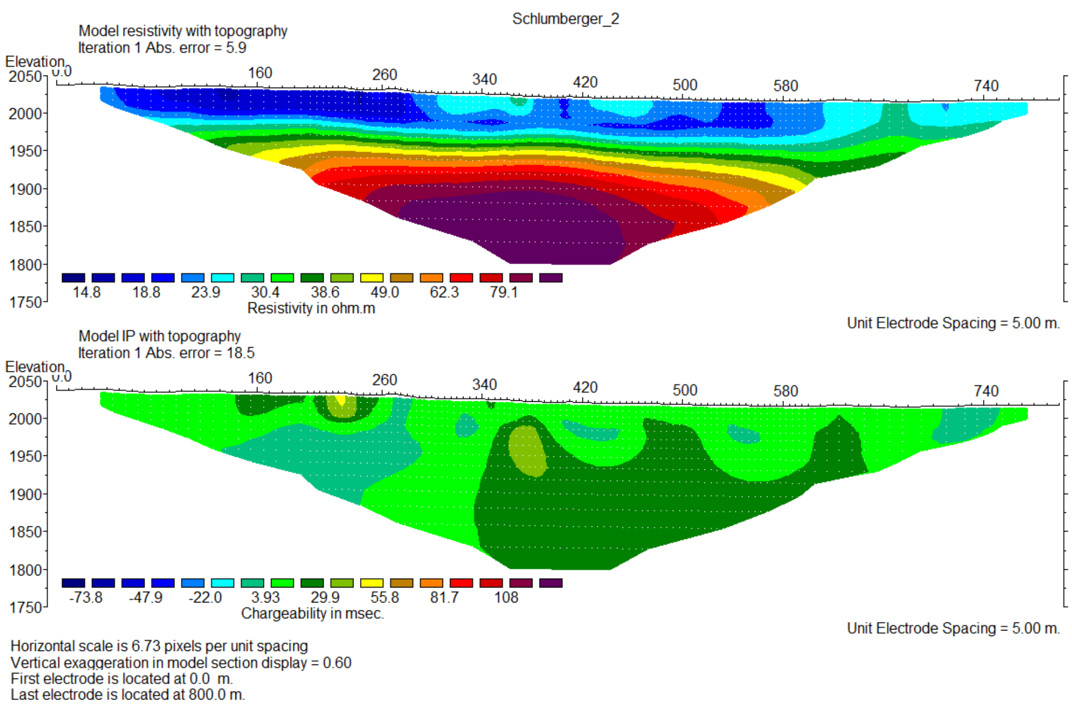

ITERACIÓN 3

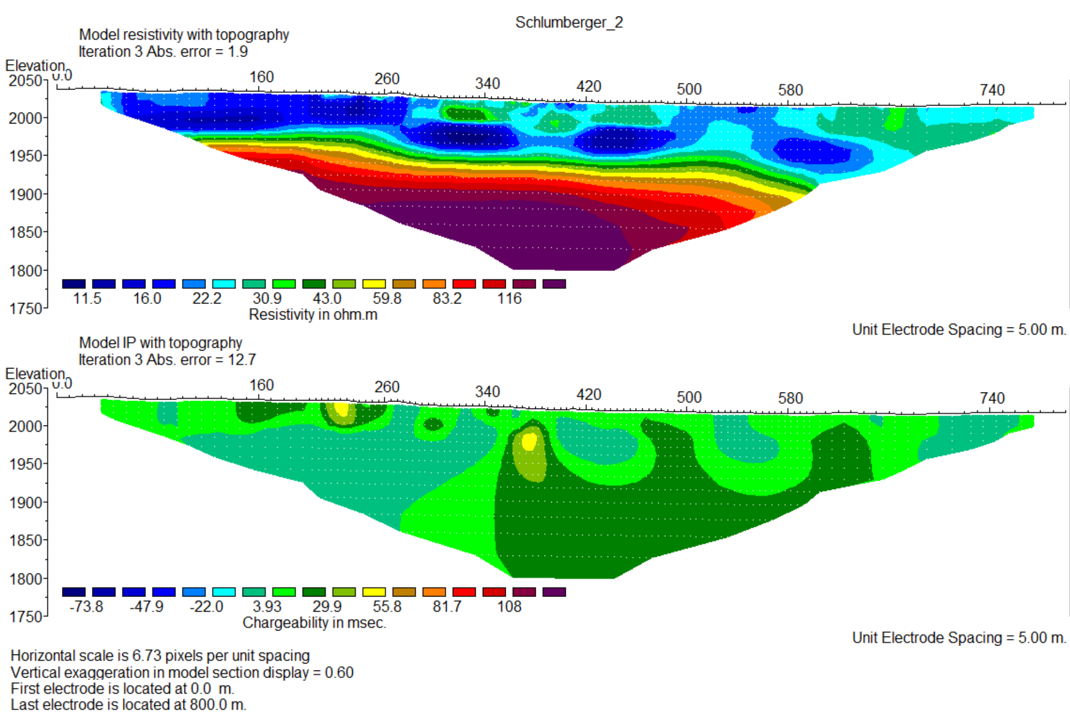

ITERACIÓN 5

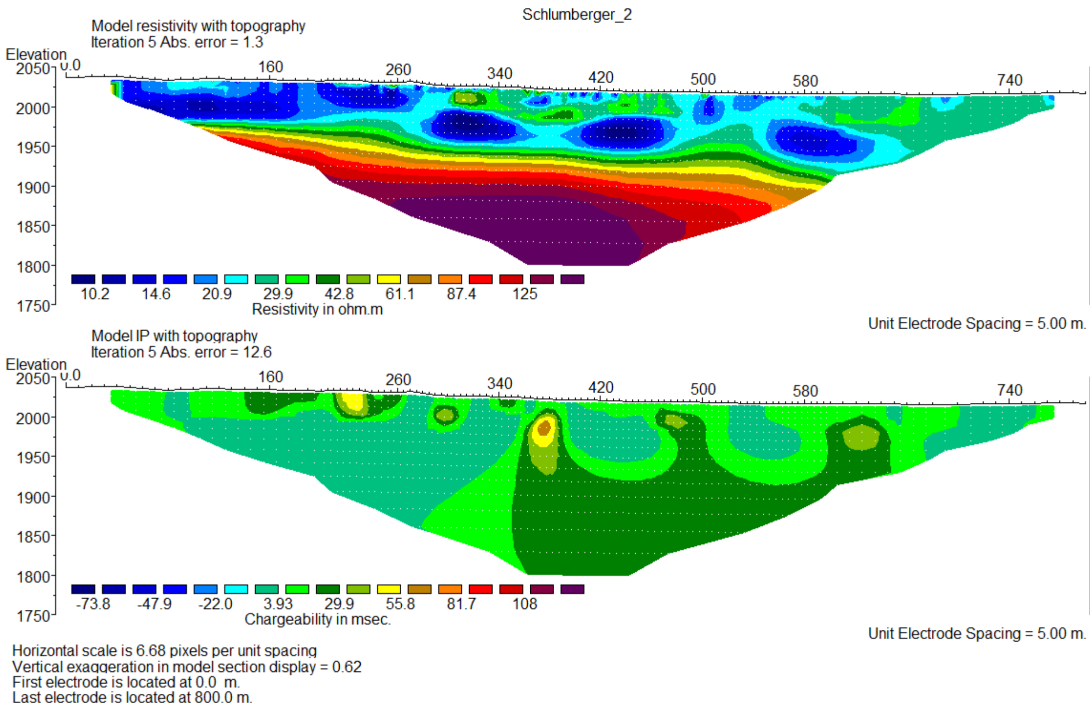

ITERACIÓN 5 BLANCO Y NEGRO

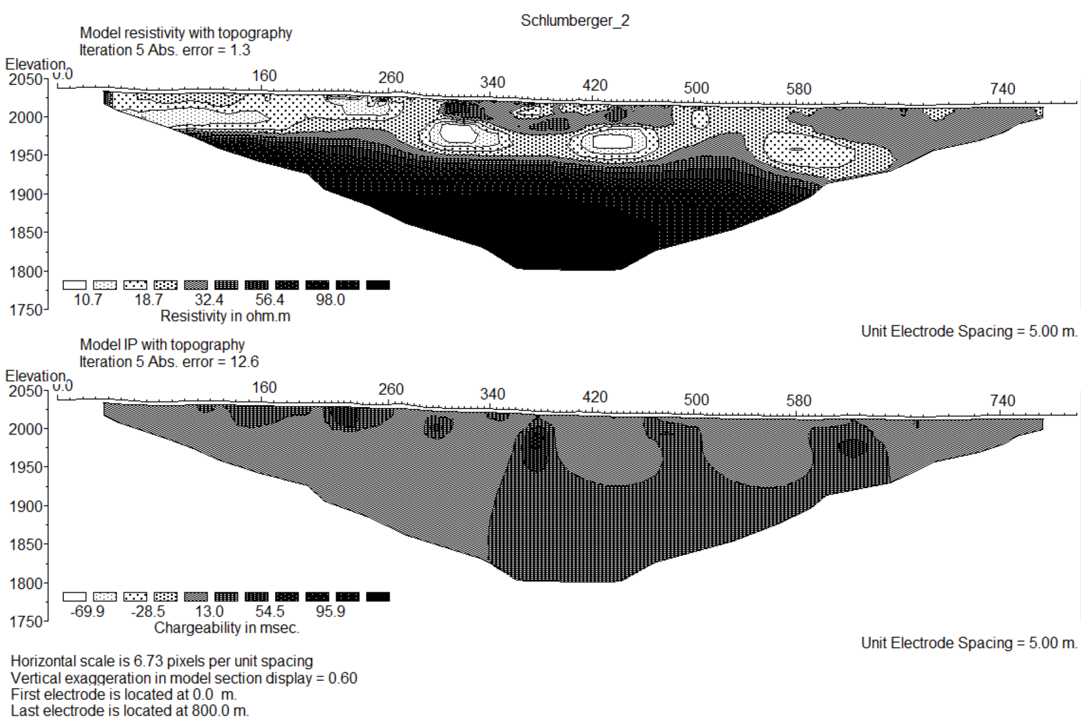

ARREGLO: SCHLUMBERGER

CABLES: 4X21

TIEMPO DE IP: 1.5 SEGUNDOS

VENTANAS IP: 10

INTERVALOS IP

VENTANA	TIEMPO EN MS
1	0.02
2	0.04
3	0.06
4	0.08
5	0.1
6	0.14
7	0.18
8	0.24
9	0.26
10	0.38
Tiempo total	1.5 MS

```
Reading file D:\Oficina\Clientes Geofisica\Tarija OB\Inversion\Tierra Linda\Schlumberger\Sch 1.5\L1-TIERRA-LINDA-SCHLUMBERGER-15TF1edit.INV

Schlumberger_2
Minimum electrode spacing is    5.0.
General array
Wenner-Schlumberger array arrangement
Total number of data points is 699.
IP values given in terms of chargeability
Half-size model blocks used for general array data set.
Model with half the unit electrode spacing is used
Number of electrodes is 119
Number of data levels is 25.
Topography present 2.
Minimum electrode location is    0.0.
Maximum electrode location is  800.0.
Minimum electrode spacing is    5.0.
Reading inversion results.
The model has 14 layers and 1264 blocks.
Iteration  1 : Abs. error   5.70   19.61.
Iteration  2 : Abs. error   2.69   13.03.
Iteration  3 : Abs. error   1.77   12.94.
Iteration  4 : Abs. error   1.38   12.88.
Iteration  5 : Abs. error   1.19   12.84.

Topographical data present in inversion file.
Schwartz-Christoffel transformation topography modelling was used.
Blocks sensitivity information present.
Average sensitivity is 1.308.
Inversion constraints information present.
Reading of file has been completed.
```

ITERACIÓN 1

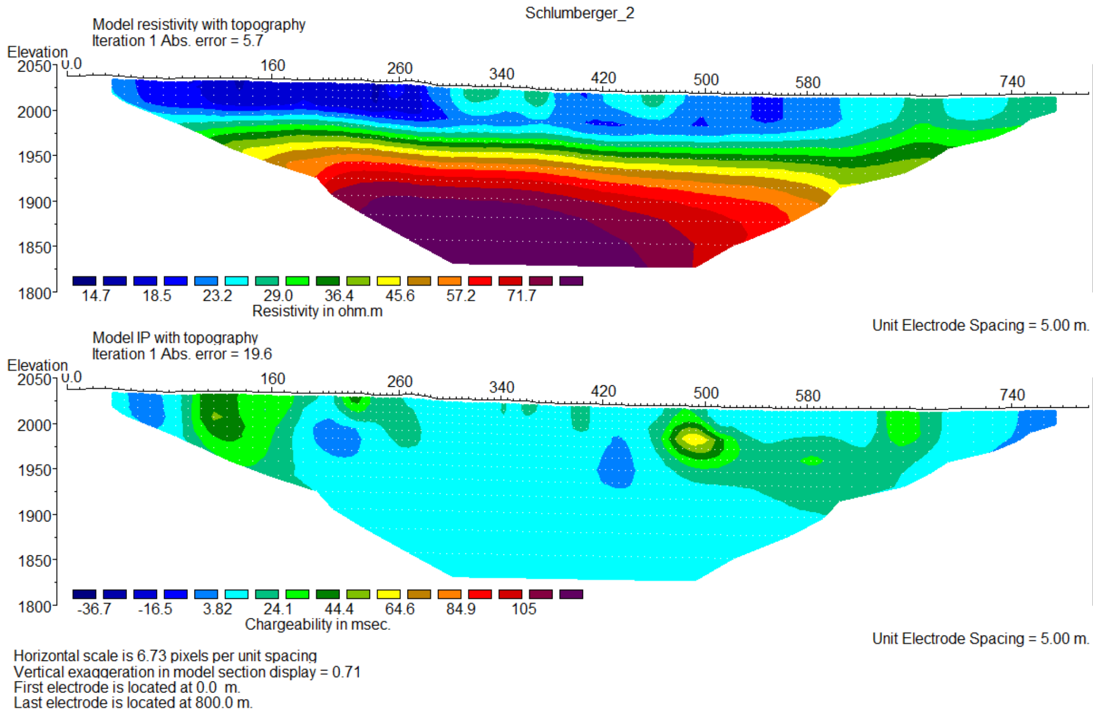

ITERACIÓN 3

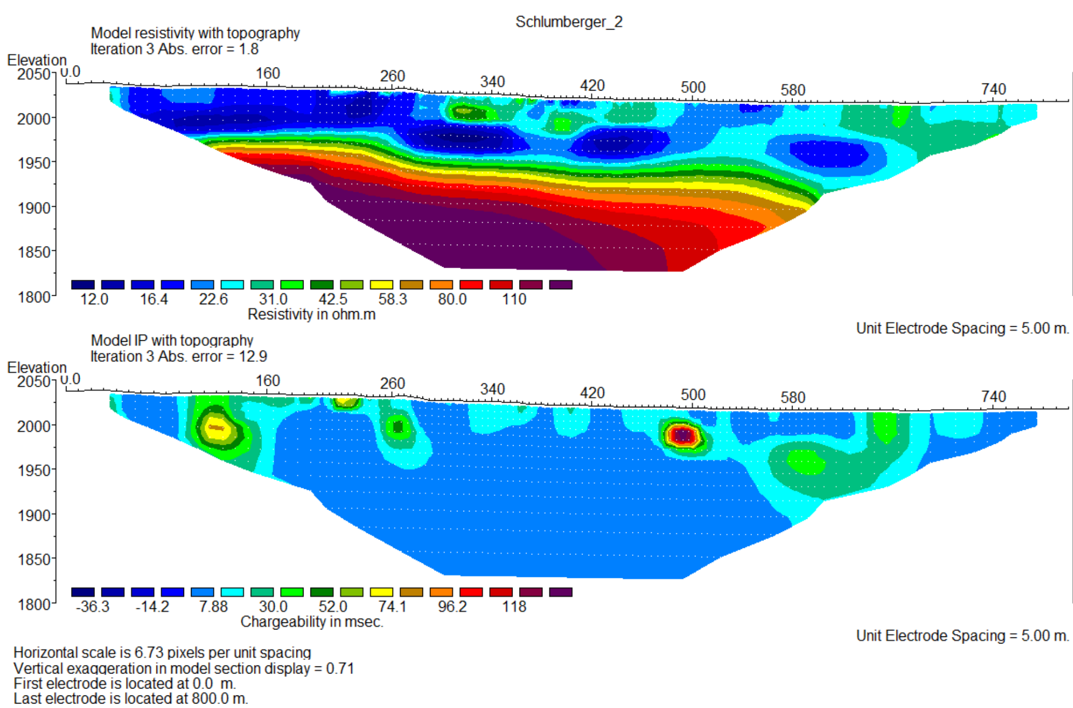

ITERACIÓN 5

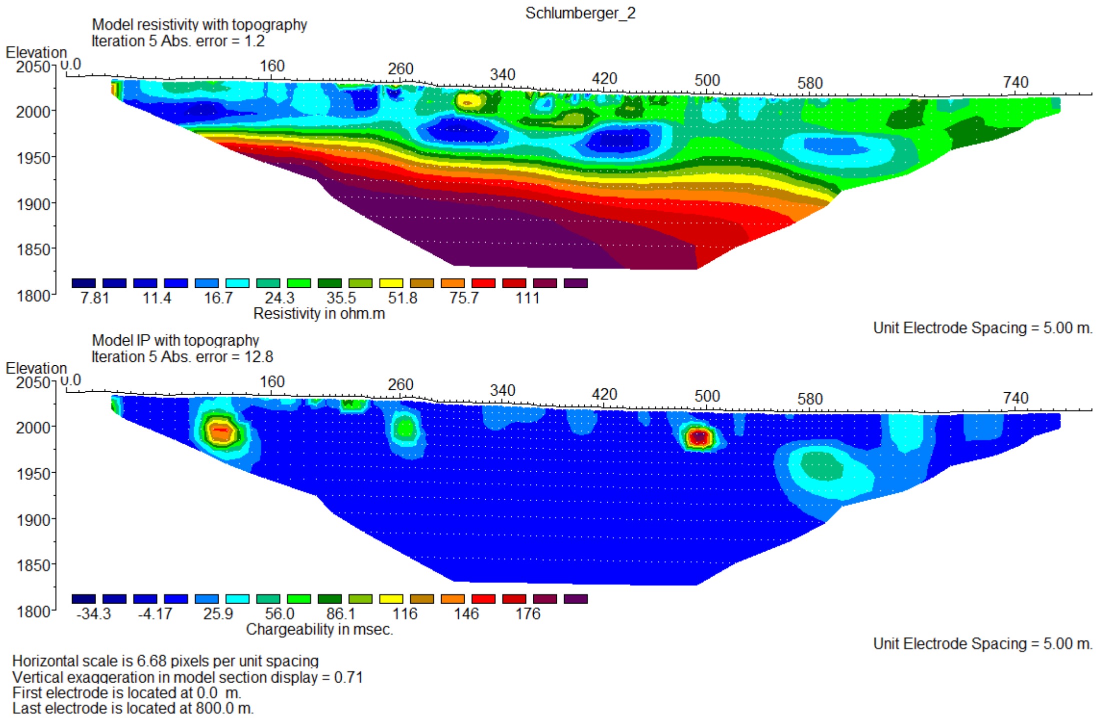

ITERACIÓN 5 – BLANCO Y NEGRO

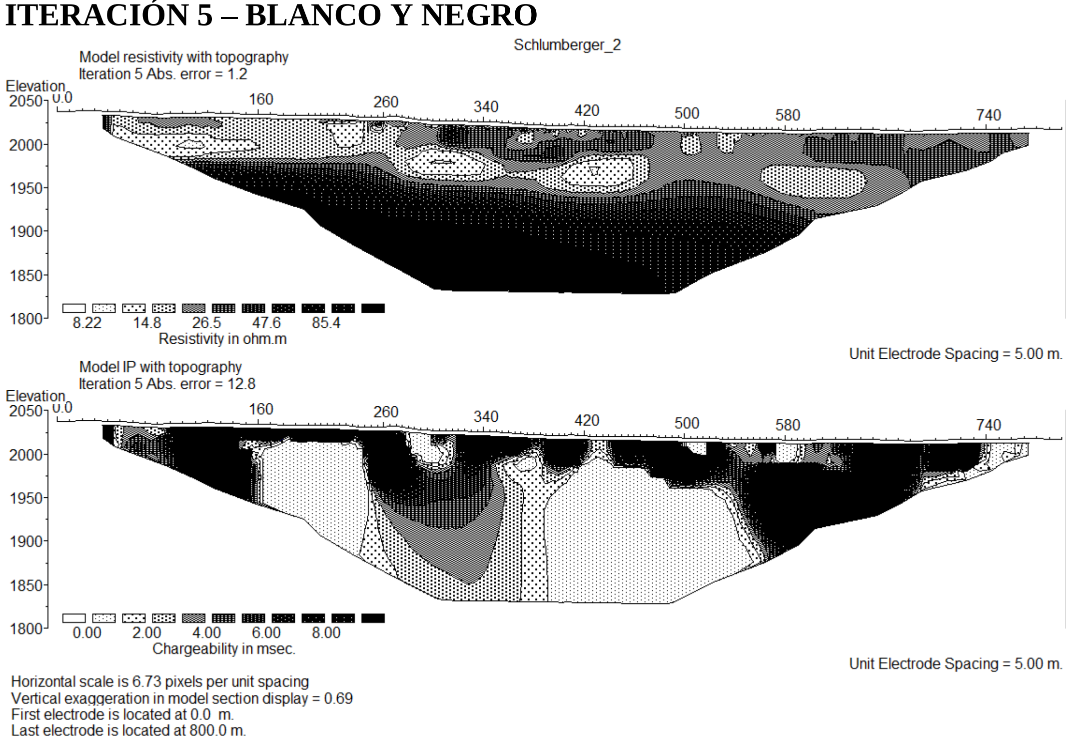

ARREGLO: GRADIENTE

CABLES: 4X21

TIEMPO DE IP: 0.5 SEGUNDOS

VENTANAS IP: 6

INTERVALOS IP

VENTANA	TIEMPO EN MS
1	0.02
2	0.04
3	0.06
4	0.08
5	0.12
6	0.18
Tiempo total	0.5 MS

```
Reading file D:\Oficina\Clientes Geofisica\Tarija OB\Inversion\Tierra Linda\Gradiente\Grad 0.5\L1-TIERRA-LINDA-GRADIENTE-05TF1edit.INV

Gradient8_1
Minimum electrode spacing is    5.0.
General array
Gradient array
Total number of data points is 682.
IP values given in terms of chargeability
Half-size model blocks used for general array data set.
Model with half the unit electrode spacing is used
Number of electrodes is 119
Number of data levels is 16.
Topography present 2.
Minimum electrode location is    0.0.
Maximum electrode location is  800.0.
Minimum electrode spacing is    5.0.
Reading inversion results.
The model has 13 layers and 1213 blocks.
Iteration  1 : Abs. error   7.48   13.16.
Iteration  2 : Abs. error   3.66    9.30.
Iteration  3 : Abs. error   2.65    9.19.
Iteration  4 : Abs. error   1.72    9.11.
Iteration  5 : Abs. error   1.41    9.06.

Topographical data present in inversion file.
Schwartz-Christoffel transformation topography modelling was used.
Blocks sensitivity information present.
Average sensitivity is 1.268.
Inversion constraints information present.
Reading of file has been completed.
```

ITERACIÓN 1

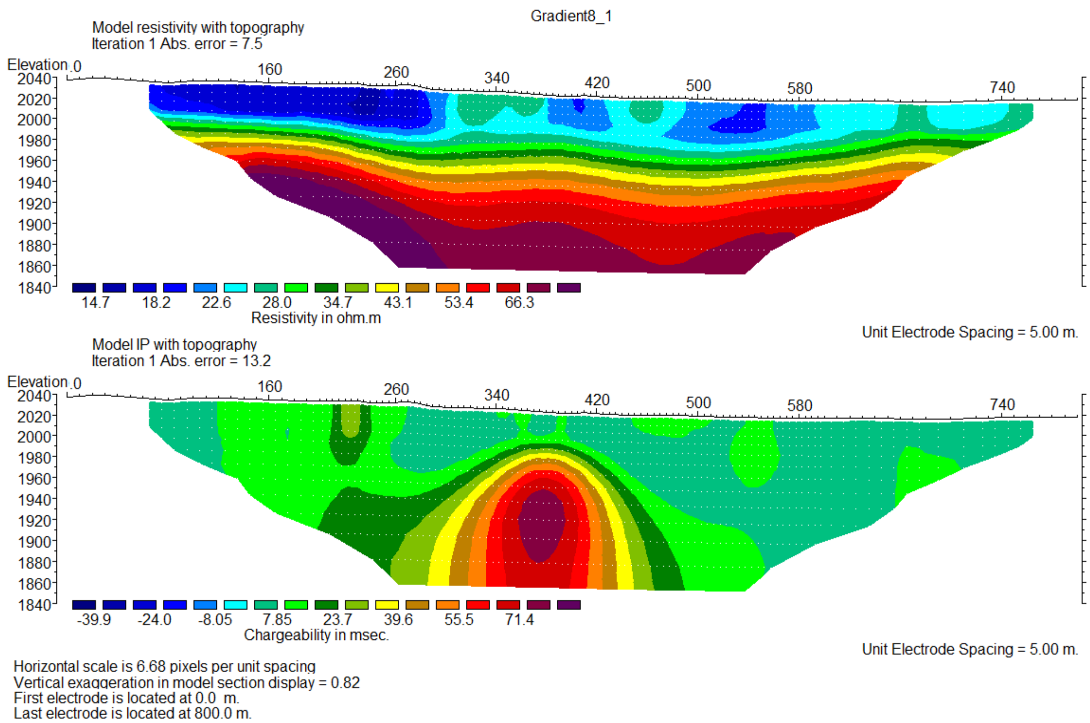

ITERACIÓN 3

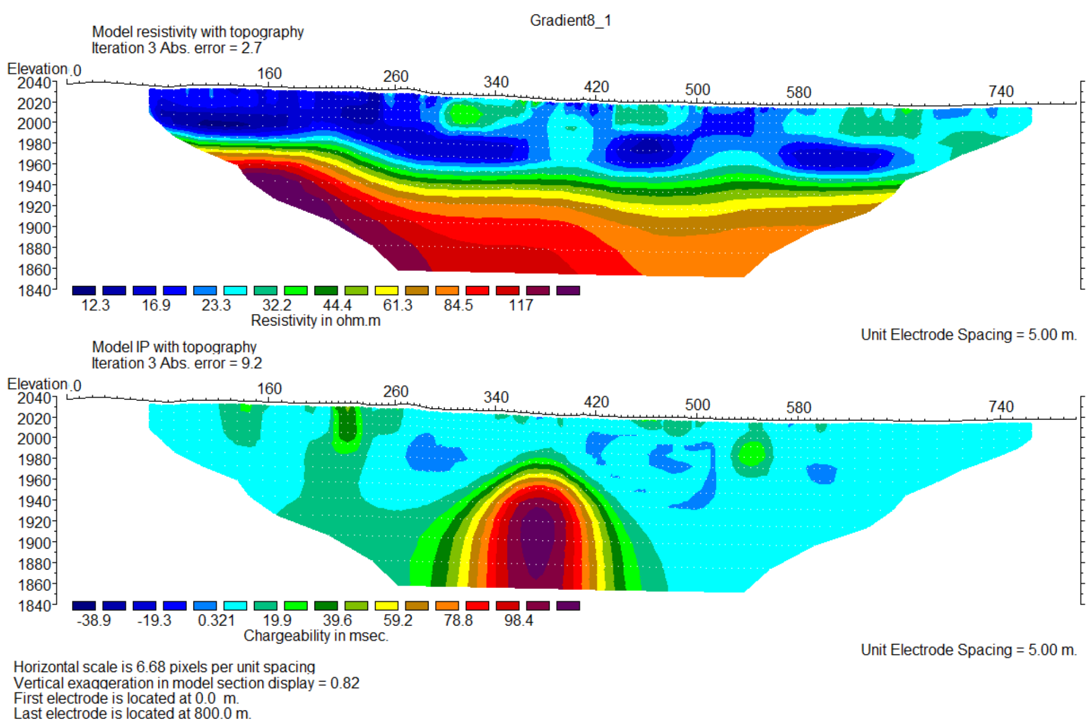

ITERACIÓN 5

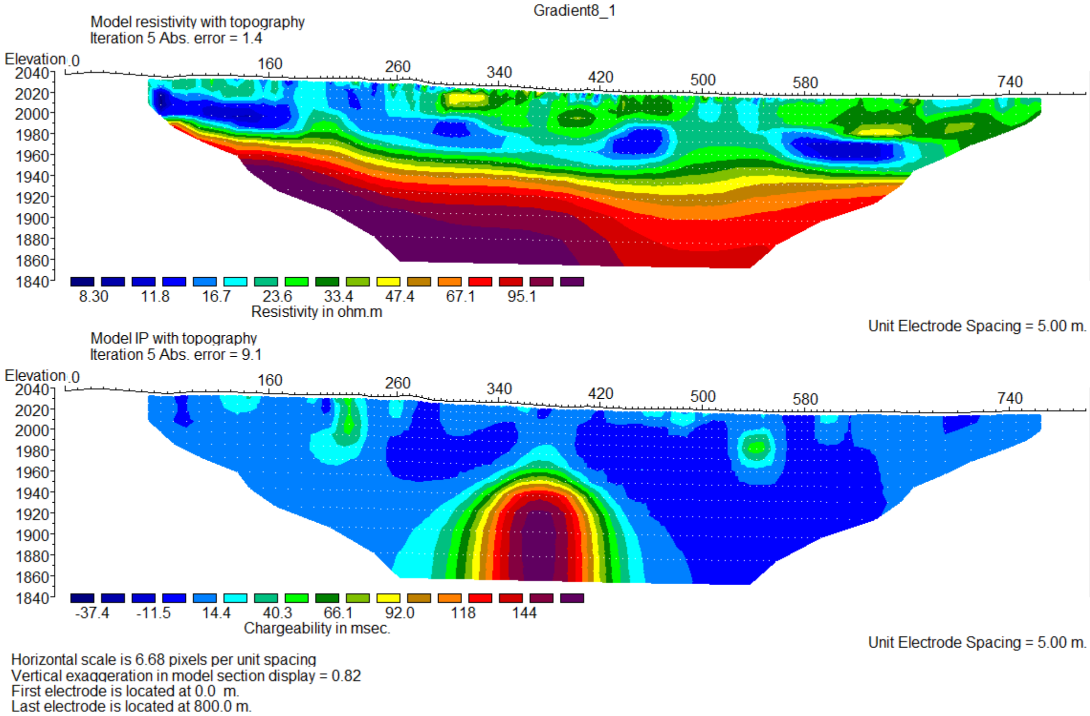

ITERACIÓN 5 – BLANCO Y NEGRO

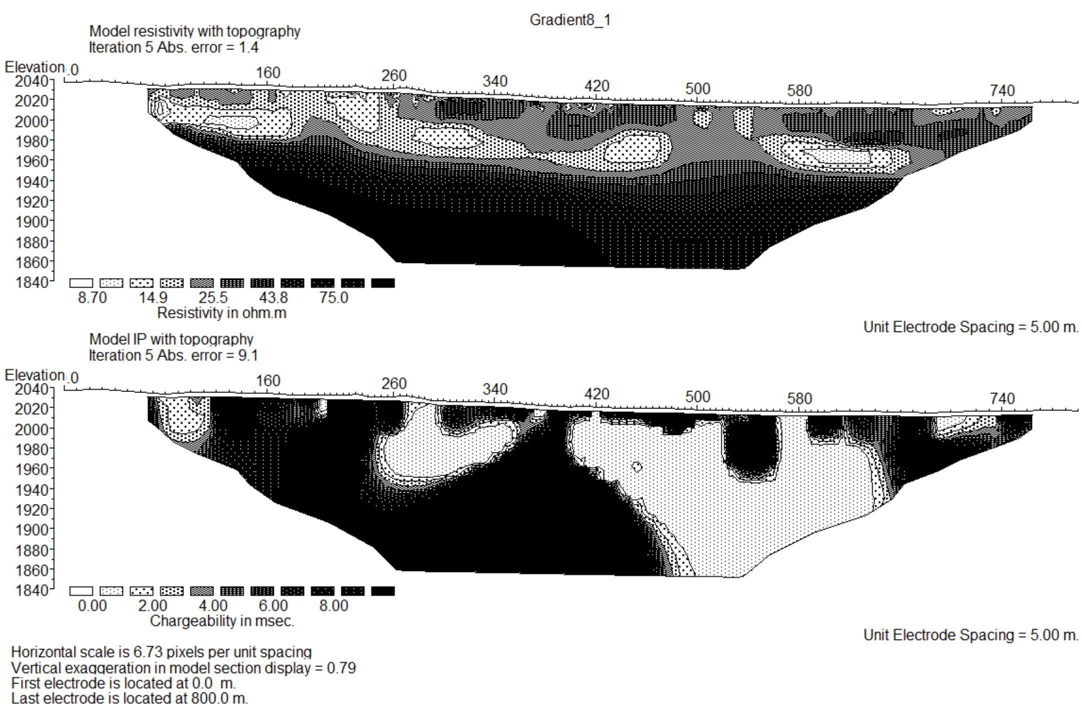

ARREGLO: GRADIENTE

CABLES: 4X21

TIEMPO DE IP: 1.0 SEGUNDO

VENTANAS IP: 8

INTERVALOS IP

VENTANA	TIEMPO EN MS
1	0.02
2	0.04
3	0.06
4	0.08
5	0.12
6	0.16
7	0.22
8	0.3
Tiempo total	1.0 MS

```
Reading file D:\Oficina\Clientes Geofisica\Tarija OB\Inversion\Tierra Linda\Gradiente\Grad 1\L1-TIERRA-LINDA-GRADIENTE-1TF1edit.INV

Gradient8_2
Minimum electrode spacing is    5.0.
General array
Gradient array
Total number of data points is 678.
IP values given in terms of chargeability
Half-size model blocks used for general array data set.
Model with half the unit electrode spacing is used
Number of electrodes is 119
Number of data levels is 16.
Topography present 2.
Minimum electrode location is    0.0.
Maximum electrode location is  800.0.
Minimum electrode spacing is    5.0.
Reading inversion results.
The model has 13 layers and 1213 blocks.
Iteration  1 : Abs. error   7.60   15.04.
Iteration  2 : Abs. error   3.73   11.28.
Iteration  3 : Abs. error   2.66   11.13.
Iteration  4 : Abs. error   1.84   11.01.
Iteration  5 : Abs. error   1.48   10.96.

Topographical data present in inversion file.
Schwartz-Christoffel transformation topography modelling was used.
Blocks sensitivity information present.
Average sensitivity is 1.260.
Inversion constraints information present.
Reading of file has been completed.
```

ITERACIÓN 1

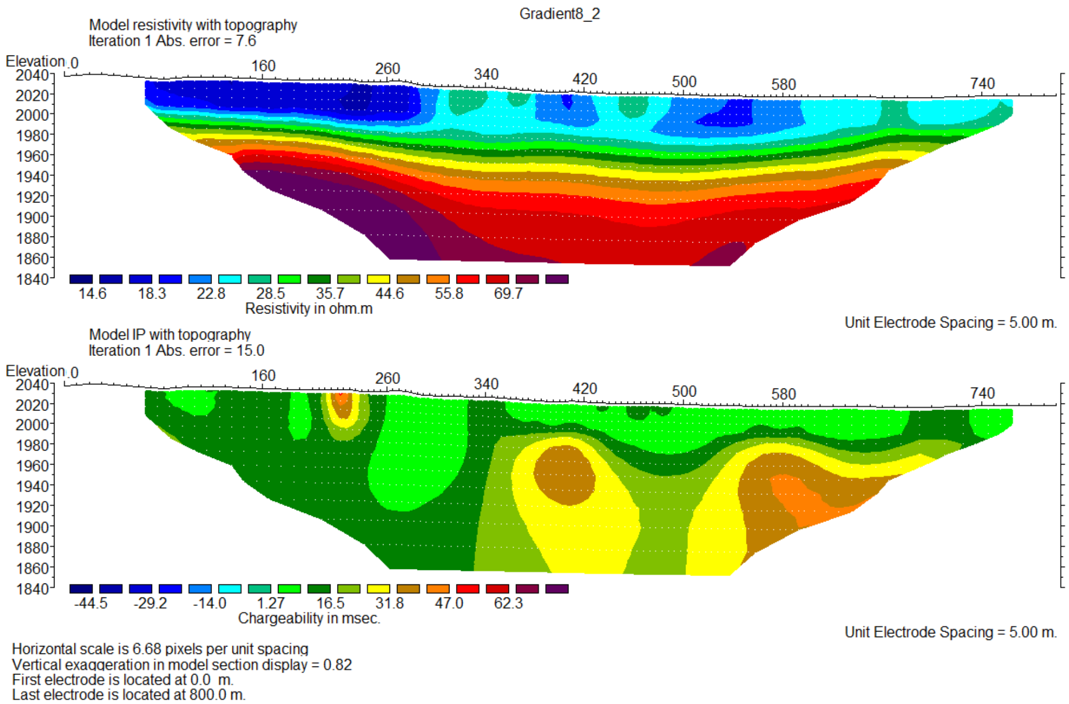

ITERACIÓN 3

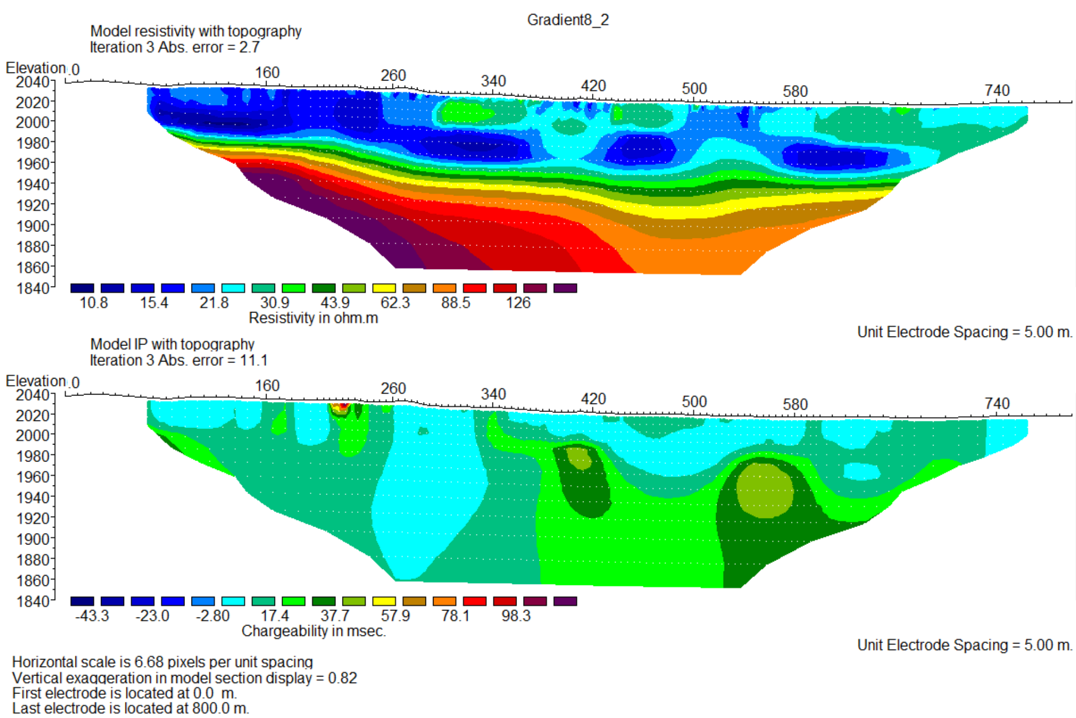

ITERACIÓN 5

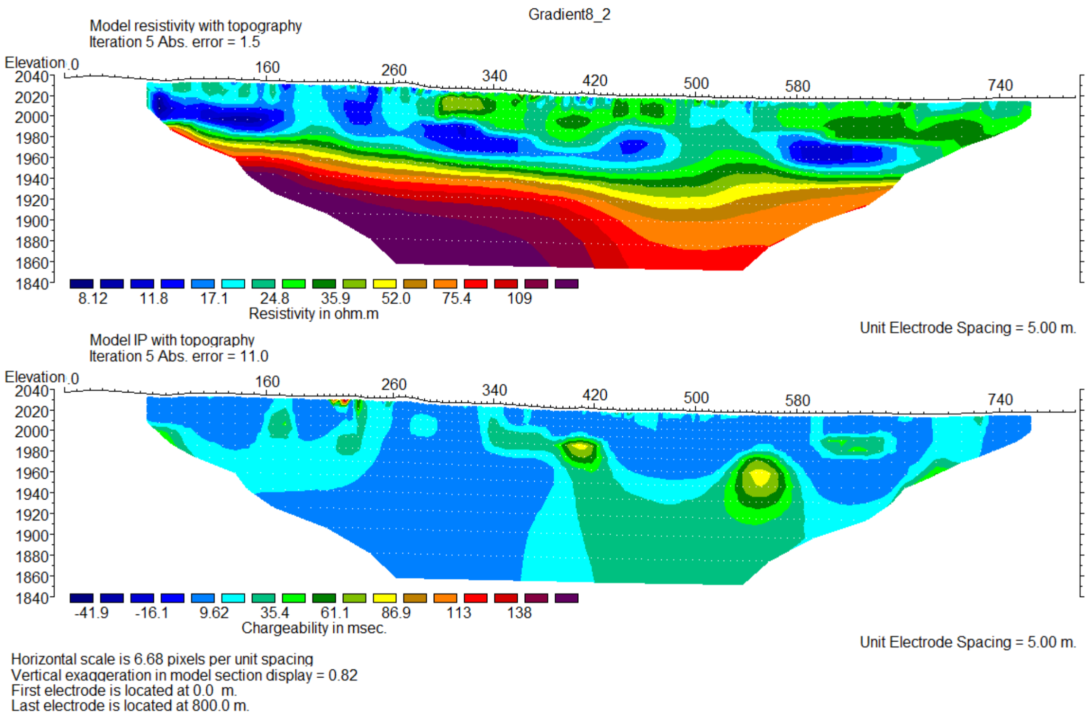

ITERACIÓN 5 – BLANCO Y NEGRO

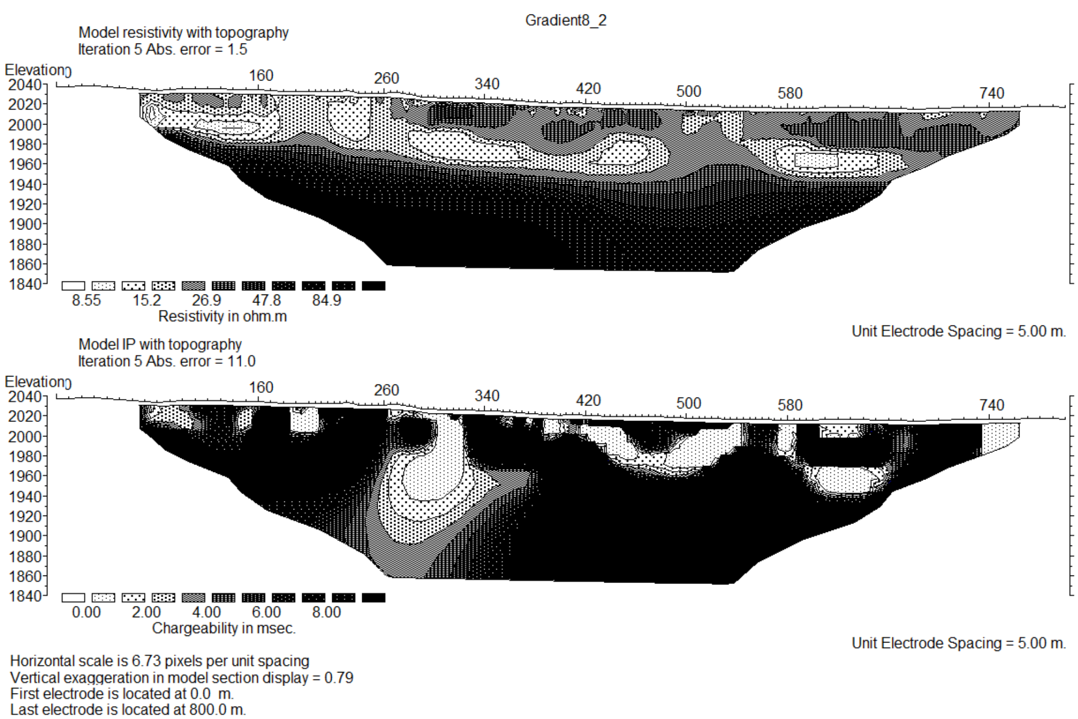

ARREGLO: GRADIENTE

CABLES: 4X21

TIEMPO DE IP: 1.5 SEGUNDOS

VENTANAS IP: 10

INTERVALOS IP

VENTANA	TIEMPO EN MS
1	0.02
2	0.04
3	0.06
4	0.08
5	0.1
6	0.14
7	0.18
8	0.24
9	0.26
10	0.38
Tiempo total	1.5 MS

```
Reading file D:\Oficina\Clientes Geofisica\Tarija OB\Inversion\Tierra Linda\Gradiente\Grad 1.5\L1-TIERRA-LINDA-GRADIENTE-15TF1edit.INV

Gradient8_1
Minimum electrode spacing is    5.0.
General array
Gradient array
Total number of data points is 668.
IP values given in terms of chargeability
Half-size model blocks used for general array data set.
Model with half the unit electrode spacing is used
Number of electrodes is 119
Number of data levels is 16.
Topography present 2.
Minimum electrode location is    0.0.
Maximum electrode location is  800.0.
Minimum electrode spacing is    5.0.
Reading inversion results.
The model has 13 layers and 1208 blocks.
Iteration  1 : Abs. error   7.41   12.55.
Iteration  2 : Abs. error   3.61    9.28.
Iteration  3 : Abs. error   2.59    9.16.
Iteration  4 : Abs. error   1.70    9.05.
Iteration  5 : Abs. error   1.36    9.04.

Topographical data present in inversion file.
Schwartz-Christoffel transformation topography modelling was used.
Blocks sensitivity information present.
Average sensitivity is 1.249.
Inversion constraints information present.
Reading of file has been completed.
```

ITERACIÓN 1

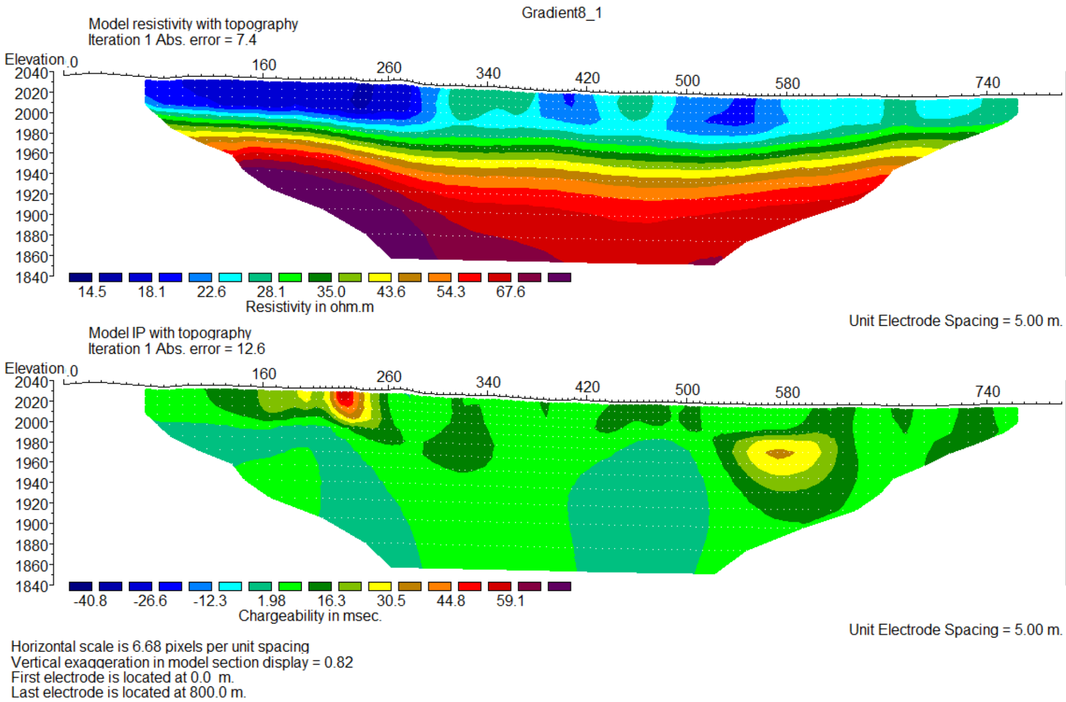

ITERACIÓN 3

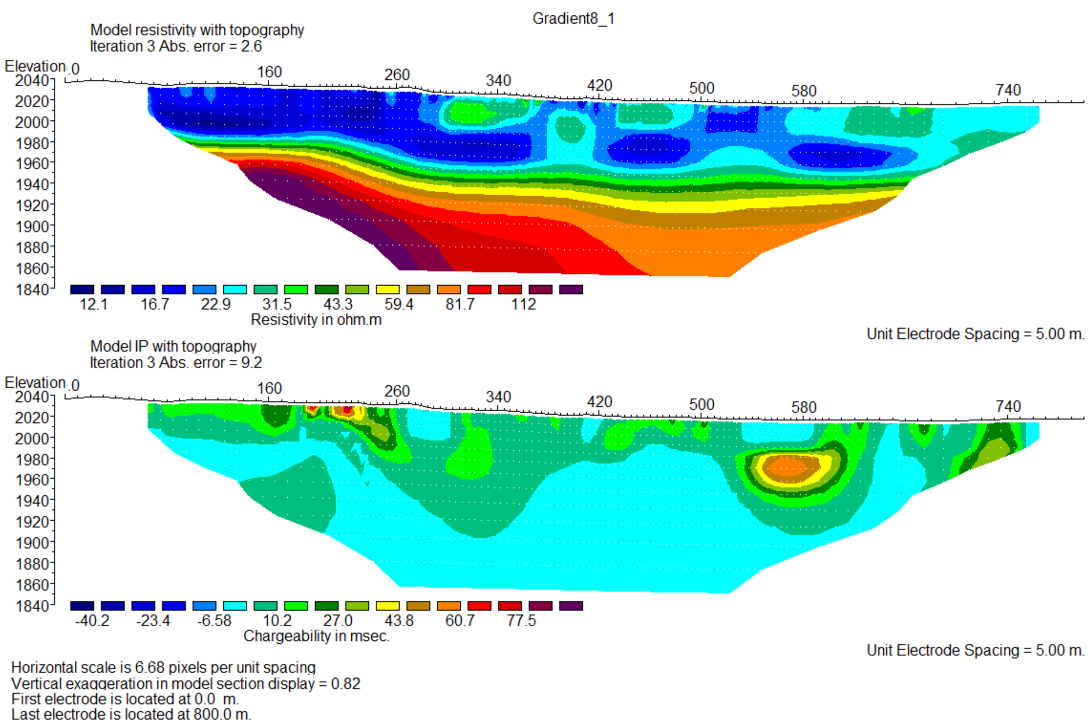

ITERACIÓN 5

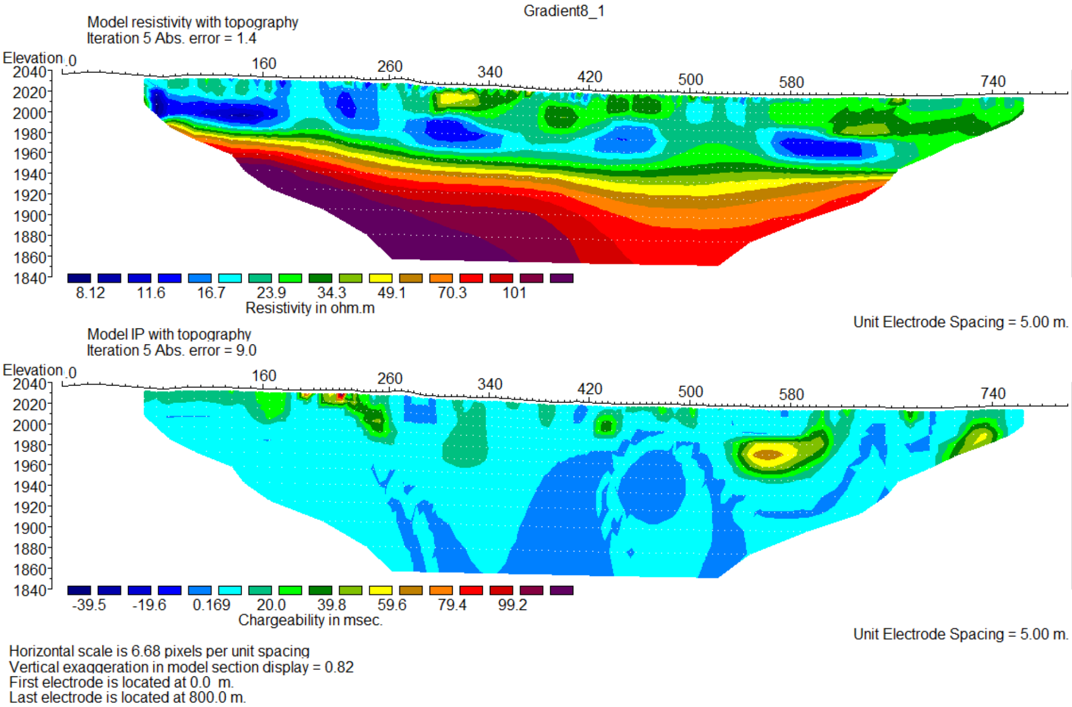

ITERACIÓN 5 BLANCO Y NEGRO

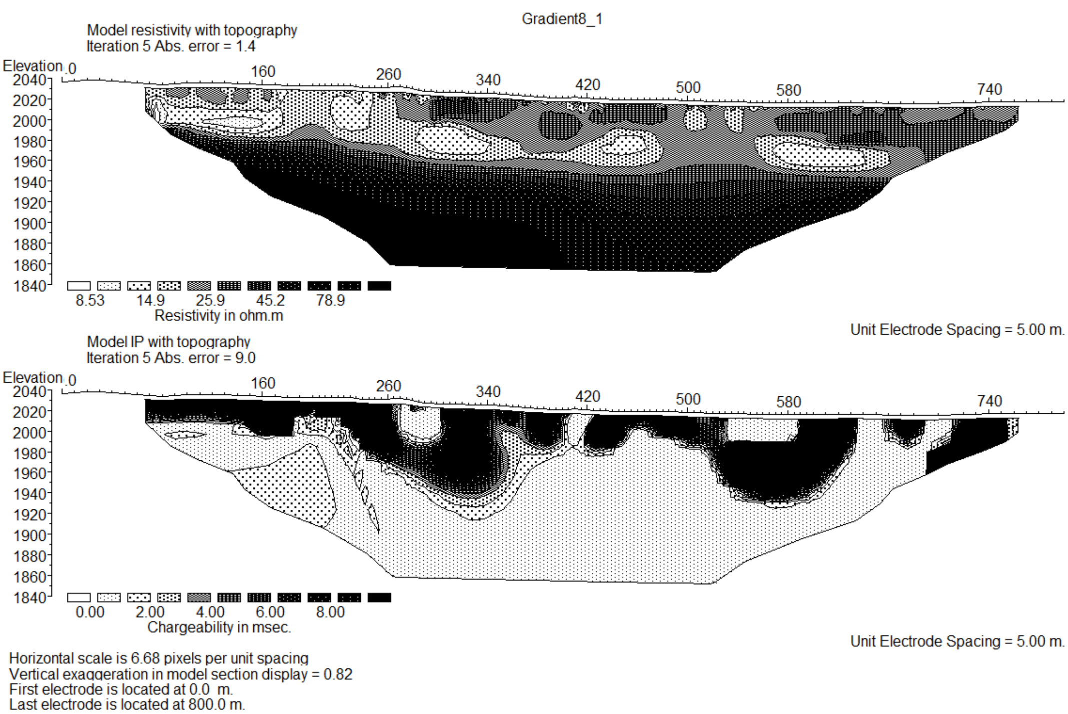

ANEXO 5b

FRAY QUEBRACHO

De acuerdo al proceso de datos tenemos lo siguiente:

ARREGLO: SCHLUMBERGER

CABLES: 4X21

TIEMPO DE IP: 0.5 SEGUNDOS

VENTANAS IP: 6

INTERVALOS IP

VENTANA	TIEMPO EN MS
1	0.02
2	0.04
3	0.06
4	0.08
5	0.12
6	0.18
Tiempo total	0.5 MS

```
Reading file D:\Oficina\Clientes Geofisica\Tarija OB\Inversion\Fray Quebracho\Schlumberger\Sch 0.5\L1-FRAY-QUEBRACHO-SCH-05-TF1edit.INV

Schlumberger_1
Minimum electrode spacing is    5.0.
General array
Wenner-Schlumberger array arrangement
Total number of data points is 683.
IP values given in terms of chargeability
Half-size model blocks used for general array data set.
Model with half the unit electrode spacing is used
Number of electrodes is 119
Number of data levels is 26.
Topography present 2.
Minimum electrode location is    0.0.
Maximum electrode location is  800.0.
Minimum electrode spacing is    5.0.
Reading inversion results.
The model has 15 layers and 1301 blocks.
Iteration  1 : Abs. error   6.76   24.21.
Iteration  2 : Abs. error   3.42   15.06.
Iteration  3 : Abs. error   2.64   14.97.
Iteration  4 : Abs. error   2.02   14.95.
Iteration  5 : Abs. error   1.75   14.95.

Topographical data present in inversion file.
Schwartz-Christoffel transformation topography modelling was used.
Blocks sensitivity information present.
Average sensitivity is 1.245.
Inversion constraints information present.
Reading of file has been completed.
```

ITERACION 1

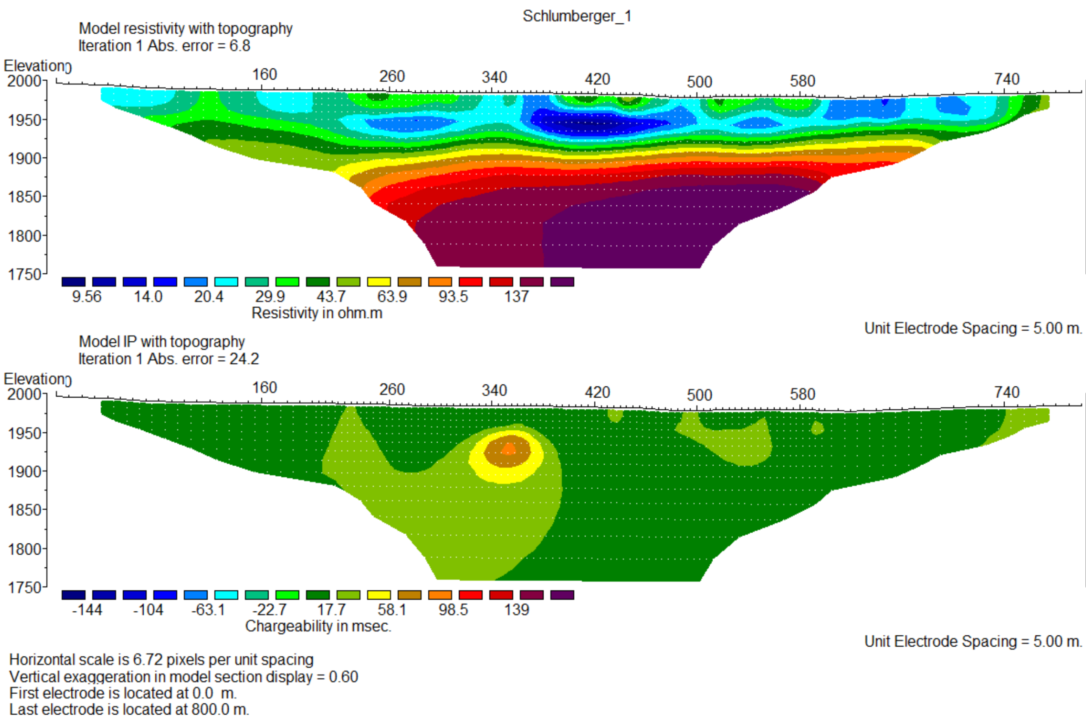

ITERACIÓN 3

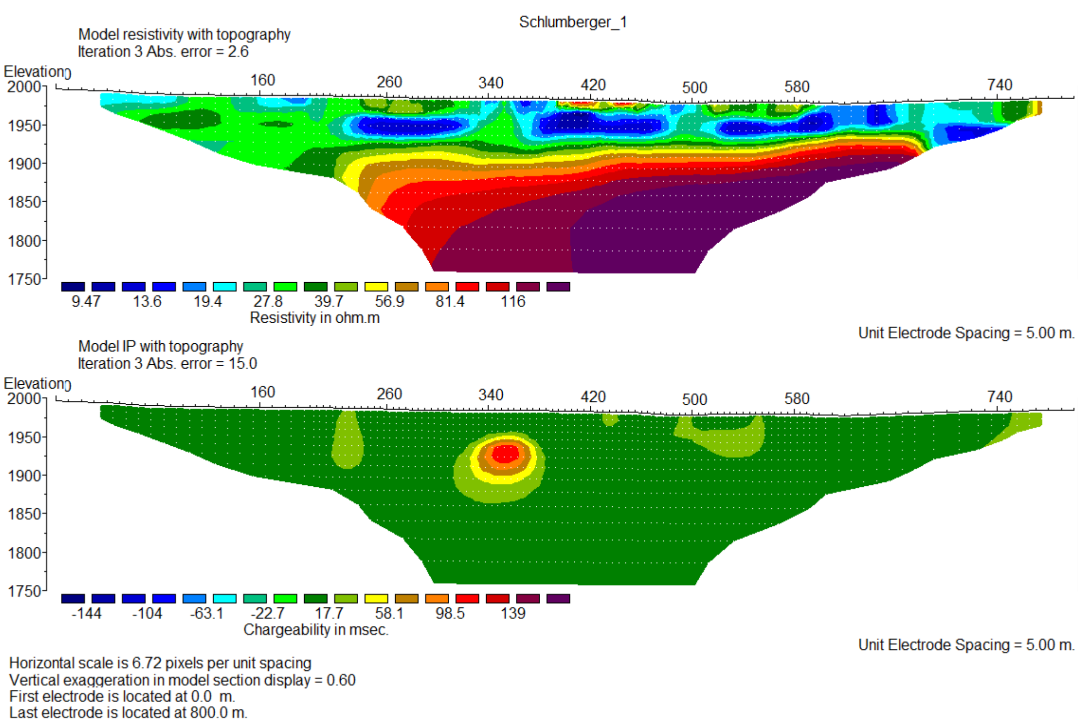

ITERACIÓN 5

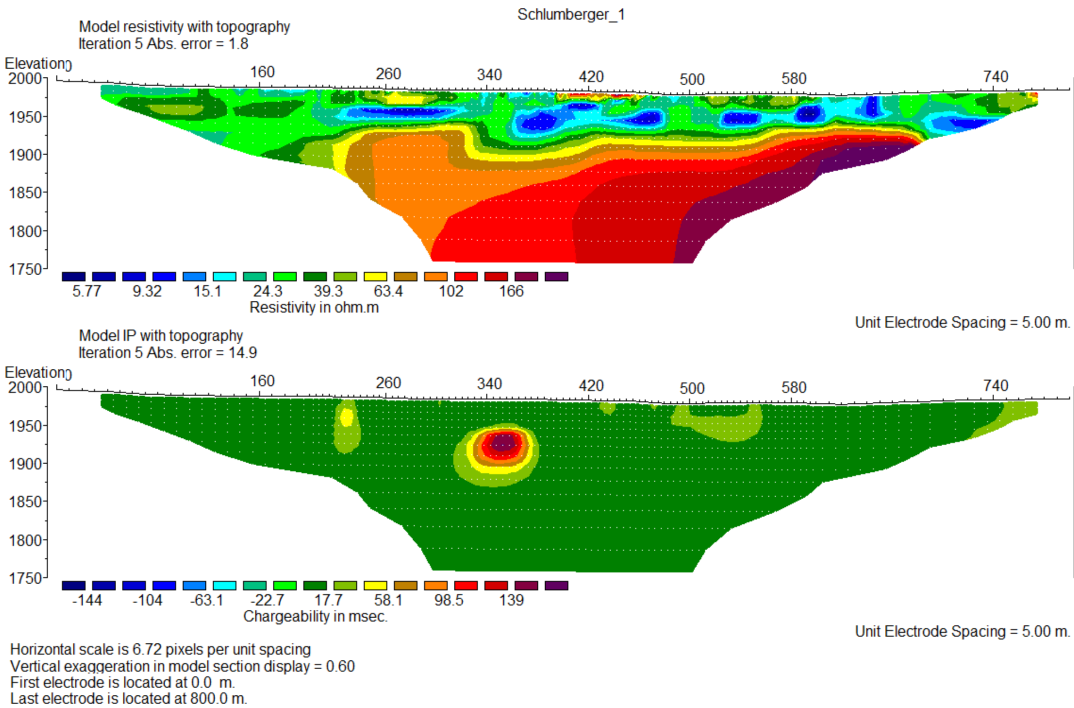

ITERACIÓN 5 – BLANCO Y NEGRO

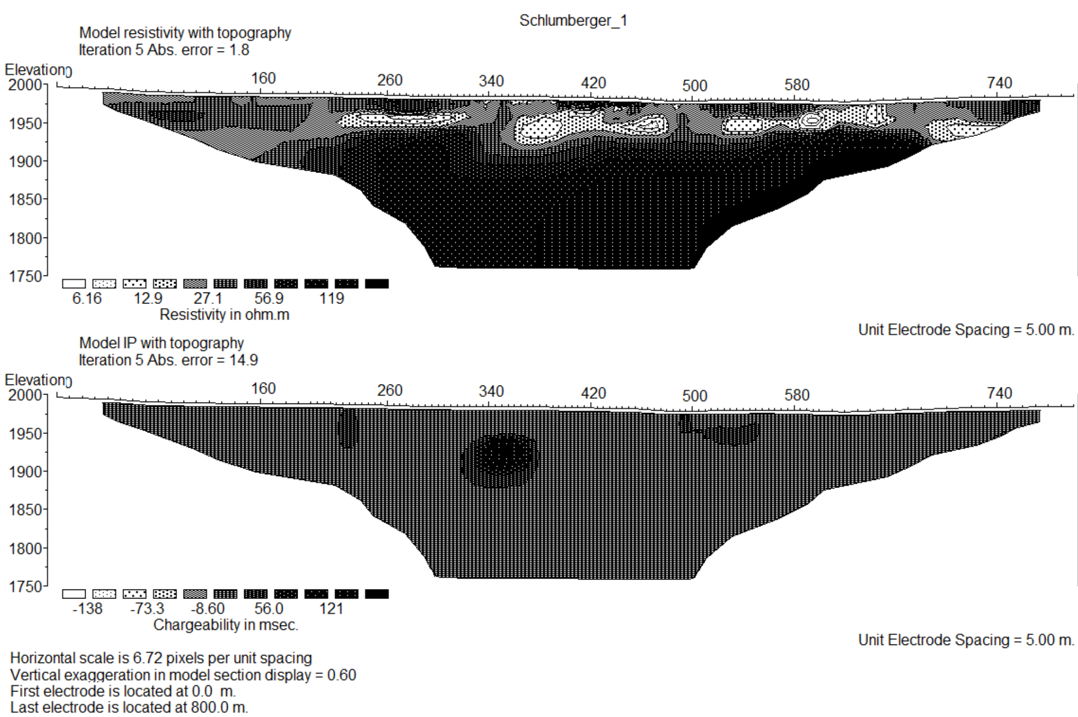

ARREGLO: SCHLUMBERGER

CABLES: 4X21

TIEMPO DE IP: 1.0 SEGUNDO

VENTANAS IP: 8

INTERVALOS IP

VENTANA	TIEMPO EN MS
1	0.02
2	0.04
3	0.06
4	0.08
5	0.12
6	0.16
7	0.22
8	0.3
Tiempo total	1.0 MS

```
Reading file D:\Oficina\Clientes Geofisica\Tarija OB\Inversion\Fray Quebracho\Schlumberger\Sch 1\L1-FRAY-QUEBRACHO-SCH-1-TF1edit.INV

Schlumberger_1
Minimum electrode spacing is    5.0.
General array
Wenner-Schlumberger array arrangement
Total number of data points is 695.
IP values given in terms of chargeability
Half-size model blocks used for general array data set.
Model with half the unit electrode spacing is used
Number of electrodes is 119
Number of data levels is 25.
Topography present 2.
Minimum electrode location is    0.0.
Maximum electrode location is  800.0.
Minimum electrode spacing is    5.0.
Reading inversion results.
The model has 14 layers and 1263 blocks.
Iteration  1 : Abs. error   6.93   23.55.
Iteration  2 : Abs. error   3.39   14.74.
Iteration  3 : Abs. error   2.63   14.58.
Iteration  4 : Abs. error   2.26   14.50.
Iteration  5 : Abs. error   1.81   14.44.

Topographical data present in inversion file.
Schwartz-Christoffel transformation topography modelling was used.
Blocks sensitivity information present.
Average sensitivity is 1.306.
Inversion constraints information present.
Reading of file has been completed.
```

ITERACIÓN 1

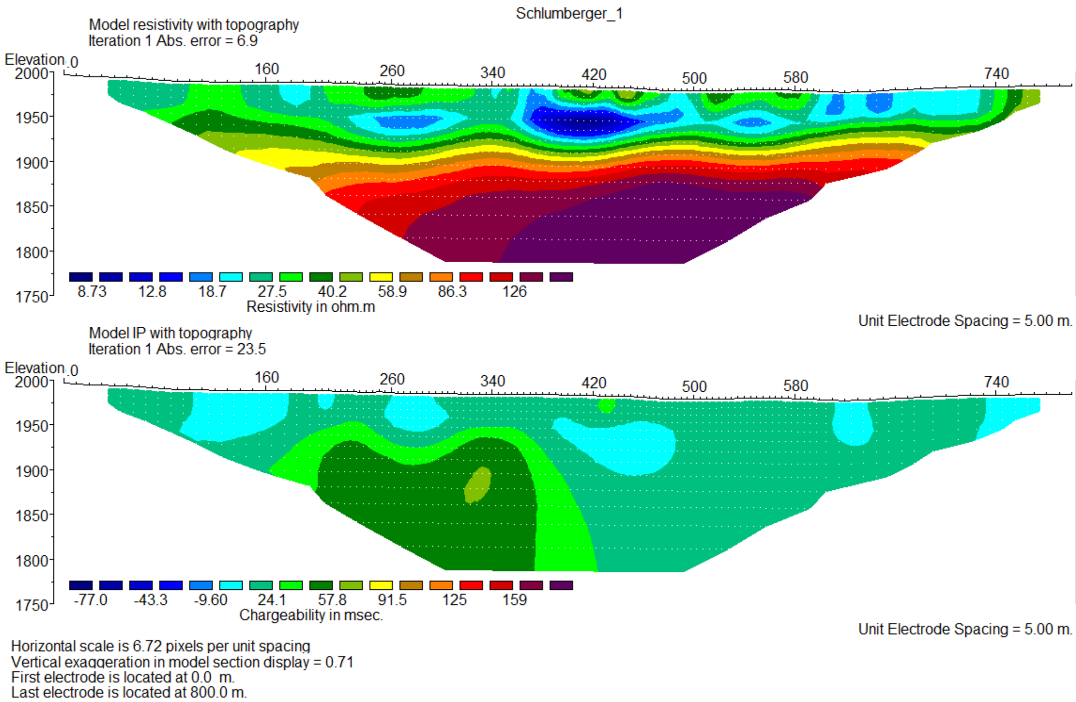

ITERACIÓN 3

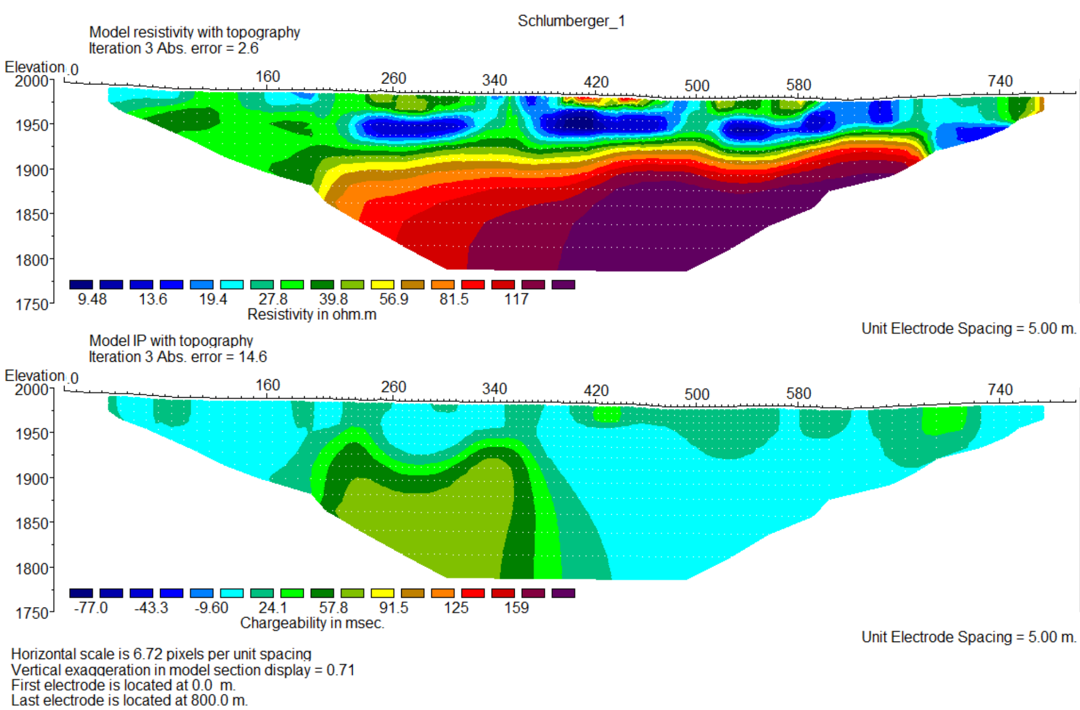

ITERACIÓN 5

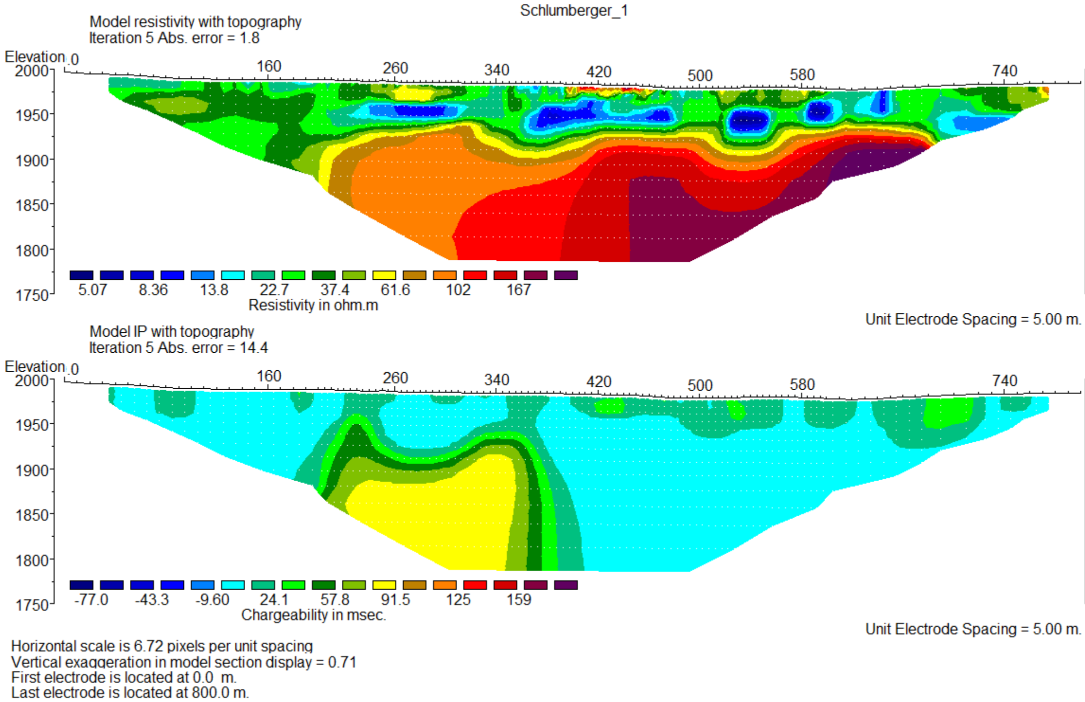

ITERACIÓN 5 BLANCO Y NEGRO

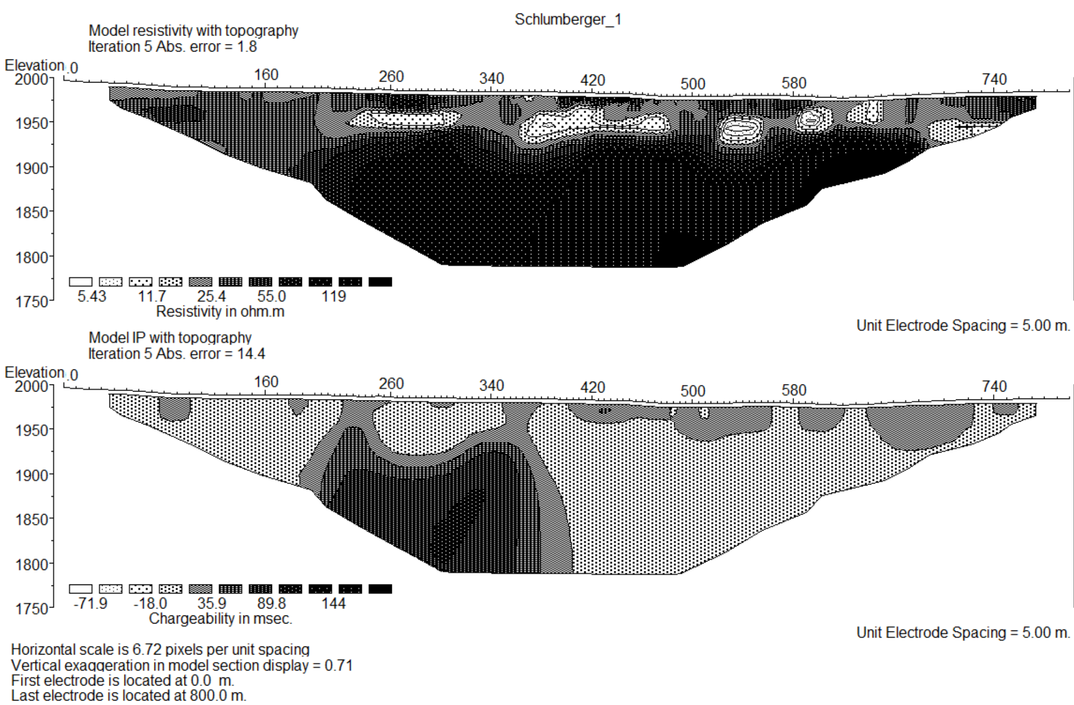

ARREGLO: SCHLUMBERGER

CABLES: 4X21

TIEMPO DE IP: 1.5 SEGUNDOS

VENTANAS IP: 10

INTERVALOS IP

VENTANA	TIEMPO EN MS
1	0.02
2	0.04
3	0.06
4	0.08
5	0.1
6	0.14
7	0.18
8	0.24
9	0.26
10	0.38
Tiempo total	1.5 MS

```
Reading file D:\Oficina\Clientes Geofisica\Tarija OB\Inversion\Fray Quebracho\Schlumberger\Sch 1.5\L1-FRAY-QUEBRACHO-SCH-15-TF1edit.INV

Schlumberger_1
Minimum electrode spacing is    5.0.
General array
Wenner-Schlumberger array arrangement
Total number of data points is 698.
IP values given in terms of chargeability
Half-size model blocks used for general array data set.
Model with half the unit electrode spacing is used
Number of electrodes is 119
Number of data levels is 26.
Topography present 2.
Minimum electrode location is    0.0.
Maximum electrode location is  800.0.
Minimum electrode spacing is    5.0.
Reading inversion results.
The model has 15 layers and 1314 blocks.
Iteration  1 : Abs. error   6.69   24.95.
Iteration  2 : Abs. error   3.56   15.25.
Iteration  3 : Abs. error   2.67   15.16.
Iteration  4 : Abs. error   2.25   15.12.
Iteration  5 : Abs. error   1.81   15.07.

Topographical data present in inversion file.
Schwartz-Christoffel transformation topography modelling was used.
Blocks sensitivity information present.
Average sensitivity is 1.260.
Inversion constraints information present.
Reading of file has been completed.
```

ITERACIÓN 1

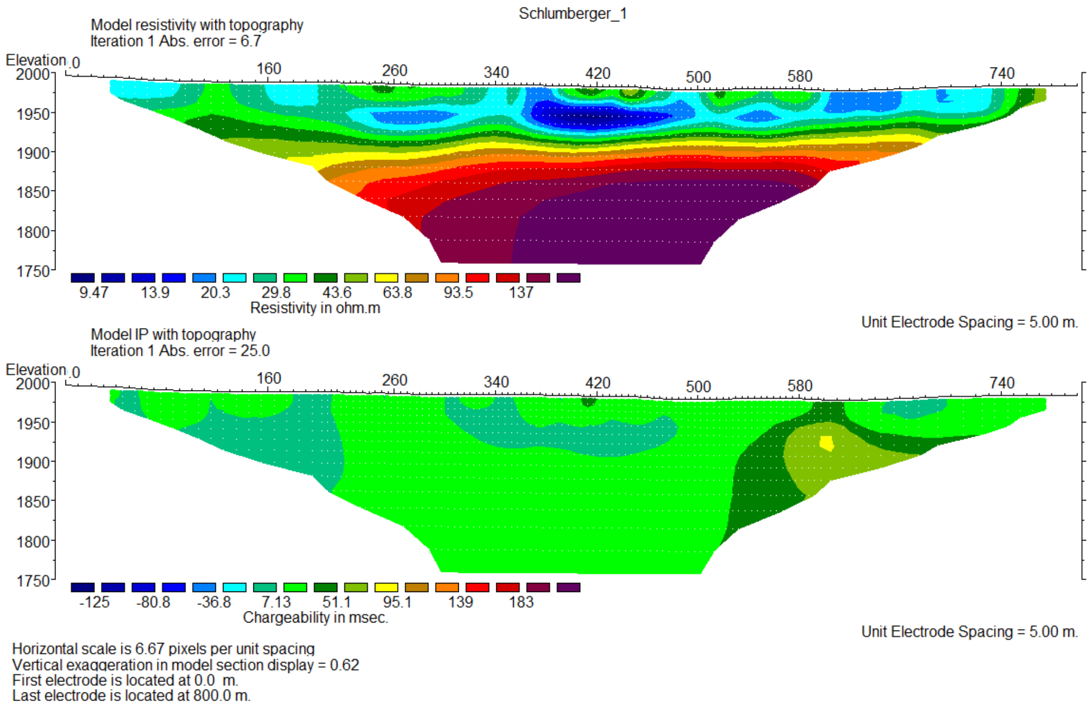

ITERACIÓN 3

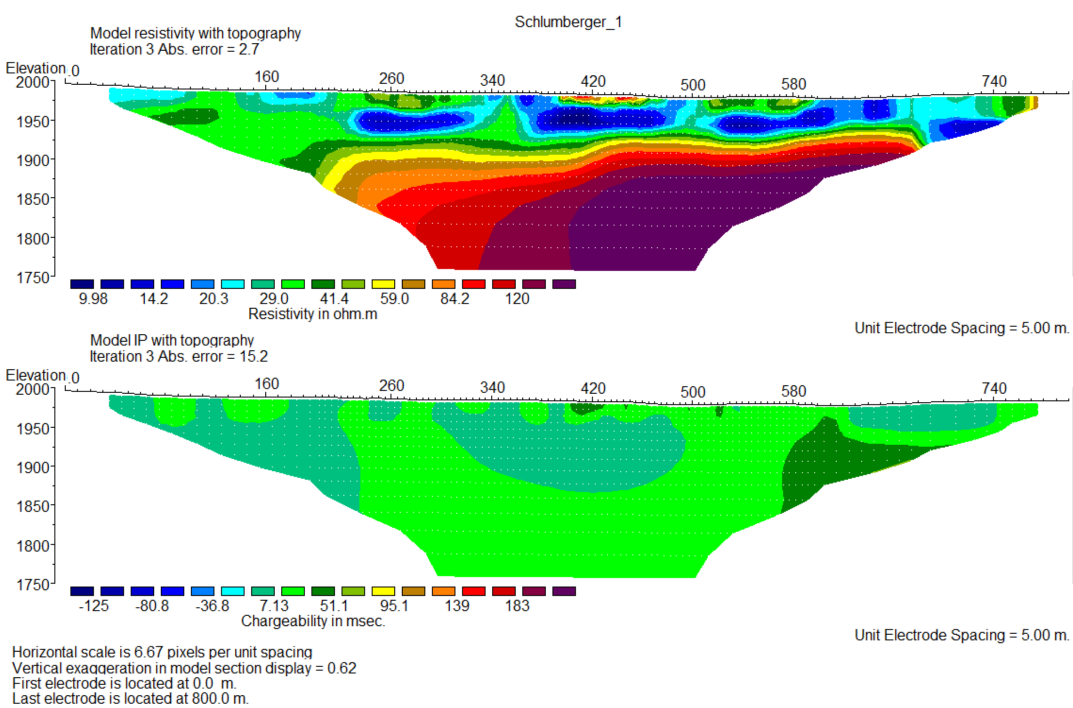

ITERACIÓN 5

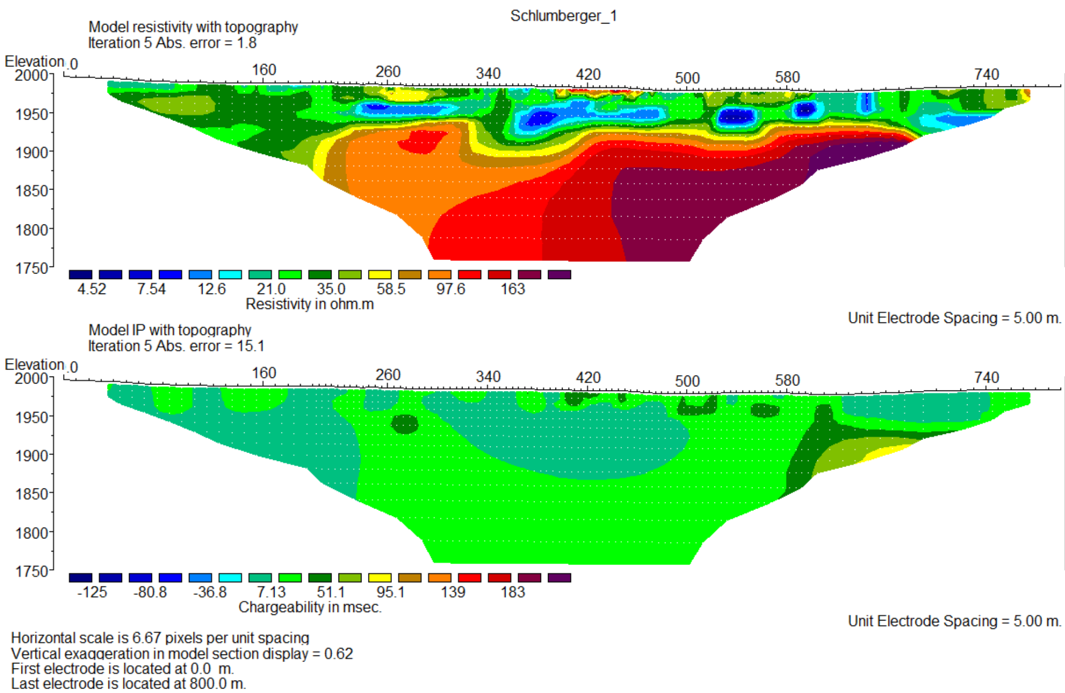

ITERACIÓN 5 – BLANCO Y NEGRO

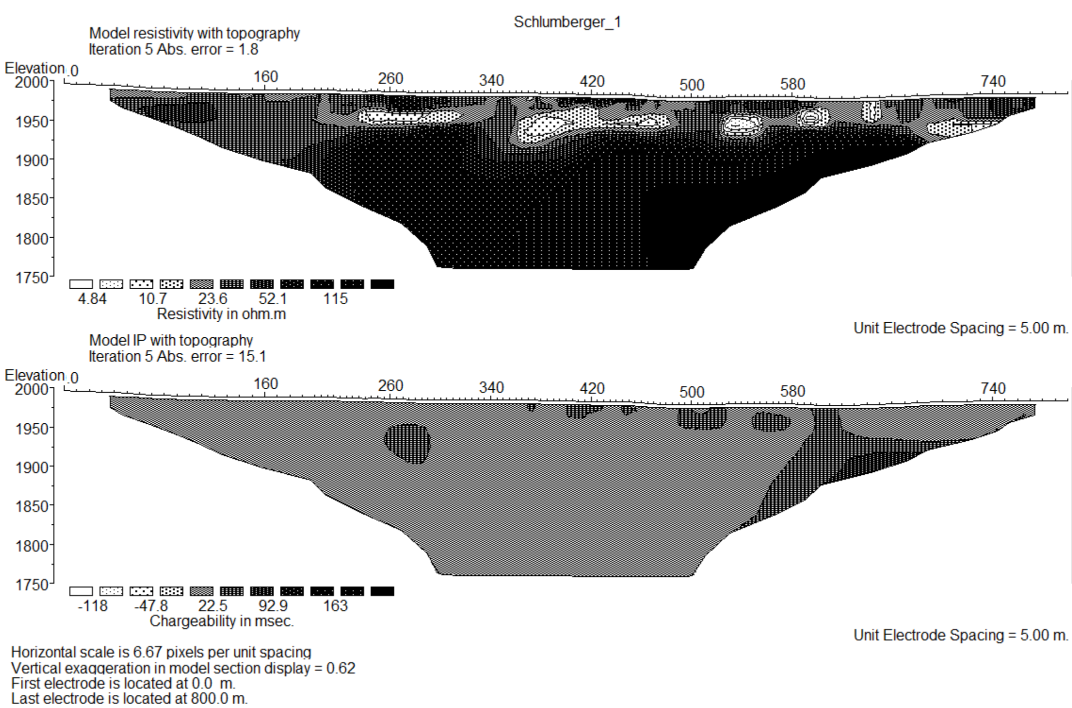

ARREGLO: GRADIENTE

CABLES: 4X21

TIEMPO DE IP: 0.5 SEGUNDOS

VENTANAS IP: 6

INTERVALOS IP

VENTANA	TIEMPO EN MS
1	0.02
2	0.04
3	0.06
4	0.08
5	0.12
6	0.18
Tiempo total	0.5 MS

```
Reading file D:\Oficina\Clientes Geofisica\Tarija OB\Inversion\Fray Quebracho\Gradiente\Grad 0.5\L1-FRAY-QUEBRACHO-GRAD-05-TF1edit.INV

Gradient8_1
Minimum electrode spacing is    5.0.
General array
Gradient array
Total number of data points is 688.
IP values given in terms of chargeability
Half-size model blocks used for general array data set.
Model with half the unit electrode spacing is used
Number of electrodes is 119
Number of data levels is 16.
Topography present 2.
Minimum electrode location is    0.0.
Maximum electrode location is  800.0.
Minimum electrode spacing is    5.0.
Reading inversion results.
The model has 13 layers and 1213 blocks.
Iteration  1 : Abs. error  10.03   17.89.
Iteration  2 : Abs. error   5.00   12.12.
Iteration  3 : Abs. error   2.90   11.99.
Iteration  4 : Abs. error   2.18   11.97.
Iteration  5 : Abs. error   1.85   11.94.

Topographical data present in inversion file.
Schwartz-Christoffel transformation topography modelling was used.
Blocks sensitivity information present.
Average sensitivity is 1.286.
Inversion constraints information present.
Reading of file has been completed.
```

ITERACIÓN 1

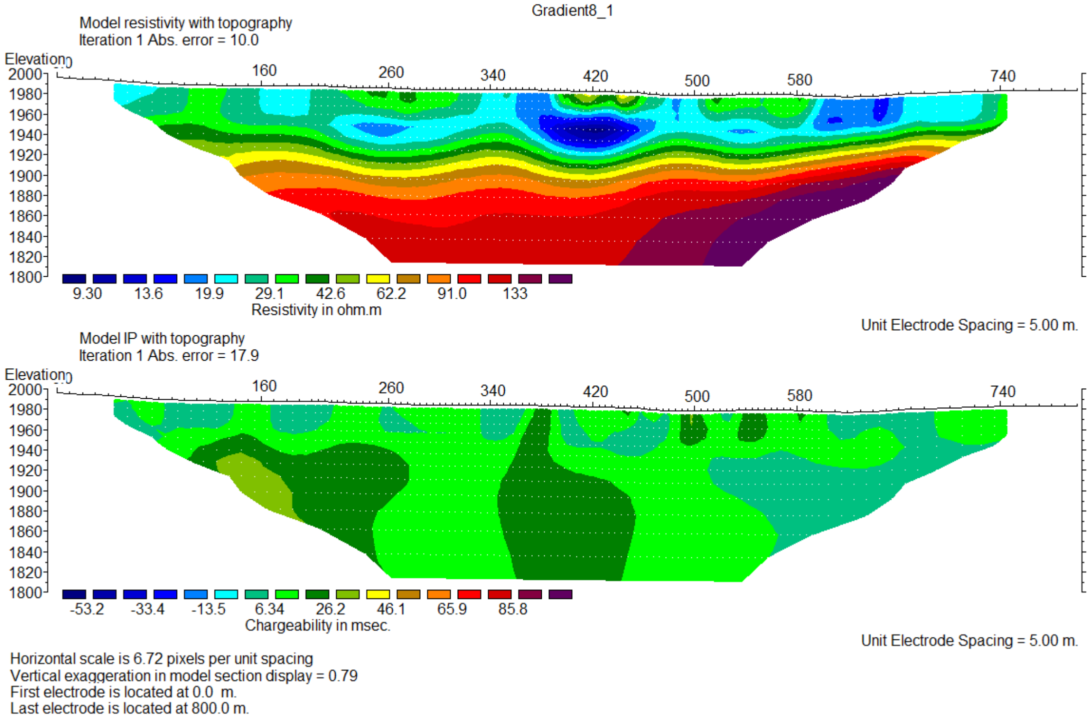

ITERACIÓN 3

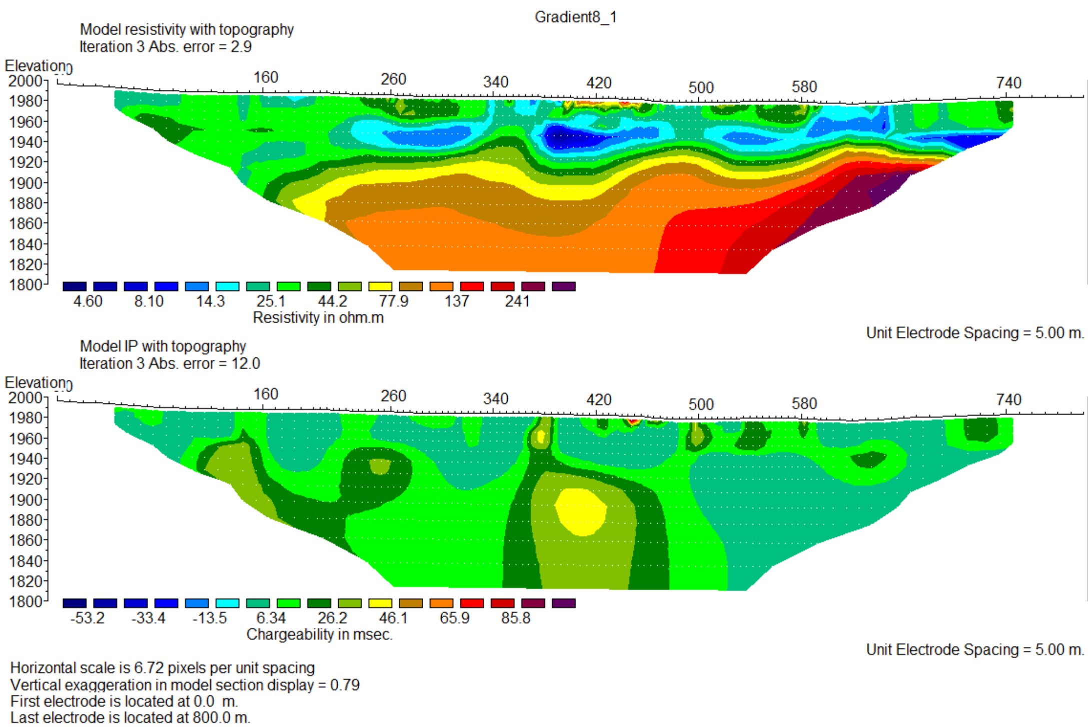

ITERACIÓN 5

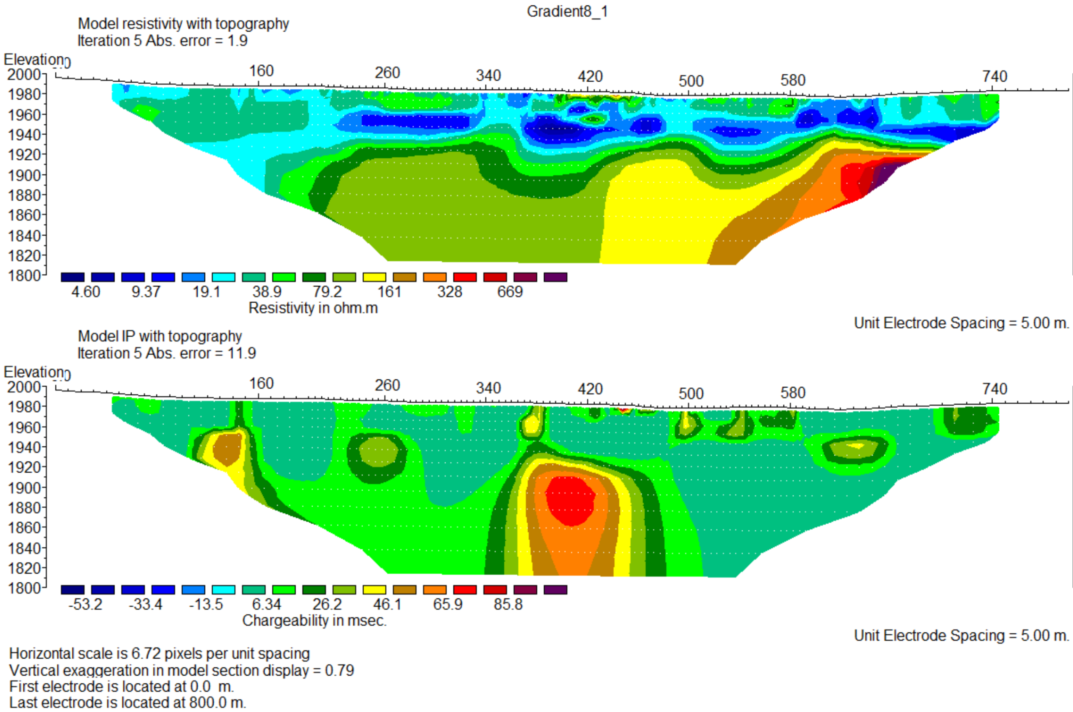

ITERACION 5 – BLANCO Y NEGRO

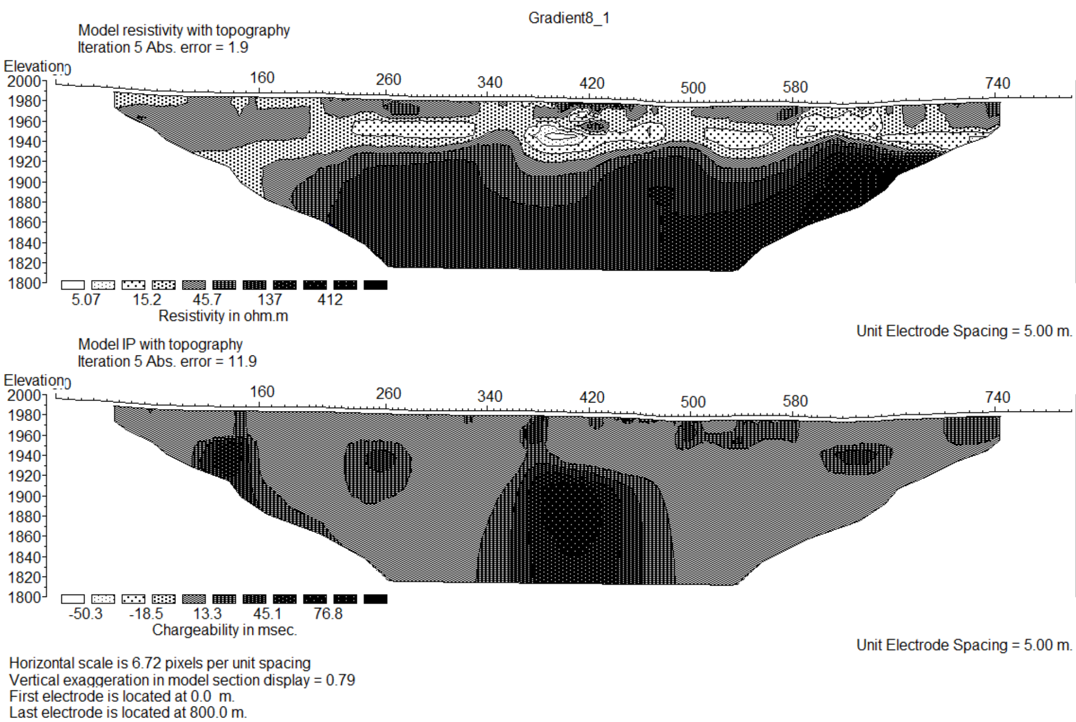

ARREGLO: GRADIENTE

CABLES: 4X21

TIEMPO DE IP: 1.0 SEGUNDO

VENTANAS IP: 8

INTERVALOS IP

VENTANA	TIEMPO EN MS
1	0.02
2	0.04
3	0.06
4	0.08
5	0.12
6	0.16
7	0.22
8	0.3
Tiempo total	1.0 MS

```
Reading file D:\Oficina\Clientes Geofisica\Tarija OB\Inversion\Fray Quebracho\Gradiente\Grad 1\L1-FRAY-QUEBRACHO-GRAD-1-TF1edit.INV

Gradient8_1
Minimum electrode spacing is    5.0.
General array
Gradient array
Total number of data points is 679.
IP values given in terms of chargeability
Half-size model blocks used for general array data set.
Model with half the unit electrode spacing is used
Number of electrodes is 119
Number of data levels is 16.
Topography present 2.
Minimum electrode location is    0.0.
Maximum electrode location is  800.0.
Minimum electrode spacing is    5.0.
Reading inversion results.
The model has 13 layers and 1213 blocks.
Iteration  1 : Abs. error   9.86   17.71.
Iteration  2 : Abs. error   4.98   12.37.
Iteration  3 : Abs. error   2.64   12.25.
Iteration  4 : Abs. error   2.17   12.16.
Iteration  5 : Abs. error   1.70   12.11.

Topographical data present in inversion file.
Schwartz-Christoffel transformation topography modelling was used.
Blocks sensitivity information present.
Average sensitivity is 1.267.
Inversion constraints information present.
Reading of file has been completed.
```

ITERACIÓN 1

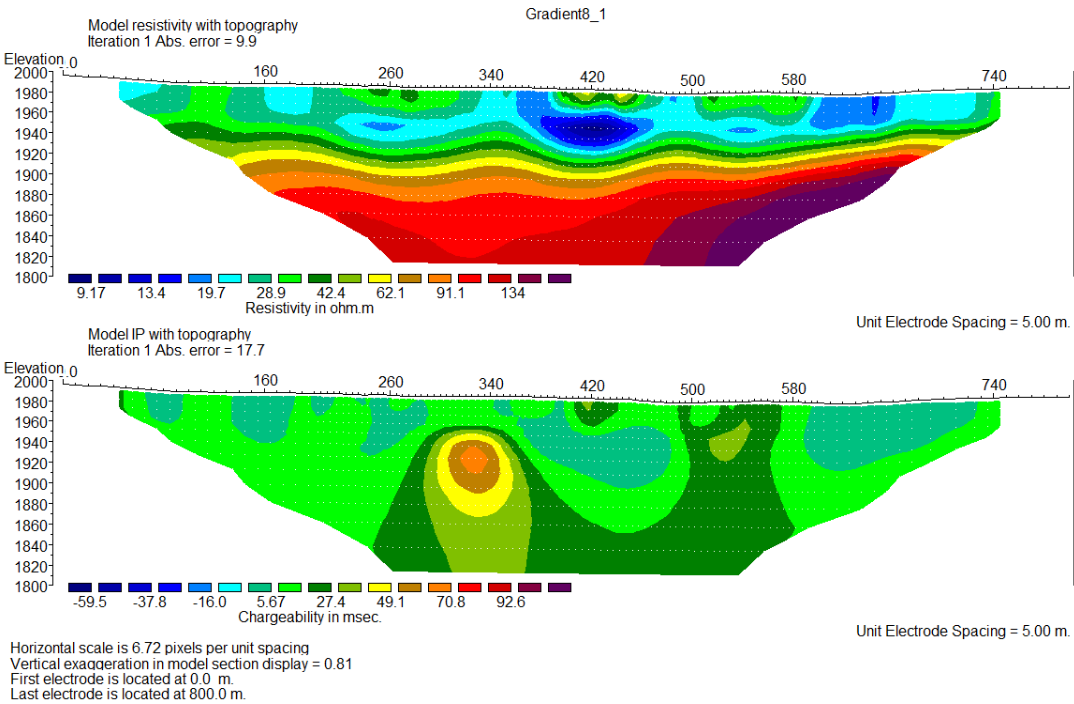

ITERACIÓN 3

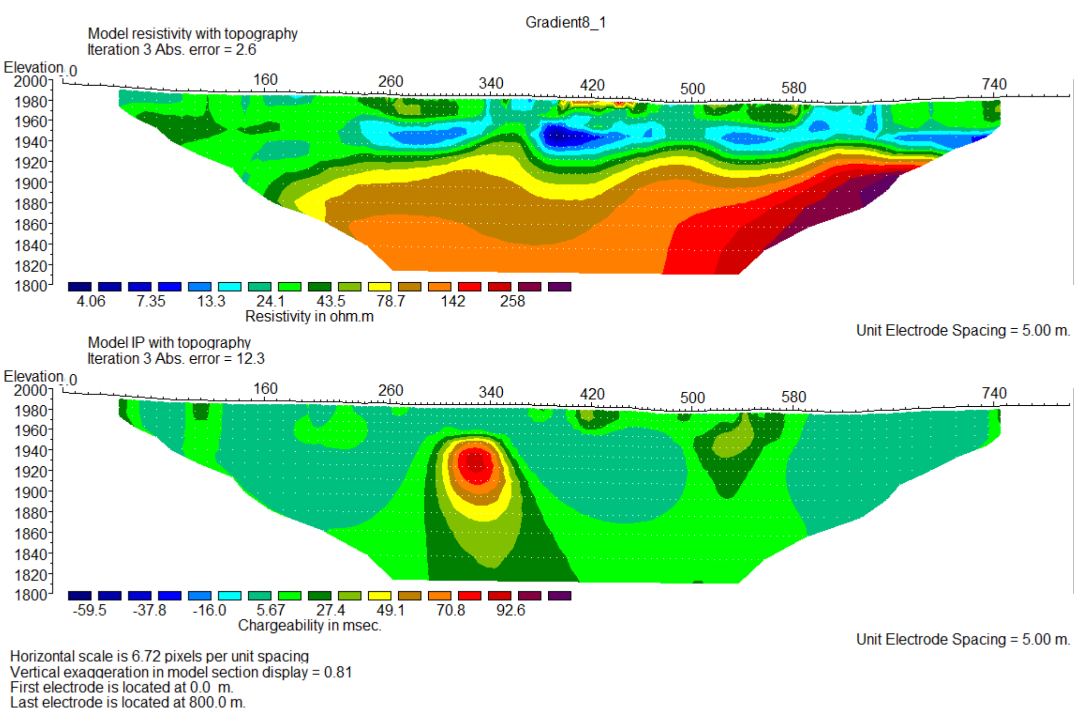

ITERACIÓN 5

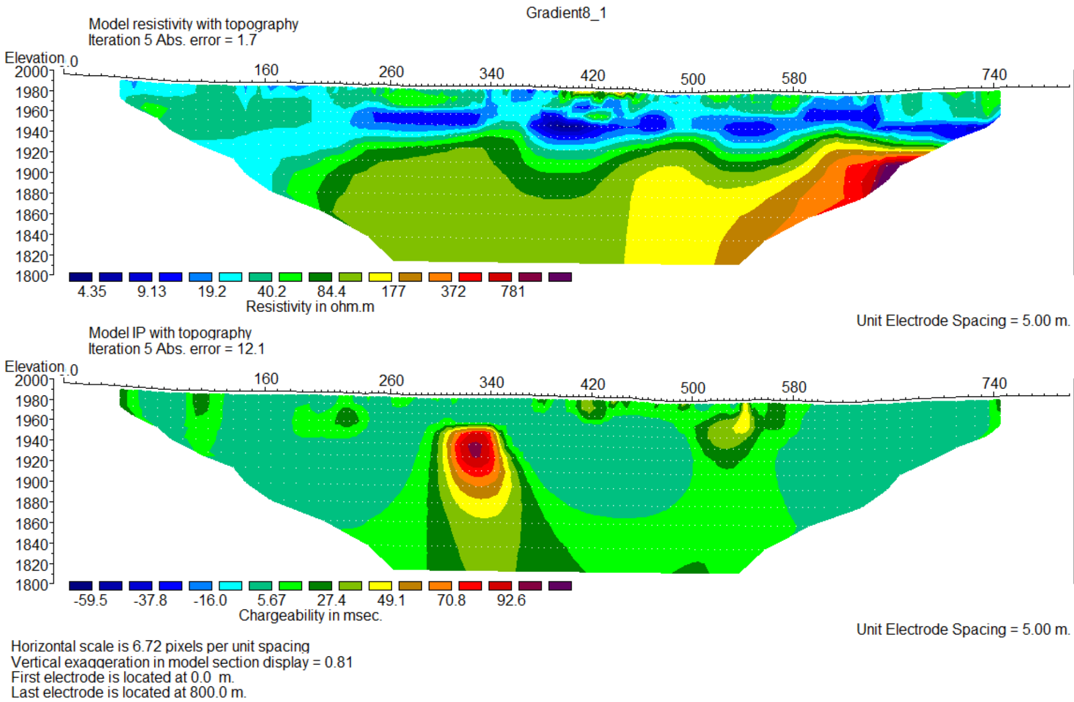

ITERACIÓN 5 – BLANCO Y NEGRO

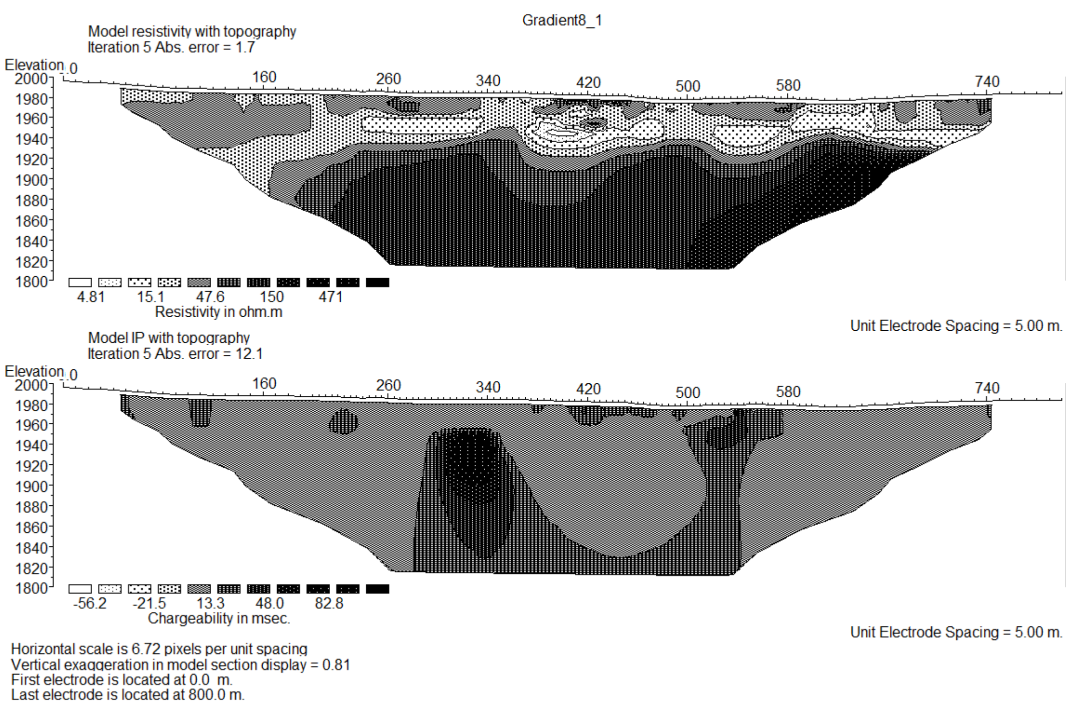

ARREGLO: GRADIENTE

CABLES: 4X21

TIEMPO DE IP: 1.5 SEGUNDOS

VENTANAS IP: 10

INTERVALOS IP

VENTANA	TIEMPO EN MS
1	0.02
2	0.04
3	0.06
4	0.08
5	0.1
6	0.14
7	0.18
8	0.24
9	0.26
10	0.38
Tiempo total	1.5 MS

```
Reading file D:\Oficina\Clientes Geofisica\Tarija OB\Inversion\Fray Quebracho\Gradiente\Grad 1.5\L1-FRAY-QUEBRACHO-GRAD-15-TF1edit.INV

Gradient8_1
Minimum electrode spacing is    5.0.
General array
Gradient array
Total number of data points is 686.
IP values given in terms of chargeability
Half-size model blocks used for general array data set.
Model with half the unit electrode spacing is used
Number of electrodes is 119
Number of data levels is 16.
Topography present 2.
Minimum electrode location is    0.0.
Maximum electrode location is  800.0.
Minimum electrode spacing is    5.0.
Reading inversion results.
The model has 13 layers and 1213 blocks.
Iteration  1 : Abs. error   9.85   14.71.
Iteration  2 : Abs. error   4.80   10.65.
Iteration  3 : Abs. error   2.68   10.51.
Iteration  4 : Abs. error   2.15   10.45.
Iteration  5 : Abs. error   1.70   10.42.

Topographical data present in inversion file.
Schwartz-Christoffel transformation topography modelling was used.
Blocks sensitivity information present.
Average sensitivity is 1.283.
Inversion constraints information present.
Reading of file has been completed.
```

ITERACIÓN 1

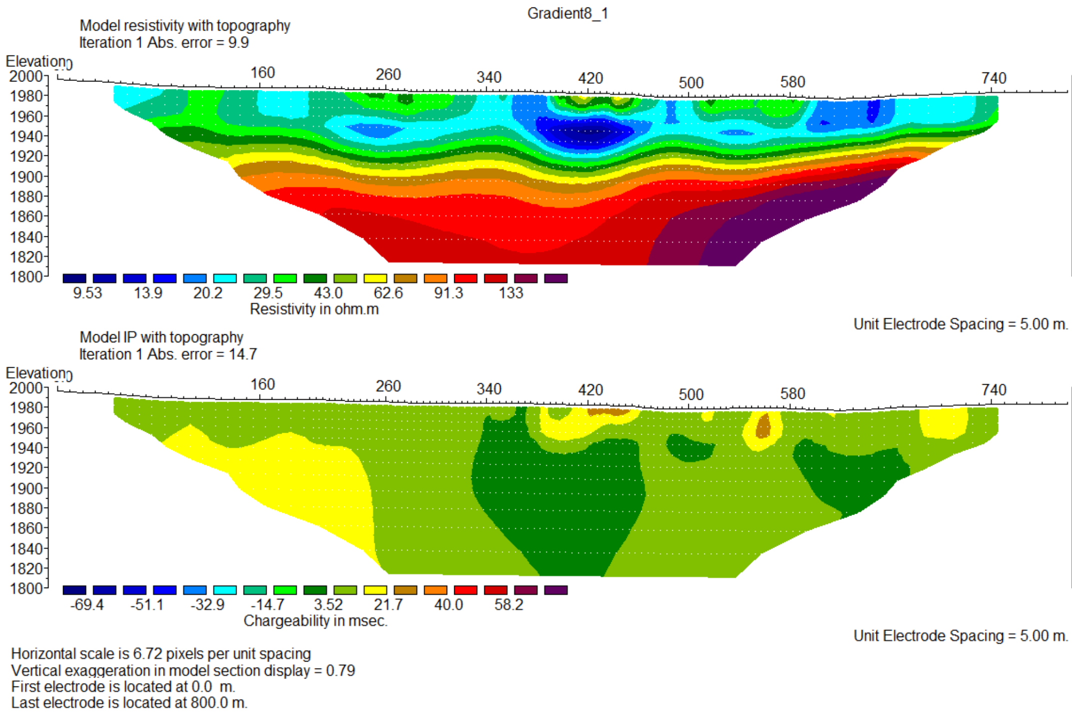

ITERACIÓN 3

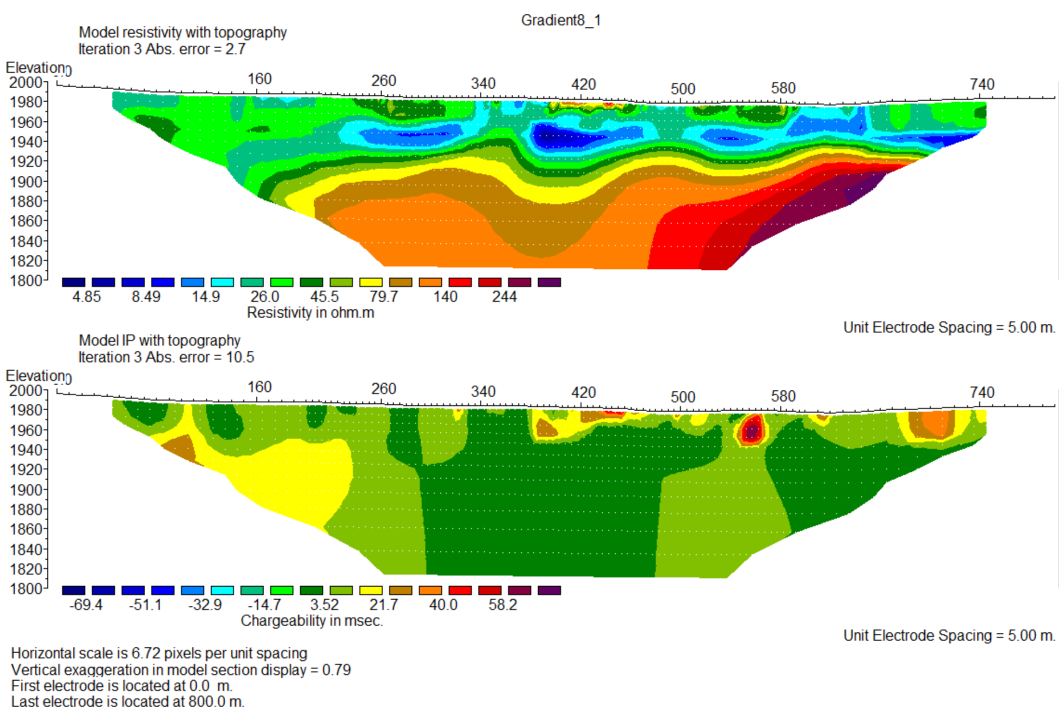

ITERACIÓN 5

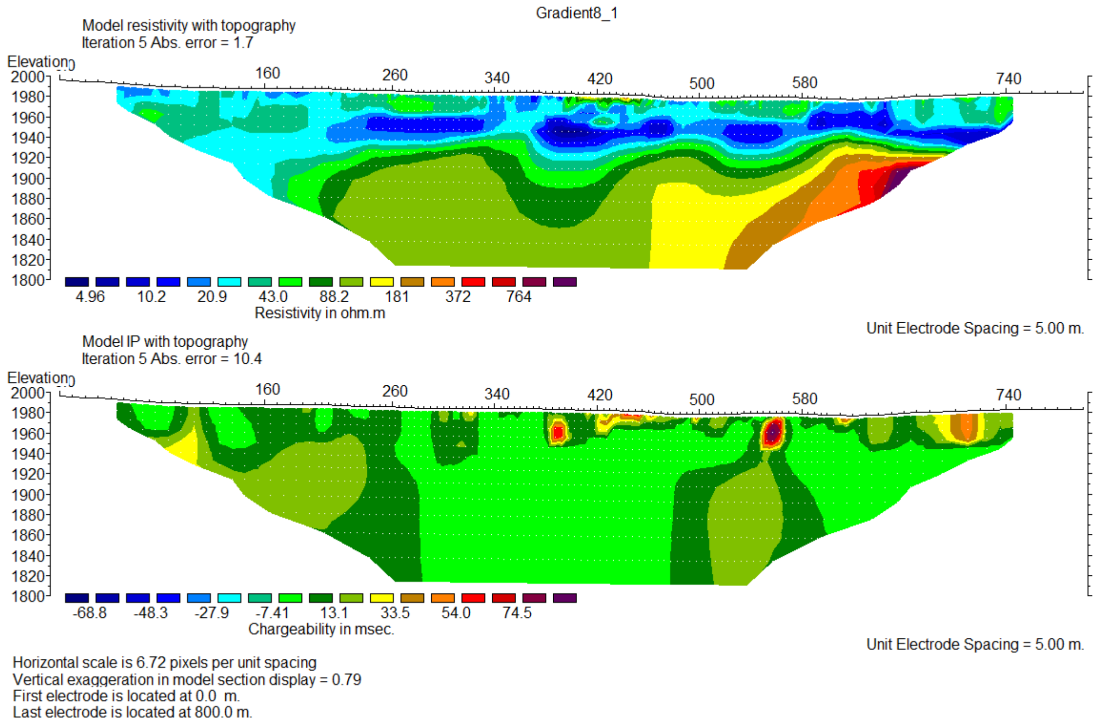

ITERACIÓN 5 – BLANCO Y NEGRO

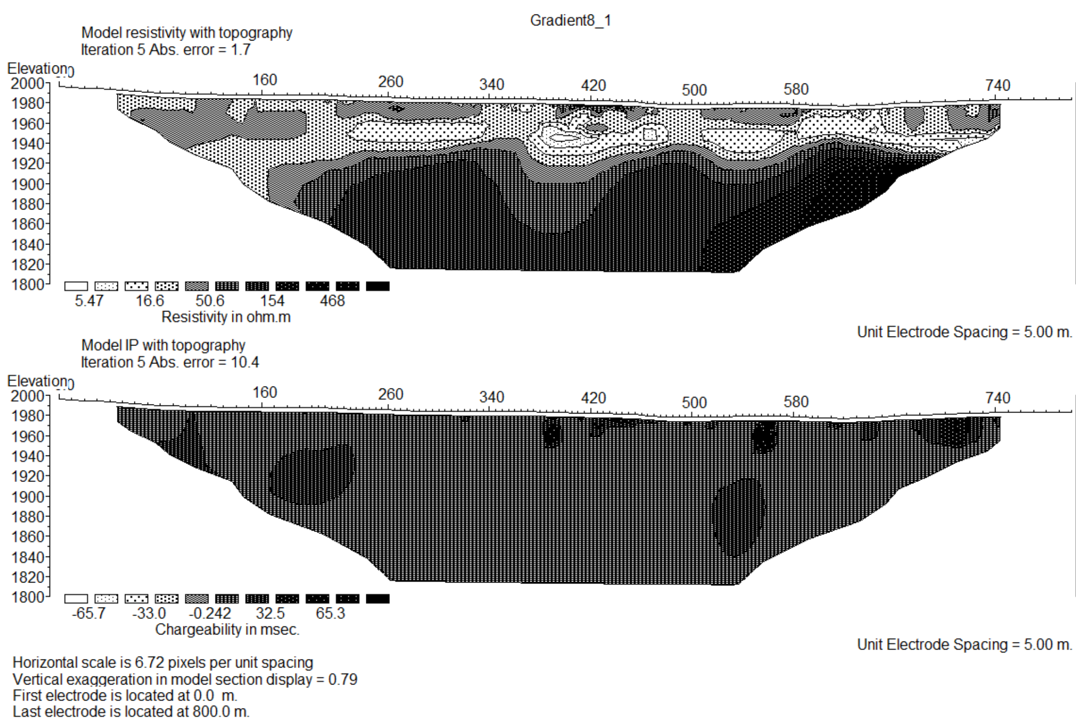

ANEXO 5c

YESERA

De acuerdo al proceso de datos tenemos lo siguiente:

ARREGLO: SCHLUMBERGER

CABLES: 4X21

TIEMPO DE IP: 0.5 SEGUNDOS

VENTANAS IP: 6

INTERVALOS IP

VENTANA	TIEMPO EN MS
1	0.02
2	0.04
3	0.06
4	0.08
5	0.12
6	0.18
Tiempo total	0.5 MS

```
Reading most recent file D:\Oficina\Clientes Geofisica\Tarija OB\Inversion\Yesera\Schlumberger\Sch 0.5\L1-YESERA-SCHLUMBERGER-05TF1edit.INV

Schlumberger_1
Minimum electrode spacing is    5.0.
General array
Wenner-Schlumberger array arrangement
Total number of data points is 698.
IP values given in terms of chargeability
Half-size model blocks used for general array data set.
Model with half the unit electrode spacing is used
Number of electrodes is 119
Number of data levels is 26.
Topography present 2.
Minimum electrode location is    0.0.
Maximum electrode location is  800.0.
Minimum electrode spacing is    5.0.
Reading inversion results.
The model has 15 layers and 1292 blocks.
Iteration  1 : Abs. error   6.74   17.32.
Iteration  2 : Abs. error   2.29   10.95.
Iteration  3 : Abs. error   1.64   10.92.
Iteration  4 : Abs. error   1.20   10.90.
Iteration  5 : Abs. error   1.05   10.89.

Topographical data present in inversion file.
Schwartz-Christoffel transformation topography modelling was used.
Blocks sensitivity information present.
Average sensitivity is 1.240.
Inversion constraints information present.
Reading of file has been completed.
```

ITERACION 1

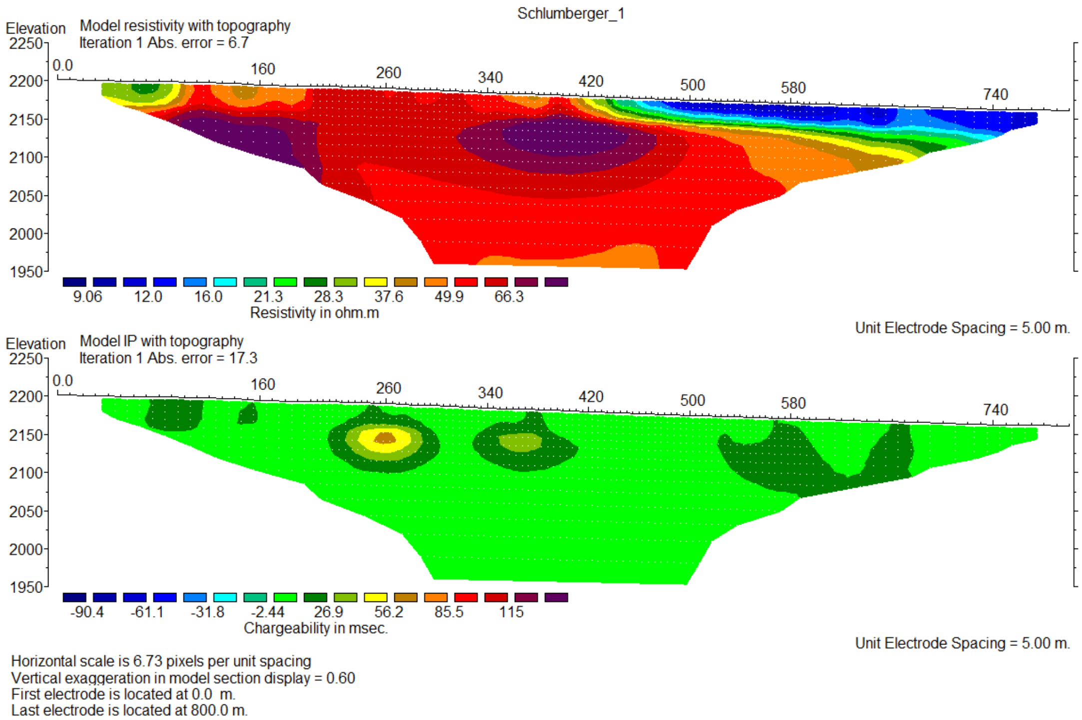

ITERACIÓN 3

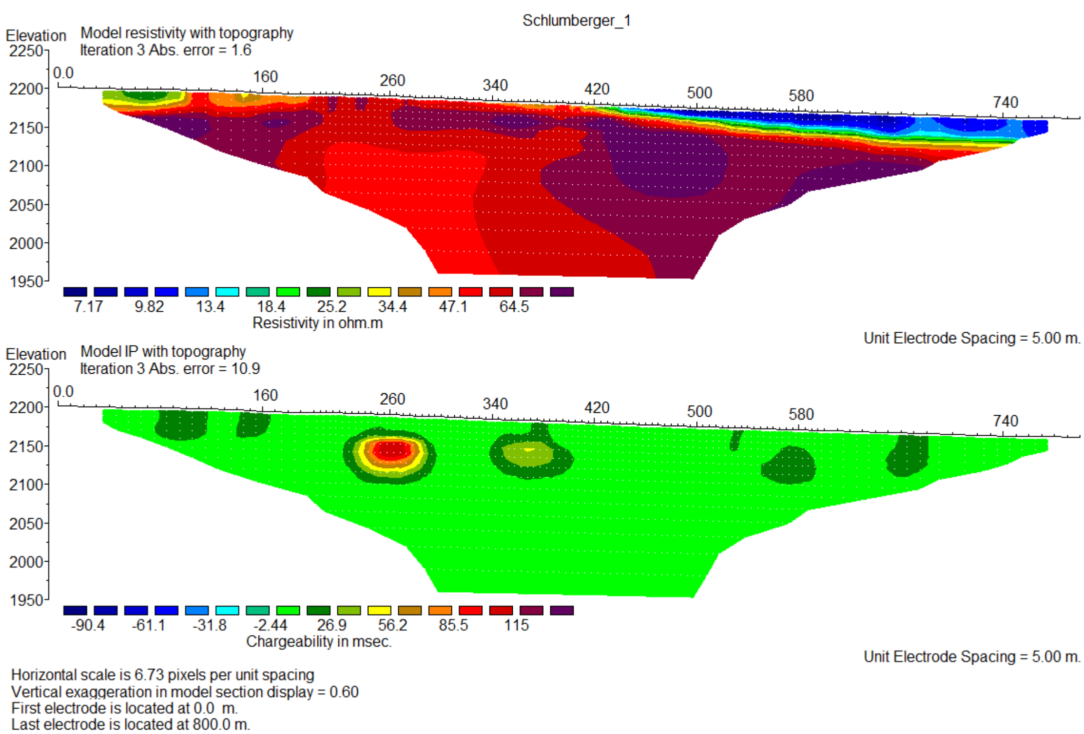

ITERACIÓN 5

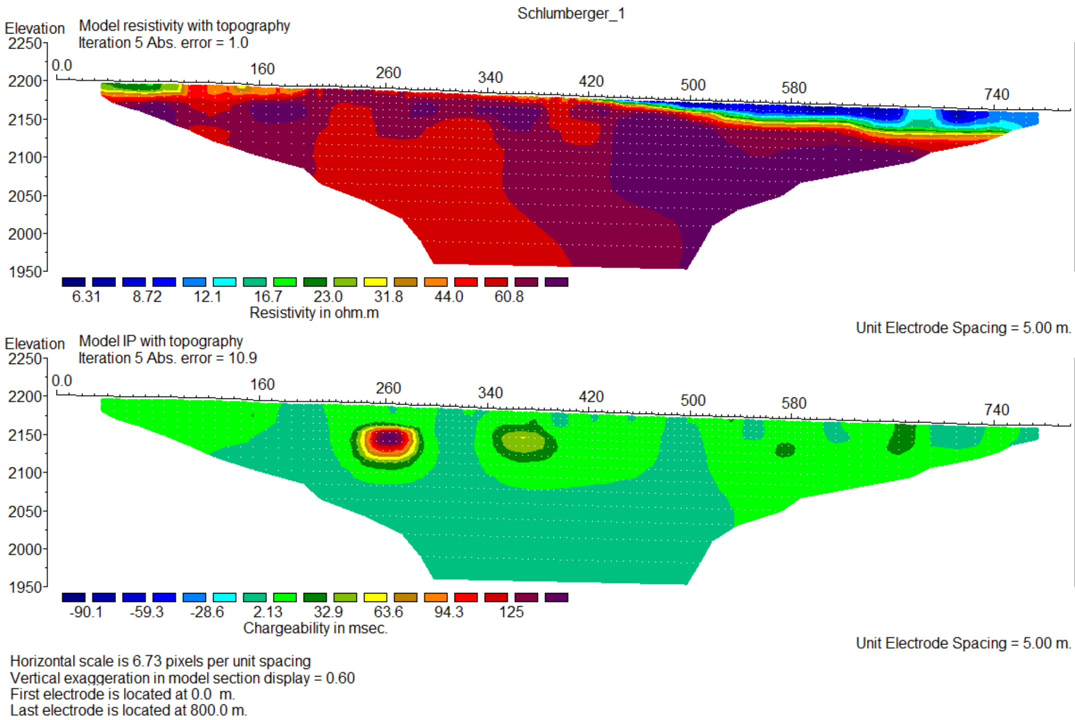

ITERACIÓN 5 – BLANCO Y NEGRO

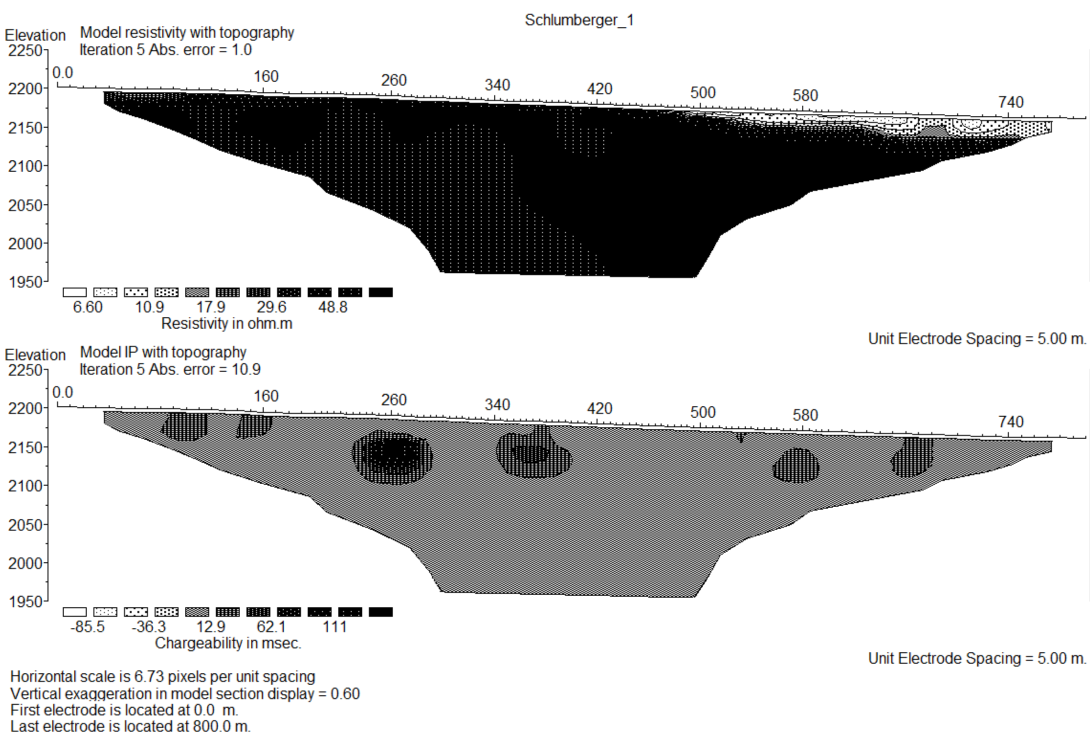

ARREGLO: SCHLUMBERGER

CABLES: 4X21

TIEMPO DE IP: 1.0 SEGUNDO

VENTANAS IP: 8

INTERVALOS IP

VENTANA	TIEMPO EN MS
1	0.02
2	0.04
3	0.06
4	0.08
5	0.12
6	0.16
7	0.22
8	0.3
Tiempo total	1.0 MS

```
Reading most recent file D:\Oficina\Clientes Geofisica\Tarija OB\Inversion\Yesera\Schlumberger\Sch 1\L1-YESERA-SCHLUMBERGER-1TF1edit.INV

Schlumberger_1
Minimum electrode spacing is    5.0.
General array
Wenner-Schlumberger array arrangement
Total number of data points is 705.
IP values given in terms of chargeability
Half-size model blocks used for general array data set.
Model with half the unit electrode spacing is used
Number of electrodes is 119
Number of data levels is 26.
Topography present 2.
Minimum electrode location is    0.0.
Maximum electrode location is  800.0.
Minimum electrode spacing is    5.0.
Reading inversion results.
The model has 15 layers and 1271 blocks.
Iteration  1 : Abs. error   6.88   18.40.
Iteration  2 : Abs. error   2.36   12.37.
Iteration  3 : Abs. error   1.66   12.35.
Iteration  4 : Abs. error   1.22   12.32.
Iteration  5 : Abs. error   1.09   12.30.

Topographical data present in inversion file.
Schwartz-Christoffel transformation topography modelling was used.
Blocks sensitivity information present.
Average sensitivity is 1.269.
Inversion constraints information present.
Reading of file has been completed.
```

ITERACIÓN 1

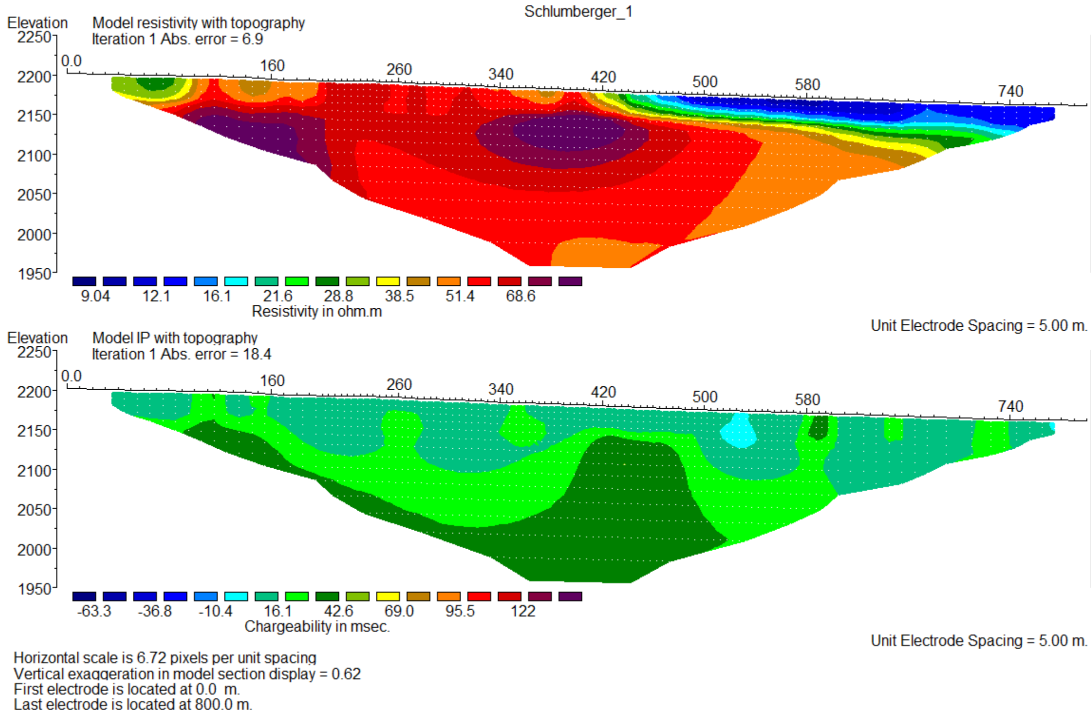

ITERACIÓN 3

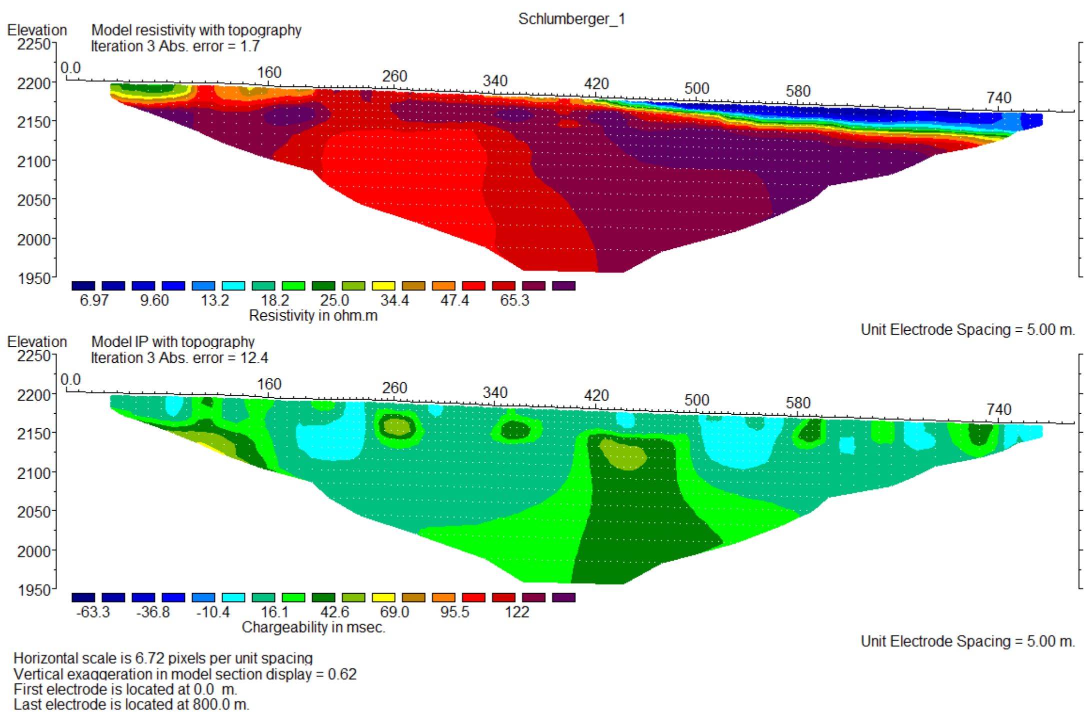

ITERACIÓN 5

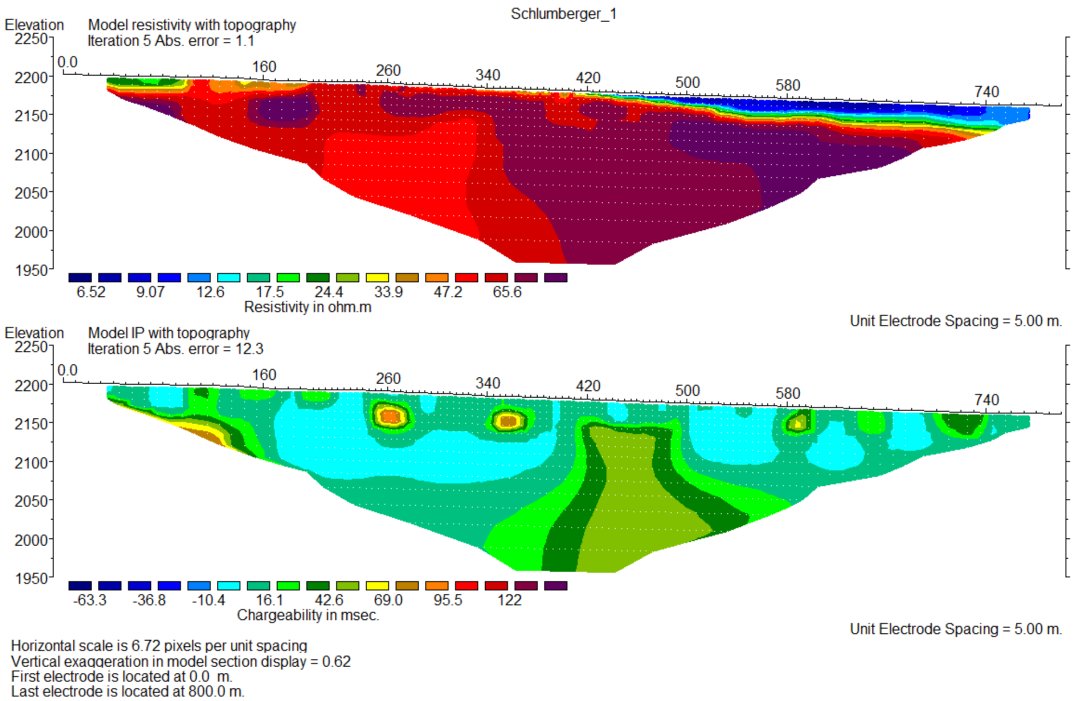

ITERACIÓN 5 – BLANCO Y NEGRO

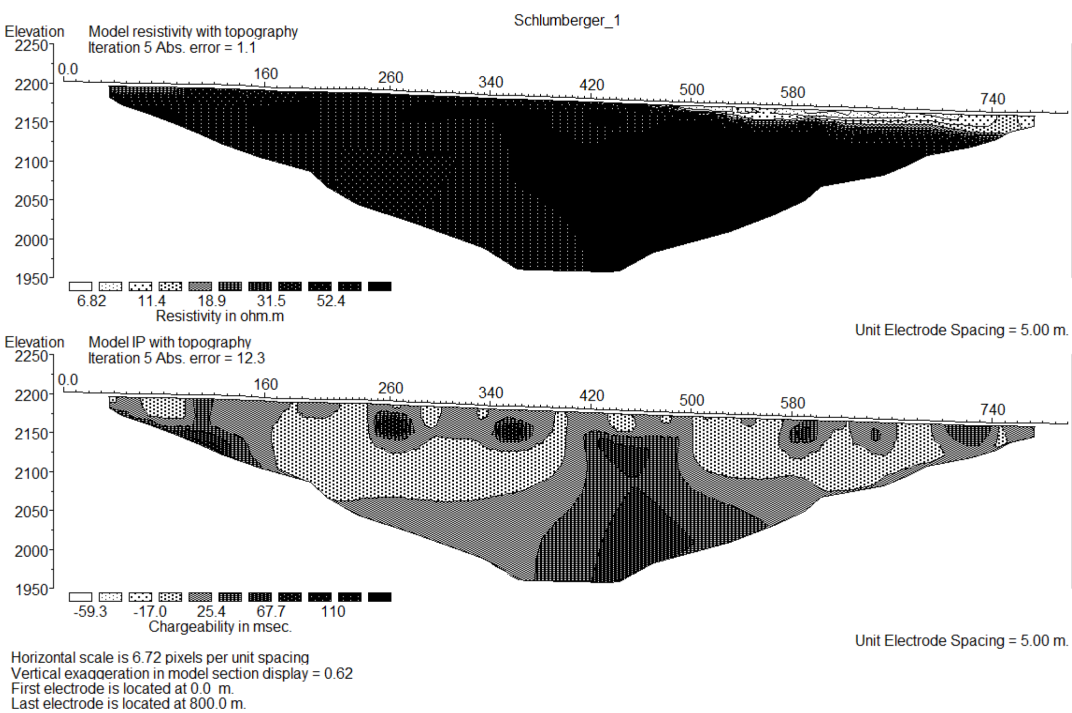

ARREGLO: SCHLUMBERGER

CABLES: 4X21

TIEMPO DE IP: 1.5 SEGUNDOS

VENTANAS IP: 10

INTERVALOS IP

VENTANA	TIEMPO EN MS
1	0.02
2	0.04
3	0.06
4	0.08
5	0.1
6	0.14
7	0.18
8	0.24
9	0.26
10	0.38
Tiempo total	1.5 MS

```
Reading file D:\Oficina\Clientes Geofisica\Tarija OB\Inversion\Yesera\Schlumberger\Sch 1.5\L1-YESERA-SCHLUMBERGER-15TF1edit.INV

Schlumberger_1
Minimum electrode spacing is    5.0.
General array
Wenner-Schlumberger array arrangement
Total number of data points is 702.
IP values given in terms of chargeability
Half-size model blocks used for general array data set.
Model with half the unit electrode spacing is used
Number of electrodes is 119
Number of data levels is 26.
Topography present 2.
Minimum electrode location is    0.0.
Maximum electrode location is  800.0.
Minimum electrode spacing is    5.0.
Reading inversion results.
The model has 15 layers and 1298 blocks.
Iteration  1 : Abs. error   6.91   15.93.
Iteration  2 : Abs. error   2.29   11.77.
Iteration  3 : Abs. error   1.58   11.73.
Iteration  4 : Abs. error   1.15   11.67.
Iteration  5 : Abs. error   1.02   11.65.

Topographical data present in inversion file.
Schwartz-Christoffel transformation topography modelling was used.
Blocks sensitivity information present.
Average sensitivity is 1.238.
Inversion constraints information present.
Reading of file has been completed.
```

ITERACIÓN 1

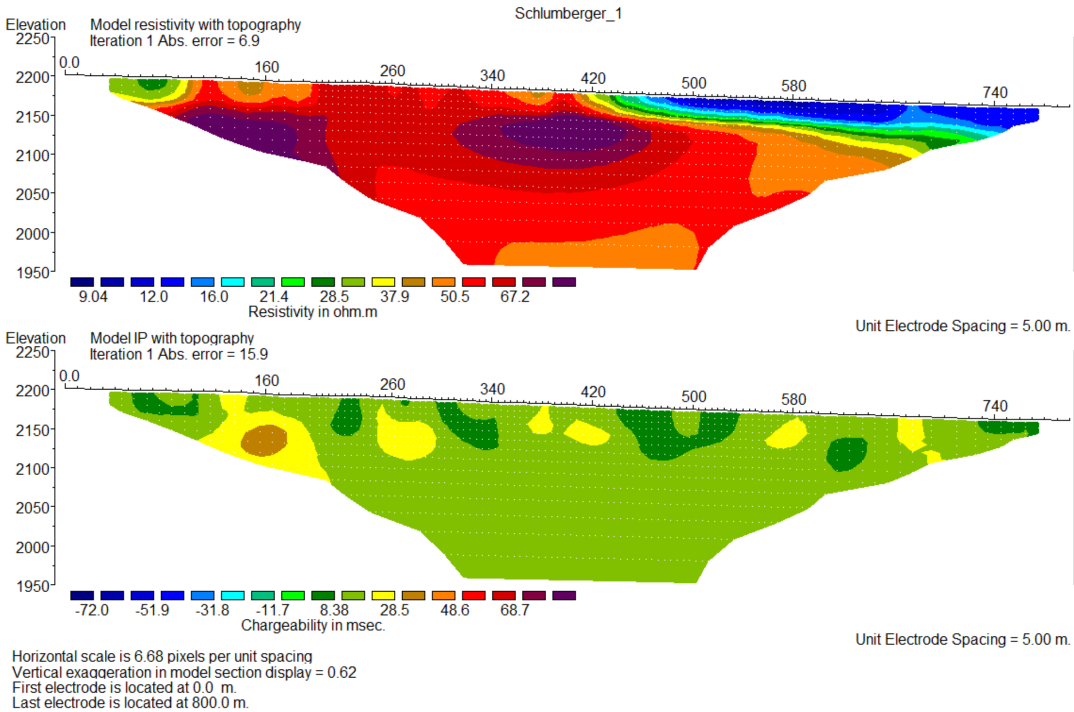

ITERACIÓN 3

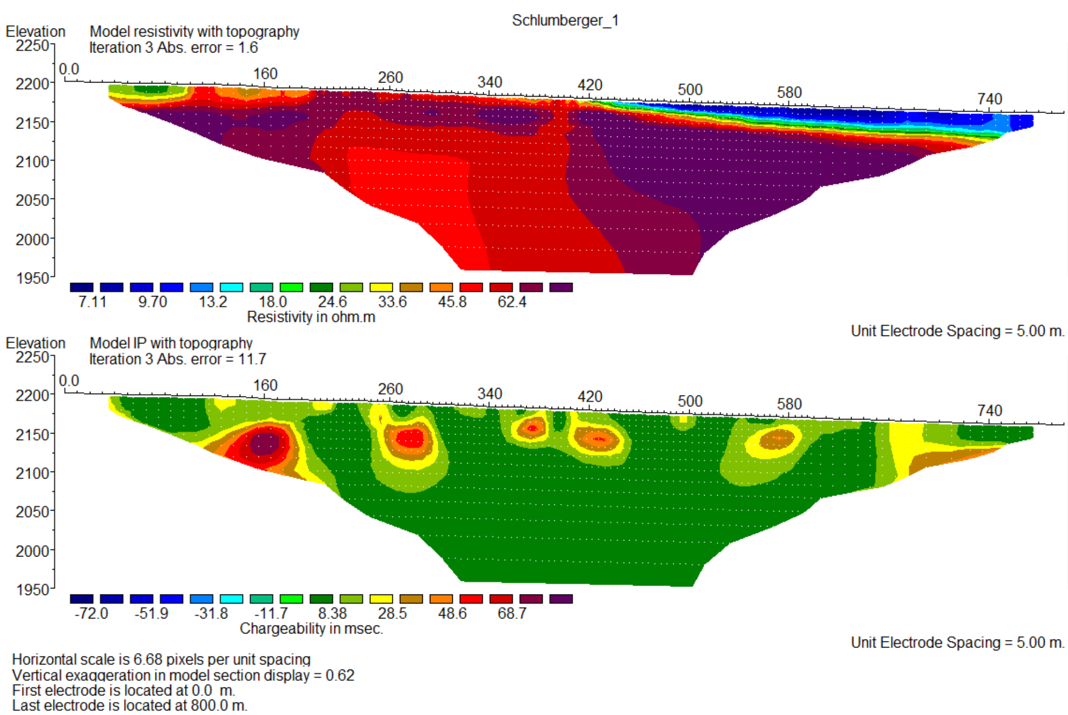

ITERACIÓN 5

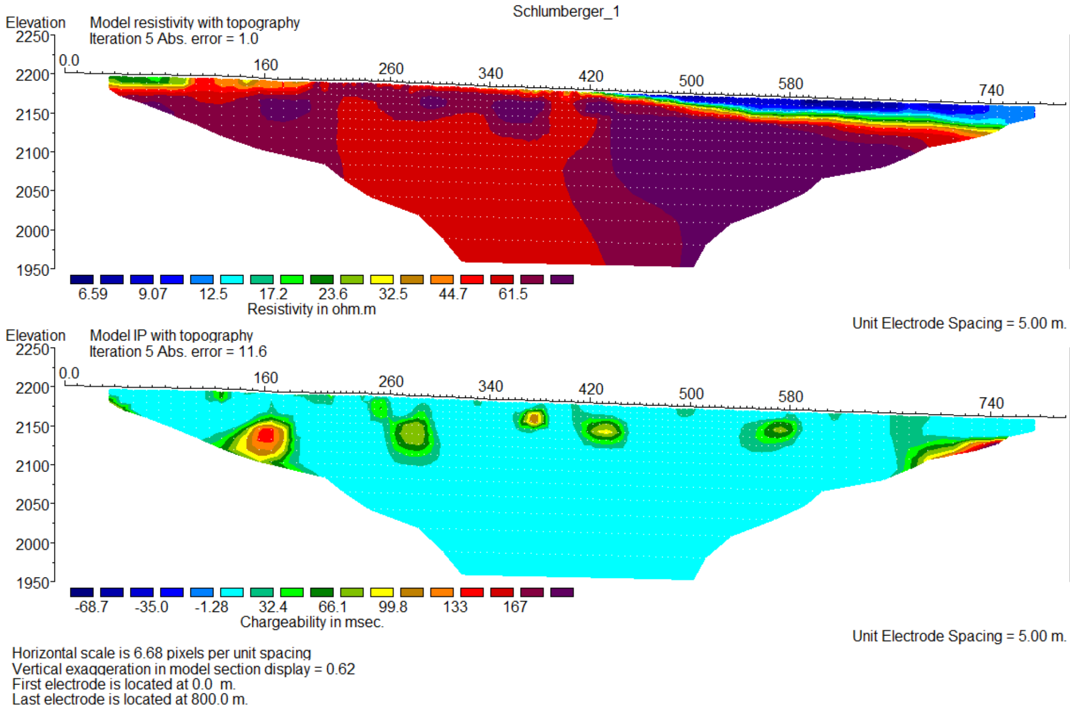

ITERACIÓN 5 – BLANCO Y NEGRO

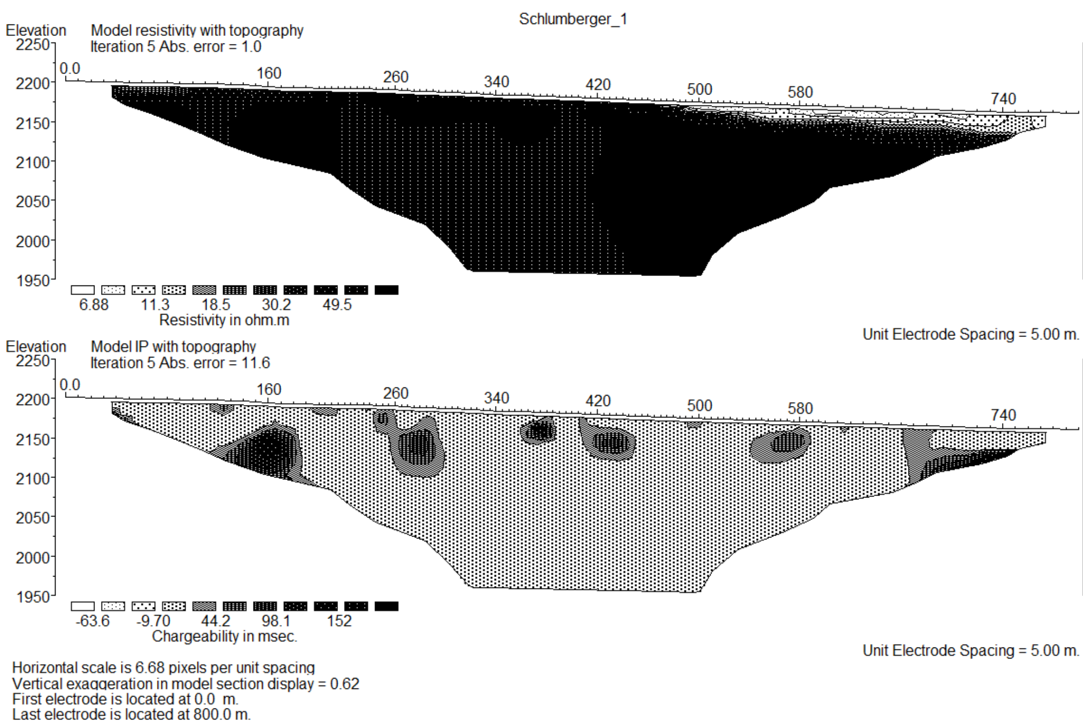

ARREGLO: GRADIENTE

CABLES: 4X21

TIEMPO DE IP: 0.5 SEGUNDOS

VENTANAS IP: 6

INTERVALOS IP

VENTANA	TIEMPO EN MS
1	0.02
2	0.04
3	0.06
4	0.08
5	0.12
6	0.18
Tiempo total	0.5 MS

```
Reading file D:\Oficina\Clientes Geofisica\Tarija OB\Inversion\Yesera\Gradiente\Grad 0.5\L1-YESERA-GRADIENTE-05TF1edit.INV

Gradient8_1
Minimum electrode spacing is    5.0.
General array
Gradient array
Total number of data points is 696.
IP values given in terms of chargeability
Half-size model blocks used for general array data set.
Model with half the unit electrode spacing is used
Number of electrodes is 119
Number of data levels is 16.
Topography present 2.
Minimum electrode location is    0.0.
Maximum electrode location is  800.0.
Minimum electrode spacing is    5.0.
Reading inversion results.
The model has 13 layers and 1196 blocks.
Iteration  1 : Abs. error   7.42   16.56.
Iteration  2 : Abs. error   3.30   10.63.
Iteration  3 : Abs. error   1.84   10.63.
Iteration  4 : Abs. error   1.23   10.60.
Iteration  5 : Abs. error   1.05   10.59.

Topographical data present in inversion file.
Schwartz-Christoffel transformation topography modelling was used.
Blocks sensitivity information present.
Average sensitivity is 1.278.
Inversion constraints information present.
Reading of file has been completed.
```

ITERACIÓN 1

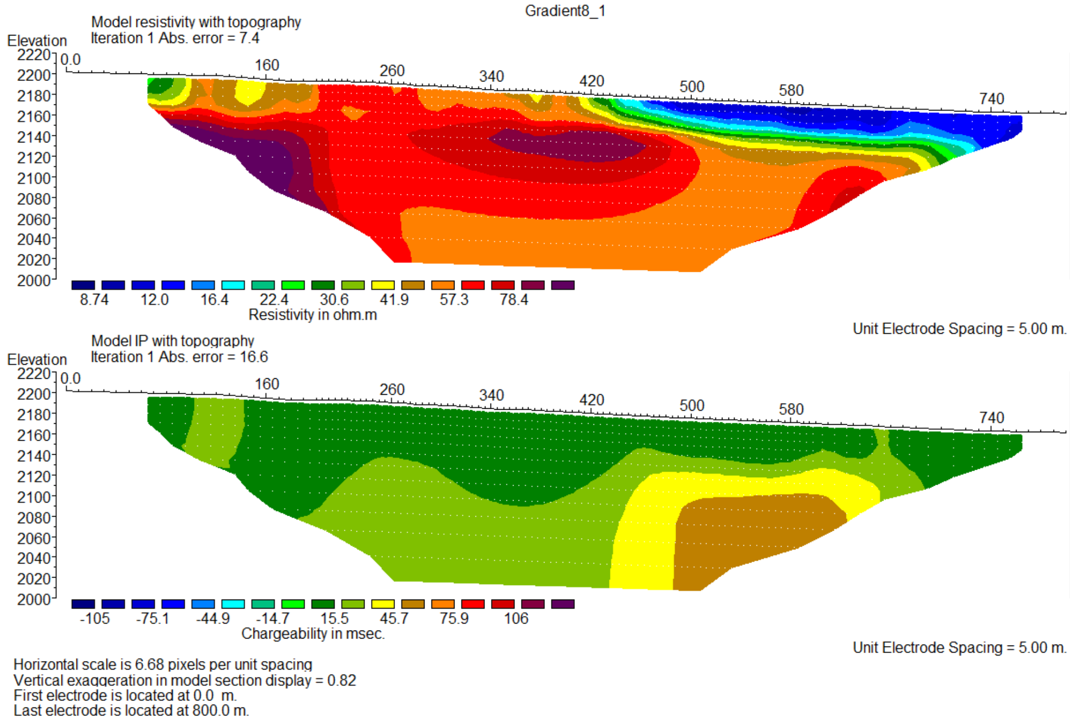

ITERACIÓN 3

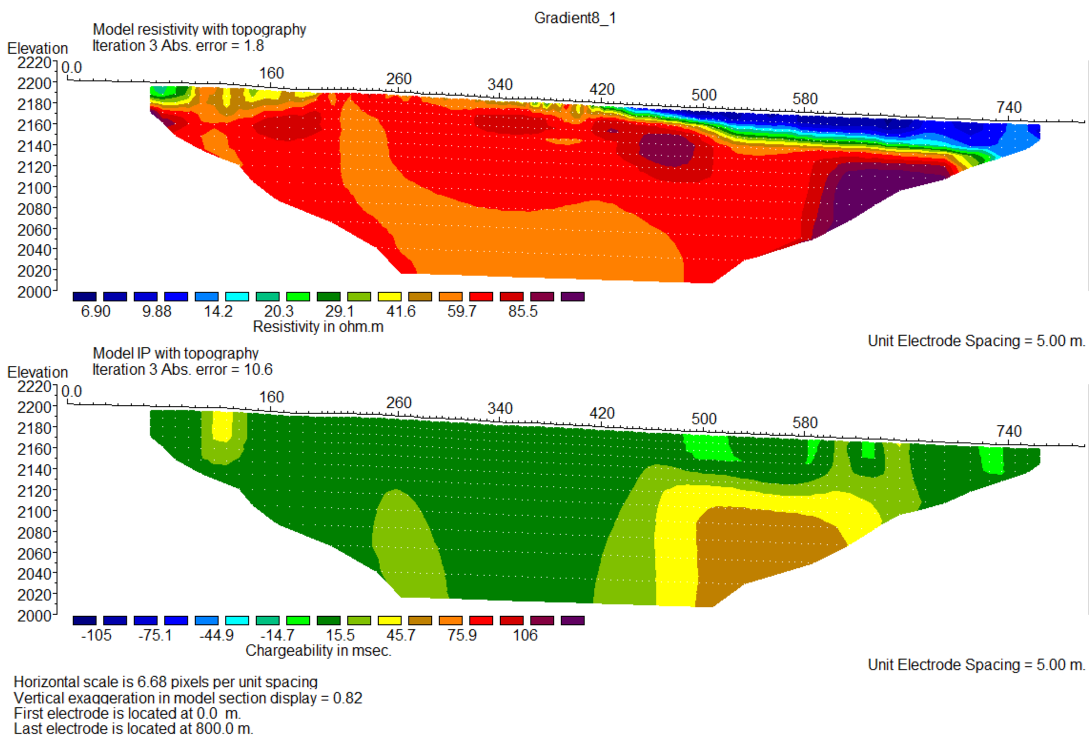

ITERACIÓN 5

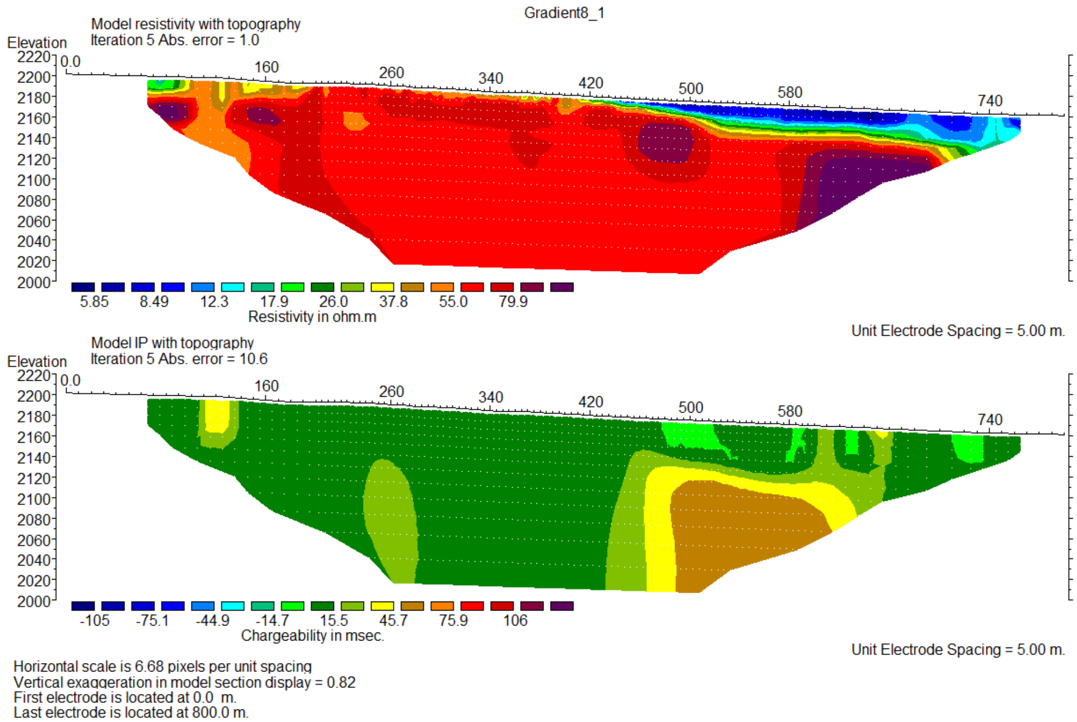

ITERACIÓN 5 BLANCO Y NEGRO

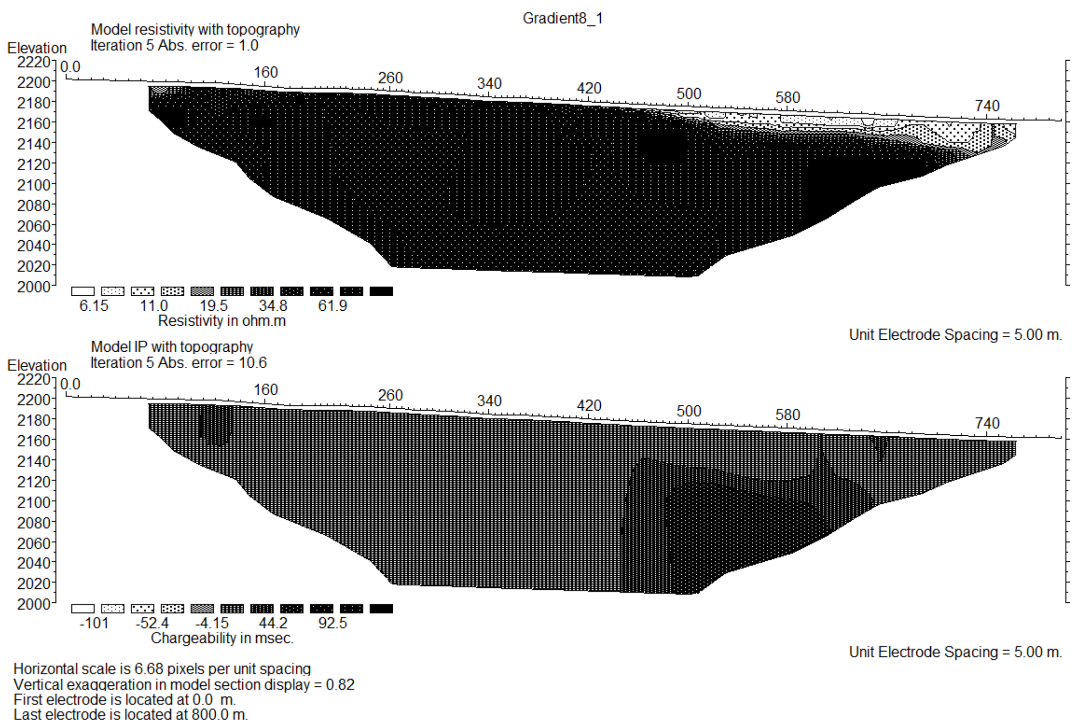

ARREGLO: GRADIENTE

CABLES: 4X21

TIEMPO DE IP: 1.0 SEGUNDO

VENTANAS IP: 8

INTERVALOS IP

VENTANA	TIEMPO EN MS
1	0.02
2	0.04
3	0.06
4	0.08
5	0.12
6	0.16
7	0.22
8	0.3
Tiempo total	1.0 MS

```
Reading file D:\Oficina\Clientes Geofisica\Tarija OB\Inversion\Yesera\Gradiente\Grad 1\L1-YESERA-GRADIENTE-1TF1edit.INV

Gradient8_1
Minimum electrode spacing is    5.0.
General array
Gradient array
Total number of data points is 695.
IP values given in terms of chargeability
Half-size model blocks used for general array data set.
Model with half the unit electrode spacing is used
Number of electrodes is 119
Number of data levels is 16.
Topography present 2.
Minimum electrode location is    0.0.
Maximum electrode location is  800.0.
Minimum electrode spacing is    5.0.
Reading inversion results.
The model has 13 layers and 1208 blocks.
Iteration  1 : Abs. error   7.52   13.93.
Iteration  2 : Abs. error   3.39    9.93.
Iteration  3 : Abs. error   1.88    9.85.
Iteration  4 : Abs. error   1.27    9.78.
Iteration  5 : Abs. error   1.04    9.77.

Topographical data present in inversion file.
Schwartz-Christoffel transformation topography modelling was used.
Blocks sensitivity information present.
Average sensitivity is 1.265.
Inversion constraints information present.
Reading of file has been completed.
```

ITERACIÓN 1

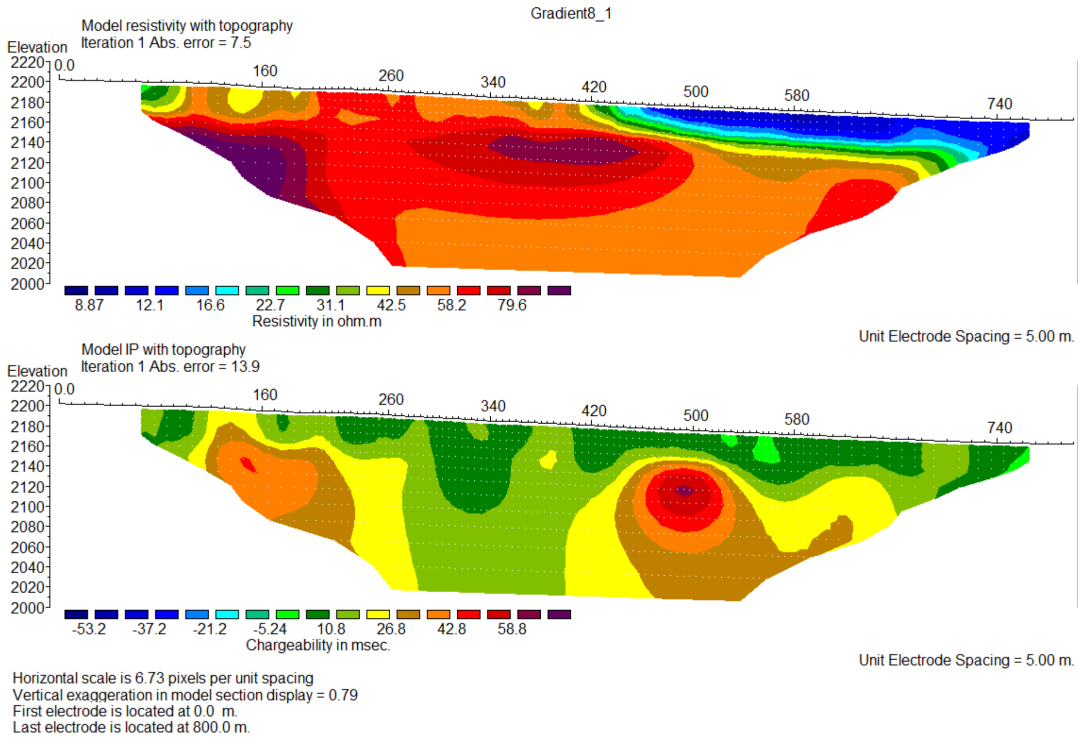

ITERACIÓN 3

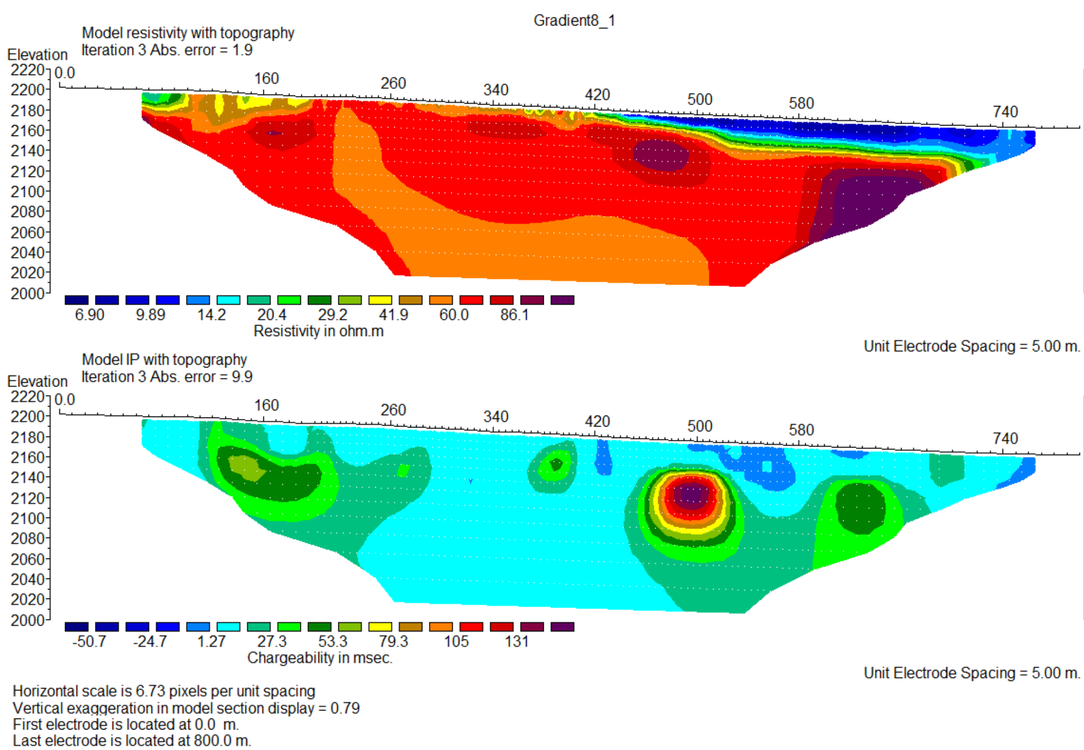

ITERACIÓN 5

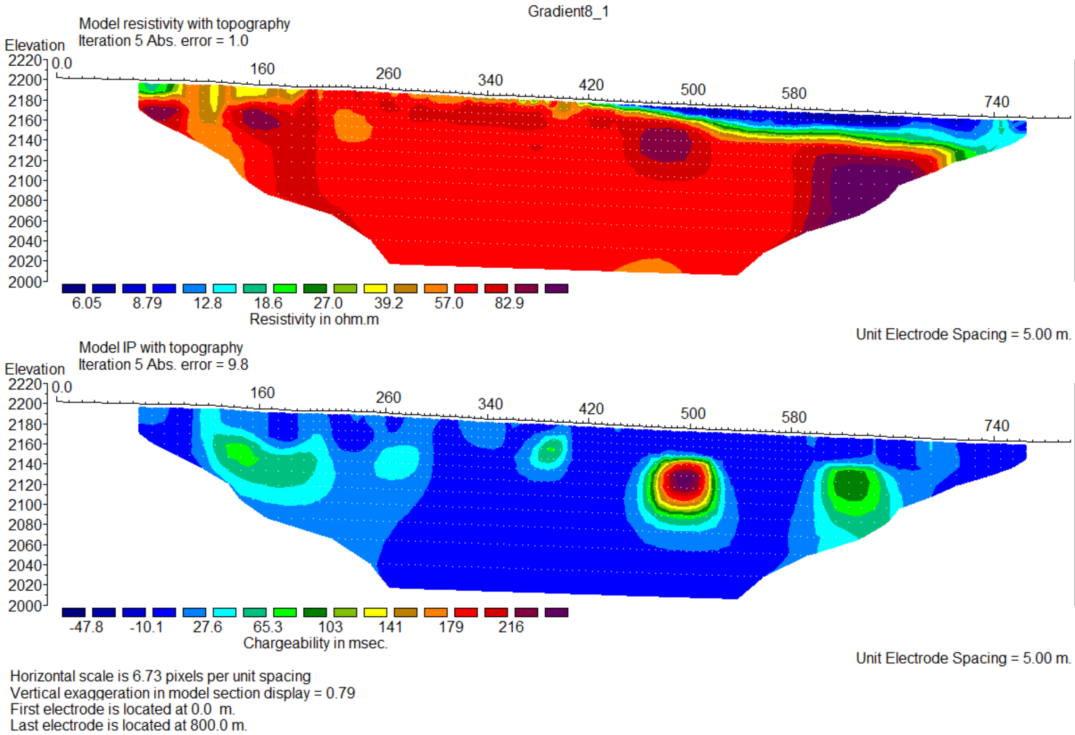

ITERACIÓN 5 – BLANCO Y NEGRO

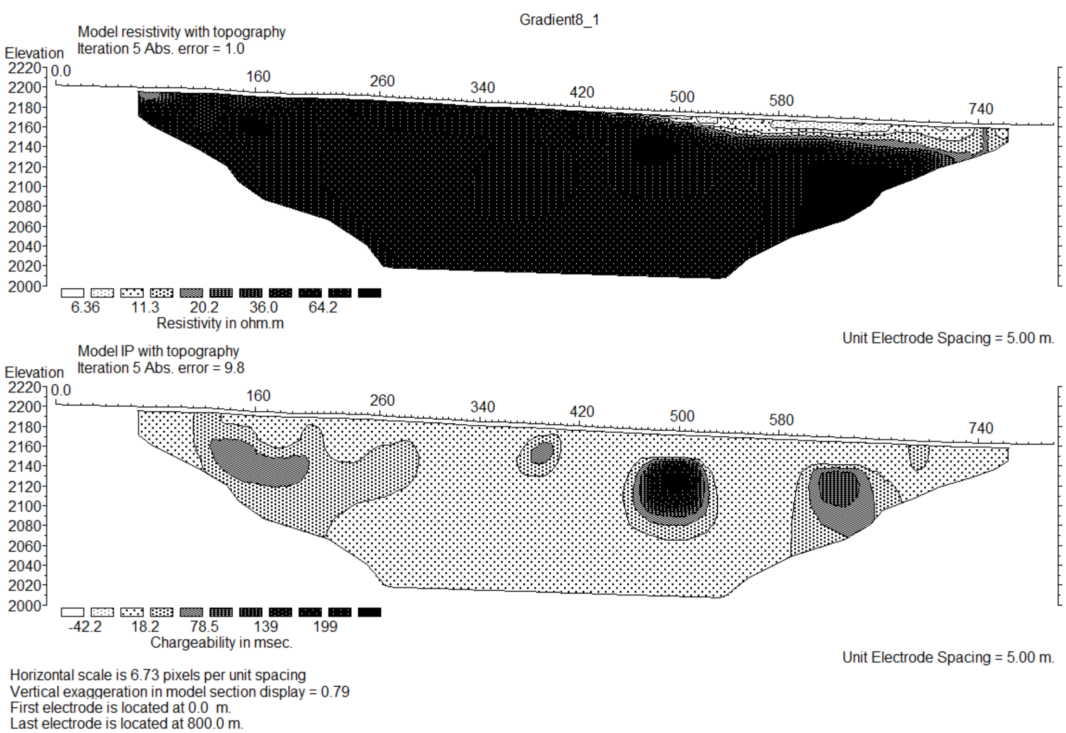

ARREGLO: GRADIENTE

CABLES: 4X21

TIEMPO DE IP: 1.5 SEGUNDOS

VENTANAS IP: 10

INTERVALOS IP

VENTANA	TIEMPO EN MS
1	0.02
2	0.04
3	0.06
4	0.08
5	0.1
6	0.14
7	0.18
8	0.24
9	0.26
10	0.38
Tiempo total	1.5 MS

```
Reading file D:\Oficina\Clientes Geofisica\Tarija OB\Inversion\Yesera\Gradiente\Grad 1.5\L1-YESERA-GRADIENTE-15TF1edit.INV

Gradient8_1
Minimum electrode spacing is    5.0.
General array
Gradient array
Total number of data points is 701.
IP values given in terms of chargeability
Half-size model blocks used for general array data set.
Model with half the unit electrode spacing is used
Number of electrodes is 119
Number of data levels is 16.
Topography present 2.
Minimum electrode location is    0.0.
Maximum electrode location is  800.0.
Minimum electrode spacing is    5.0.
Reading inversion results.
The model has 13 layers and 1208 blocks.
Iteration  1 : Abs. error   7.58   12.47.
Iteration  2 : Abs. error   3.38    9.17.
Iteration  3 : Abs. error   1.90    9.11.
Iteration  4 : Abs. error   1.25    9.05.
Iteration  5 : Abs. error   1.04    9.03.

Topographical data present in inversion file.
Schwartz-Christoffel transformation topography modelling was used.
Blocks sensitivity information present.
Average sensitivity is 1.274.
Inversion constraints information present.
Reading of file has been completed.
```

ITERACIÓN 1

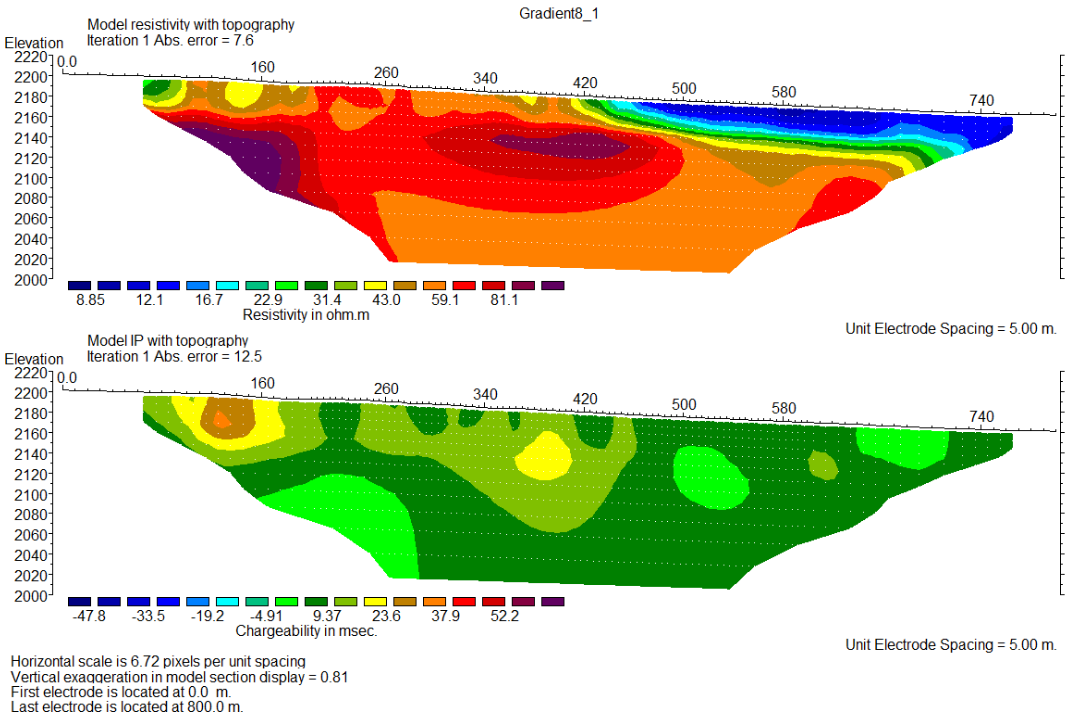

ITERACIÓN 3

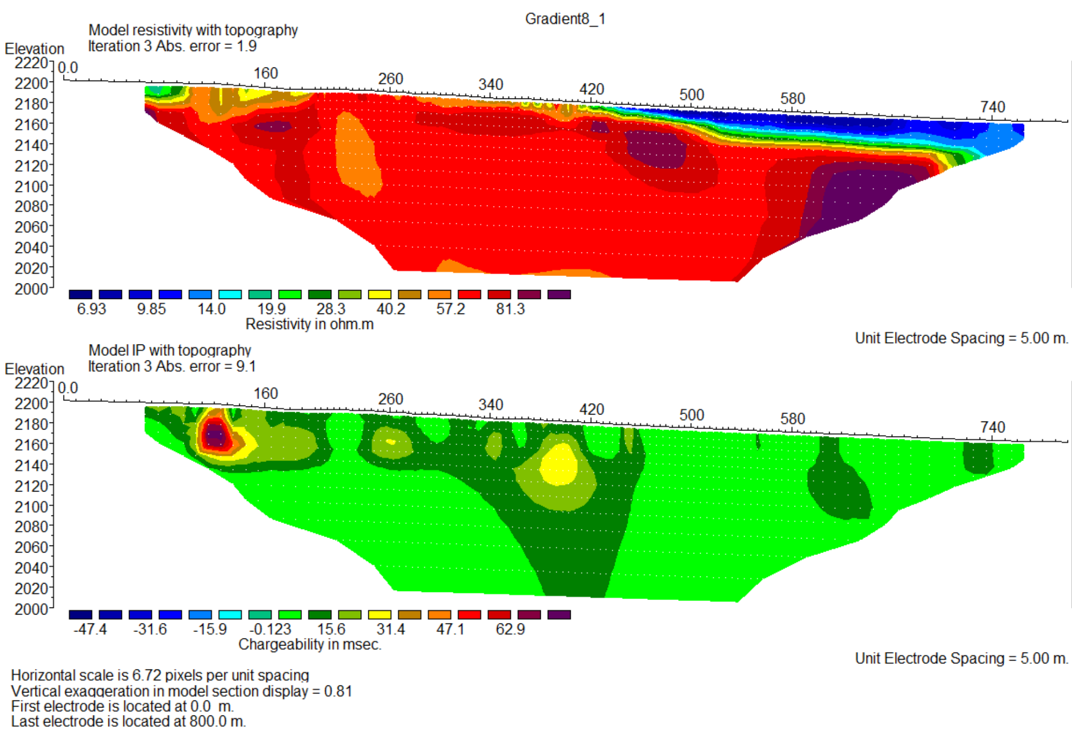

ITERACIÓN 5

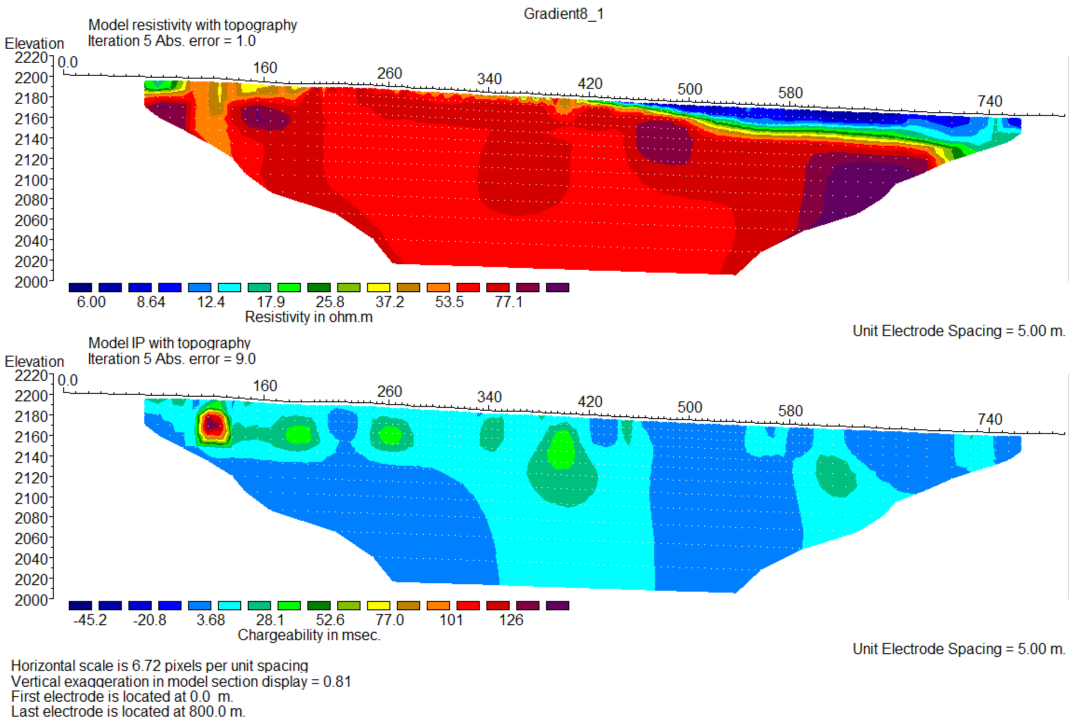

ITERACION 5 – BLANCO Y NEGRO

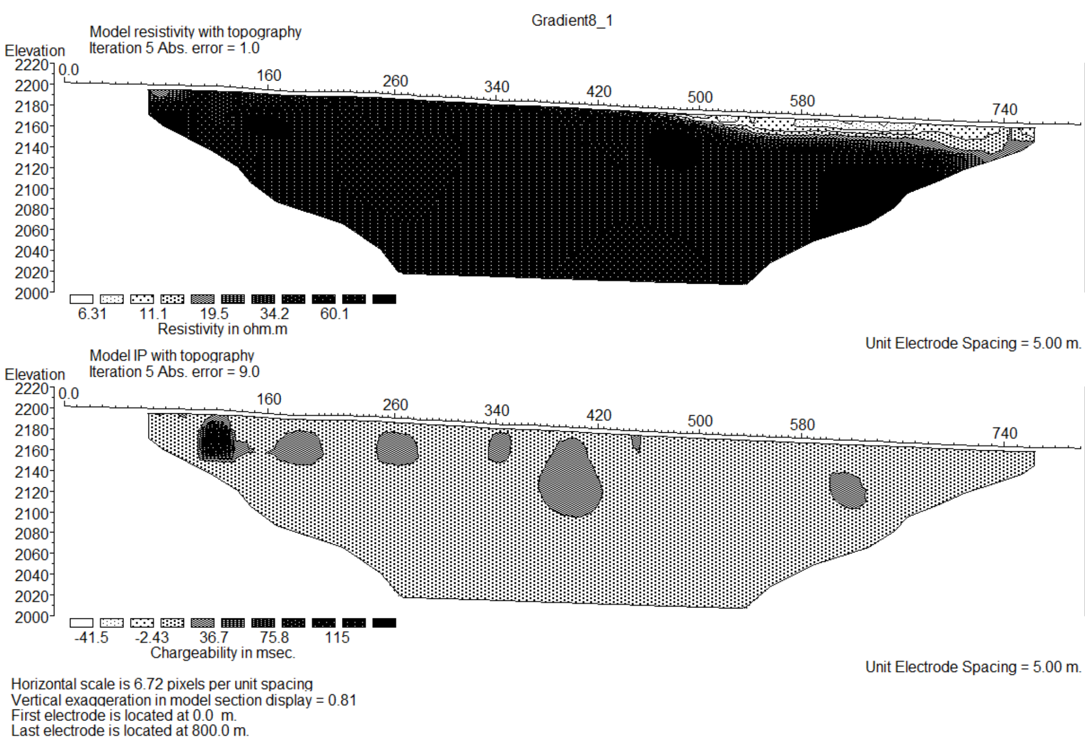

REGISTRO ELECTRICO VERTICAL
POZO TIERRA LINDA

PROF. LOGGEO DE MUESTRAS DE CAMPO

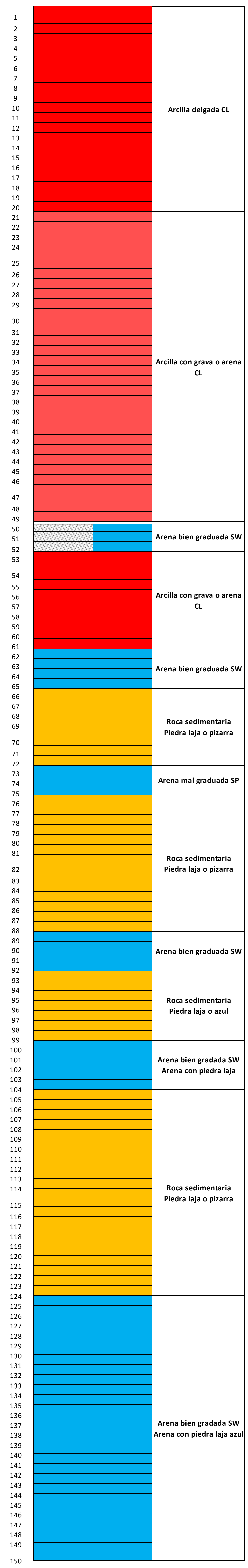

REGISTRO ELECTRICO VERTICAL
TIERRA LINDA

PROF	SP	RES CORTA	RES LARGA
1			
2			
3			
4			
5			
6			
7	43	14	22
8	38	18	22
9	32	46	55
10	31	25	52
11	30	18	18
12	30	12	16
13	28	12	16
14	24	12	14
15	21	12	15
16	20	15	10
17	19	10	15
18	18	10	15
19	14	10	15
20	10	15	15
21	4	17	19
22	2	14	20
23	0	16	22
24	-2	21	30
25	-5	30	30
26	-5	35	60
27	-10	100	115
28	-14	130	70
29	-12	40	19
30	-10	12	18
31	-10	10	12
32	-12	11	10
33	-10	11	8
34	-10	10	6
35	-10	12	6
36	-12	10	6
37	-14	12	10
38	-14	11	10
39	-12	12	8
40	-14	12	8
41	-16	12	8
42	-16	12	12
43	-18	18	20
44	-16	16	20
45	-16	16	20
46	-18	15	24
47	-22	35	30
48	-28	40	40
49	-26	40	40
50	-22	42	36
51	-24	46	46
52	-24	46	48
53	-26	30	44
54	-26	25	25
55	-20	20	16
56	-20	20	10
57	-20	20	10
58	-22	20	20
59	-24	22	26
60	-26	25	28
61	-24	28	30
62	-24	25	34
63	-26	30	35
64	-24	35	38
65	-24	38	42
66	-26	38	45
67	-30	40	50
68	-30	48	58
69	-30	55	70
70	-30	70	72
71	-30	90	100
72	-30	102	130
73	-30	105	122
74	-32	105	132
75	-30	108	140
76	-30	115	135
77	-30	98	126
78	-32	110	150
79	-36	120	150
80	-30	126	122
81	-30	120	95
82	-30	78	81
83	-32	72	80
84	-32	110	115
85	-36	130	115
86	-36	140	110
87	-36	160	140
88	-34	135	165
89	-34	100	120
90	-34	100	110
91	-38	95	115
92	-36	140	130
93	-36	120	120
94	-36	85	100
95	-36	80	84
96	-36	60	98
97	-30	90	92
98	-36	130	120
99	-36	115	110
100	-36	100	122
101	-38	130	140
102	-36	140	140
103	-36	170	165
104	-40	160	190
105	-38	160	195
106	-32	188	186
107	-30	150	155
108	-32	130	158
109	-34	135	130
110	-32	90	105
111	-36	100	118
112	-38	110	105
113	-36	90	82
114	-40	80	100
115	-38	80	95
116	-40	180	155
117	-34	170	155
118	-42	130	130
119	-44	135	120
120	-38	100	90
121	-38	72	100
122	-38	170	160
123	-32	155	160
124	-36	115	140
125	-44	140	155
126	-44	200	200
127	-38	200	200
128	-38	160	180
129	-40	135	180
130	-40	138	120
131	-40	160	160
132	-50	195	195
133	-40	180	135
134	-36	95	130
135	-38	148	150
136	-38	150	135
137	-42	100	98
138	-40	68	85
139	-34	70	88
140	-40	90	90
141	-38	110	100
142	-36	90	105
143	-38	118	105
144	-38	95	110
145	-40	102	150
146	-42	180	200
147	-38	160	150
148	-32		
149	-30		
150	-30		

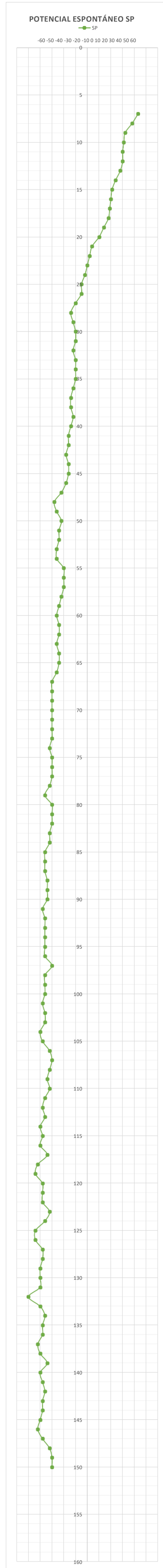

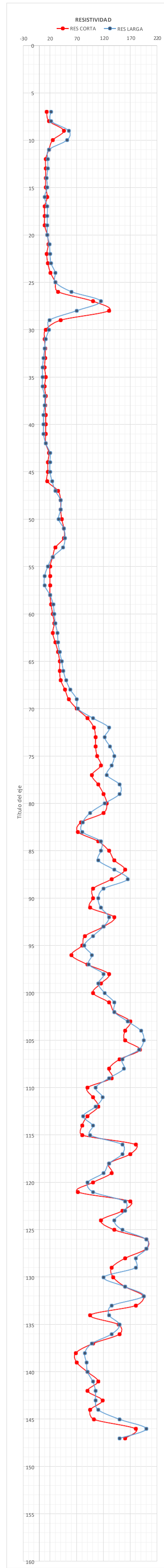

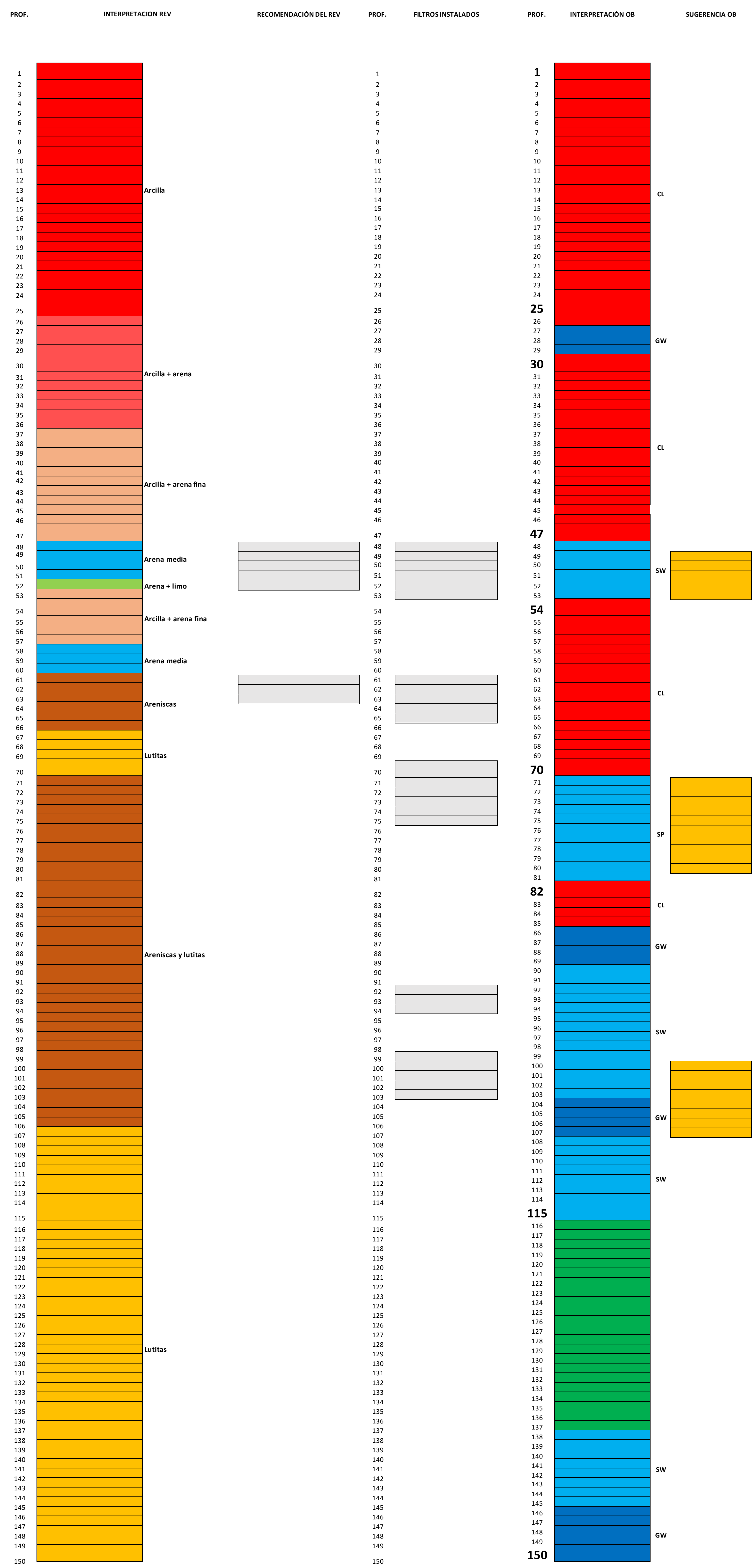
PROF.
INTERPRETACION REV
RECOMENDACIÓN DEL REV
PROF.
FILTROS INSTALADOS
PROF.
INTERPRETACIÓN OB
SUGERENCIA OB
Arcilla
Arcilla + arena
Arcilla + arena fina
Arena media
Arena + limo
Arcilla + arena fina
Arena media
Areniscas
Lutitas
Areniscas y lutitas
Lutitas
CL
GW
CL
SW
CL
SP
CL
GW
SW
GW
SW
SW
GW

REGISTRO ELECTRICO VERTICAL
POZO FRAY QUEBRACHO

REGISTRO ELECTRICO VERTICAL FRAY QUEBRACHO

PROF. LOGGEO DE MUESTRAS DE CAMPO

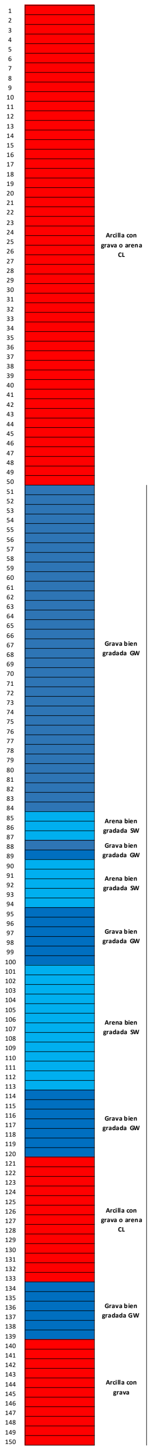

PROF	SP	RES CORTA	RES LARGA
1			
2			
3			
4			
5			
6			
7			
8			
9	45	20	20
10	45	20	20
11	46	20	19
12	46	20	20
13	48	20	20
14	48	20	20
15	48	20	19
16	48	20	20
17	48	20	20
18	48	20	20
19	48	20	20
20	49	20	20
21	49	20	20
22	49	40	20
23	49	40	18
24	49	20	20
25	50	20	20
26	50	20	20
27	55	20	20
28	55	20	20
29	55	20	22
30	50	20	20
31	50	20	22
32	50	20	20
33	50	20	20
34	55	20	20
35	50	20	25
36	50	20	20
37	50	20	20
38	55	20	22
39	55	20	20
40	55	20	18
41	58	20	25
42	57	20	22
43	57	20	22
44	56	20	30
45	53	40	40
46	55	140	130
47	55	130	160
48	55	140	150
49	50	135	175
50	50	150	180
51	48	150	210
52	48	170	250
53	48	160	250
54	48	160	240
55	47	170	240
56	47	200	250
57	47	170	270
58	47	180	290
59	47	205	350
60	47	250	360
61	47	260	400
62	47	260	370
63	47	250	340
64	47	240	380
65	45	230	350
66	45	240	370
67	44	240	380
68	44	240	300
69	44	240	350
70	43	220	300
71	43	220	250
72	42	200	270
73	43	180	150
74	44	120	70
75	44	50	80
76	44	60	60
77	45	70	40
78	44	50	60
79	47	40	50
80	44	80	80
81	43	190	240
82	44	225	200
83	44	180	250
84	44	170	250
85	44	170	120
86	44	180	200
87	44	220	300
88	44	220	280
89	44	250	200
90	44	250	270
91	44	230	330
92	44	220	175
93	44	200	280
94	44	240	330
95	43	220	270
96	42	180	300
97	44	240	350
98	44	250	320
99	44	250	360
100	44	250	330
101	44	230	280
102	44	200	280
103	44	180	260
104	44	170	240
105	43	200	275
106	44	210	250
107	44	140	140
108	44	170	250
109	44	230	230
110	44	230	230
111	44	220	270
112	44	230	200
113	44	230	300
114	44	220	200
115	44	220	200
116	44	170	270
117	44	190	120
118	44	200	240
119	44	150	160
120	41	160	140
121	42	170	200
122	42	200	120
123	42	200	240
124	42	170	100
125	43	190	190
126	48	180	140
127	46	150	40
128	46	30	50
129	50	30	40
130	50	50	50
131	46	160	180
132	46	180	110
133	44	210	260
134	44	210	170
135	43	200	240
136	43	200	240
137	44	210	100
138	42	200	175
139	44	170	100
140	44	180	100
141	44	130	70
142	46	50	40
143	46	50	50
144	46	50	50
145	48	50	70
146	44	170	20
147	43	170	200
148	42	190	30
149	42	160	100
150	50	120	30

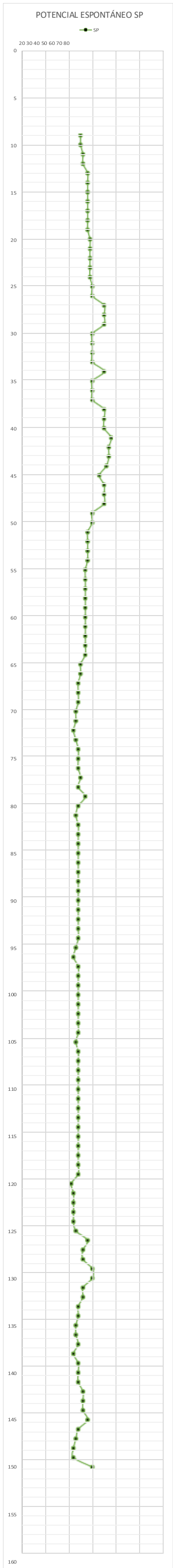

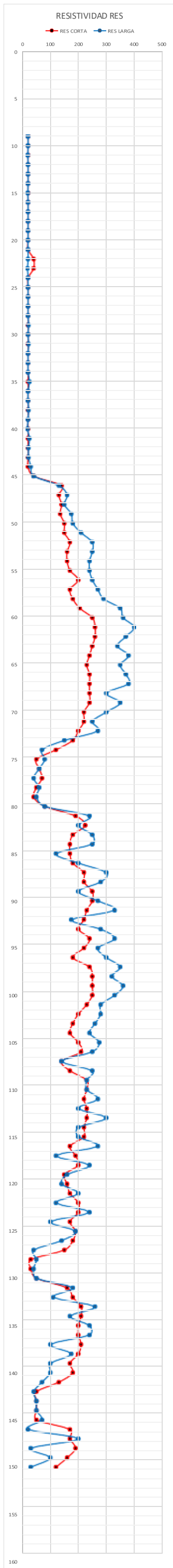

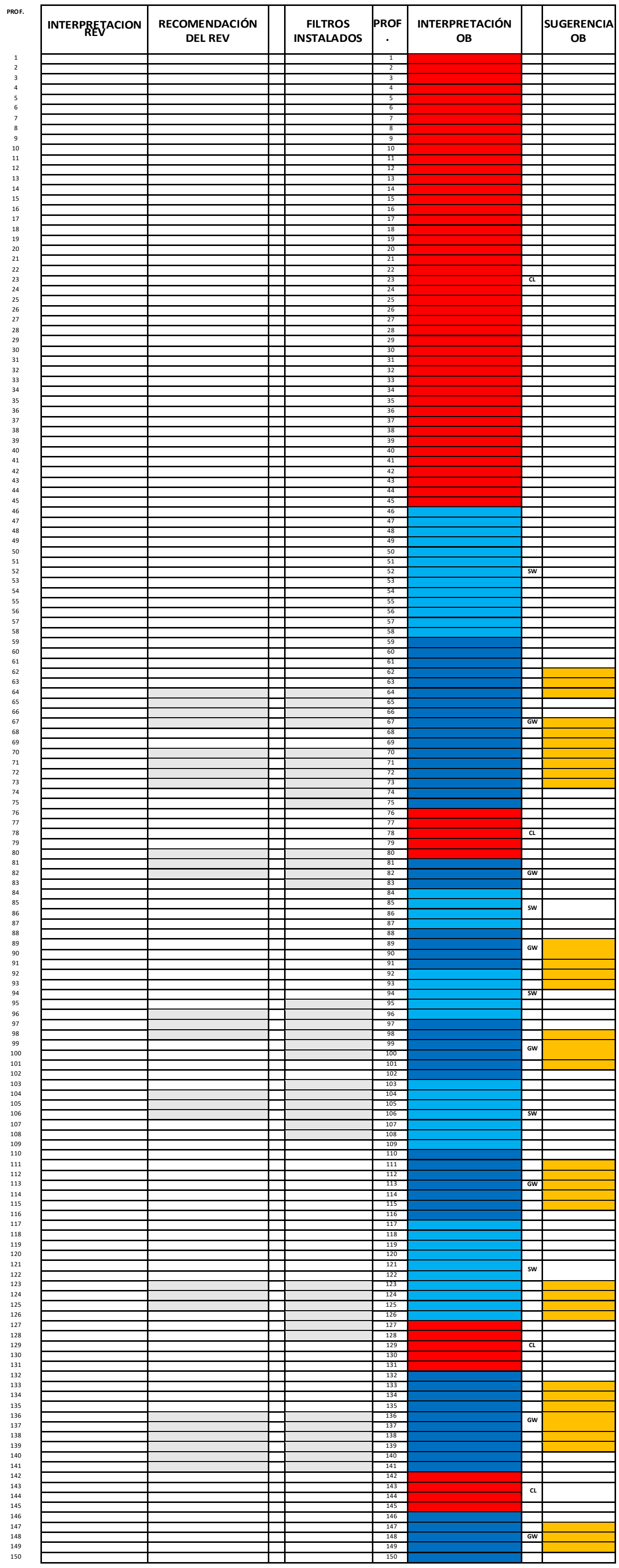

PERFILES HISTÓRICOS: PERFIL LITOLÓGICO

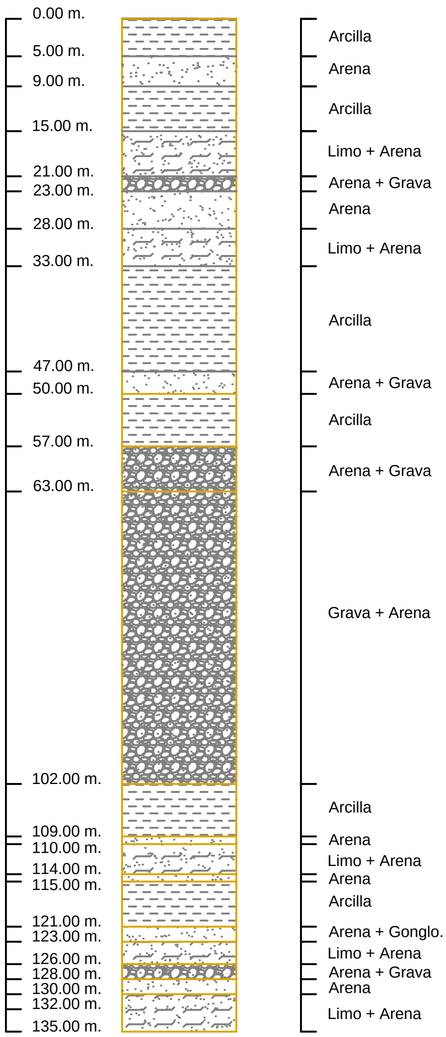

ADEME: PERFIL DE UBICACIÓN DE FILTROS

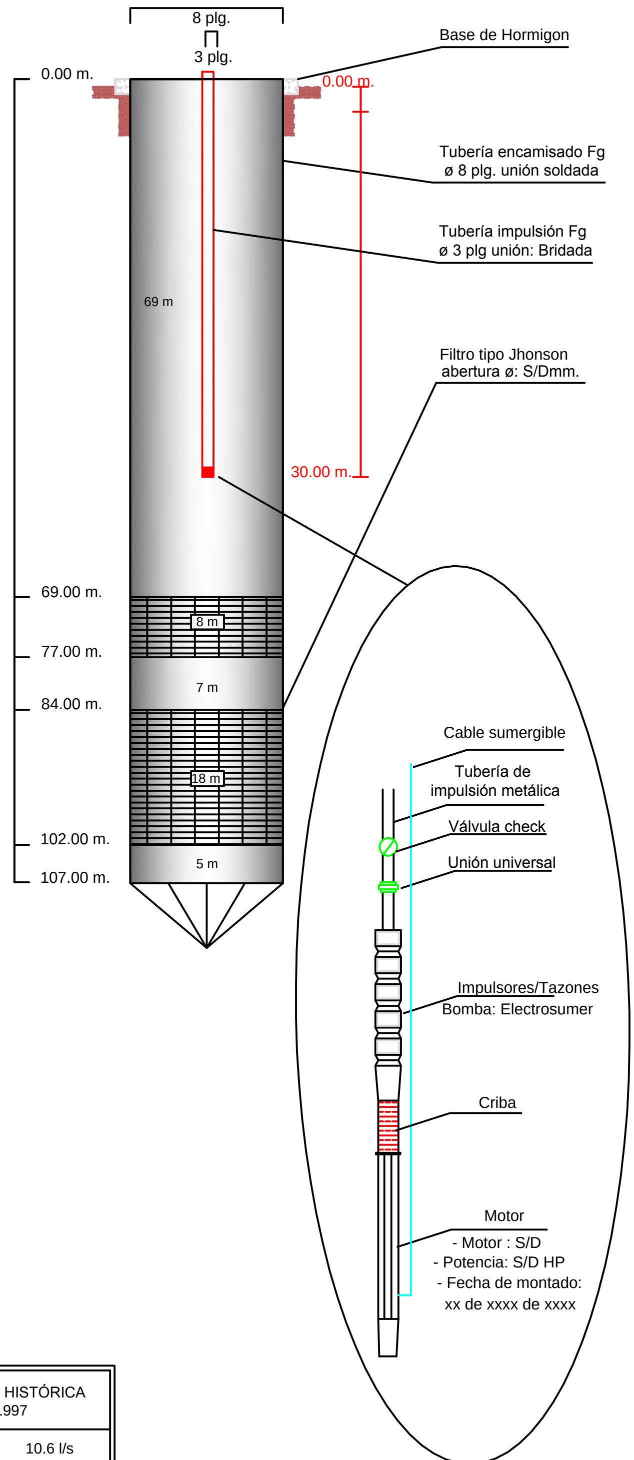

CAUDAL ACTUAL	
GESTIÓN JUNIO 2019	14.96 l/s
PROFUNDIDAD DE LA BOMBA	..........m
POTENCIA DE BOMBA	..........HP
DIÁMETRO IMPULSIÓN	..........Plg

INFORMACIÓN HISTÓRICA 30/02/1997	
CAUDAL	10.6 l/s
NIVEL ESTATICO	8.73 m
NIVEL DINÁMICO	9.27 m
LONG. DE FILTROS	26 m

COSAALT LTDA. TARIJA	COSAAL LTDA GESTION 2019	POZO : OSCAR ZAMORA	CÓDIGO TEC : P2	CÓDIGO NÚM.: 1020	REVISADO - APROBADO : MSc.ING.ALARCÓN R.GUALBERTO	FECHA DE PERFORACIÓN: 21 DE FEBRERO DE 1997
	GERENCIA DE OPERACIONES	DPTO. PROD. Y TRATAMIENTO UNIDAD SARH	ESC.V.: 1:100 ESC.H. : 1:10	FECHA ELAB. PLANO: ABR. 2018 - EN. 2019	ELABORADO - DIBUJANTE: EST. UNIV. ENCINAS M. LUIS A. EST. UNIV. TACACHO C. GUSTAVO	COORDENADAS: X: 320029 Y:7621136 Z: 1947

LAMINA: 02/61

PERFILES HISTÓRICOS: PERFIL LITOLÓGICO

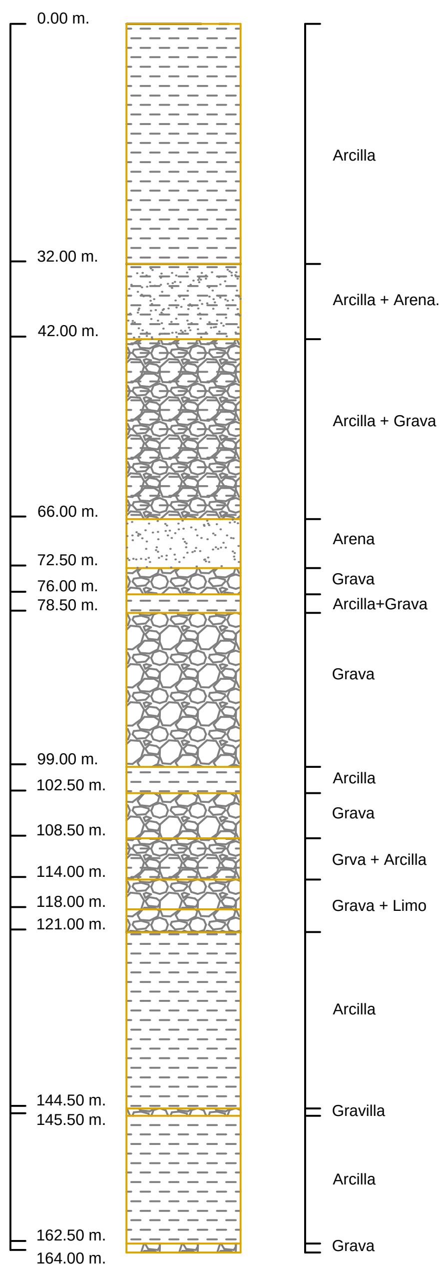

ADEME: PERFIL DE UBICACIÓN DE FILTROS

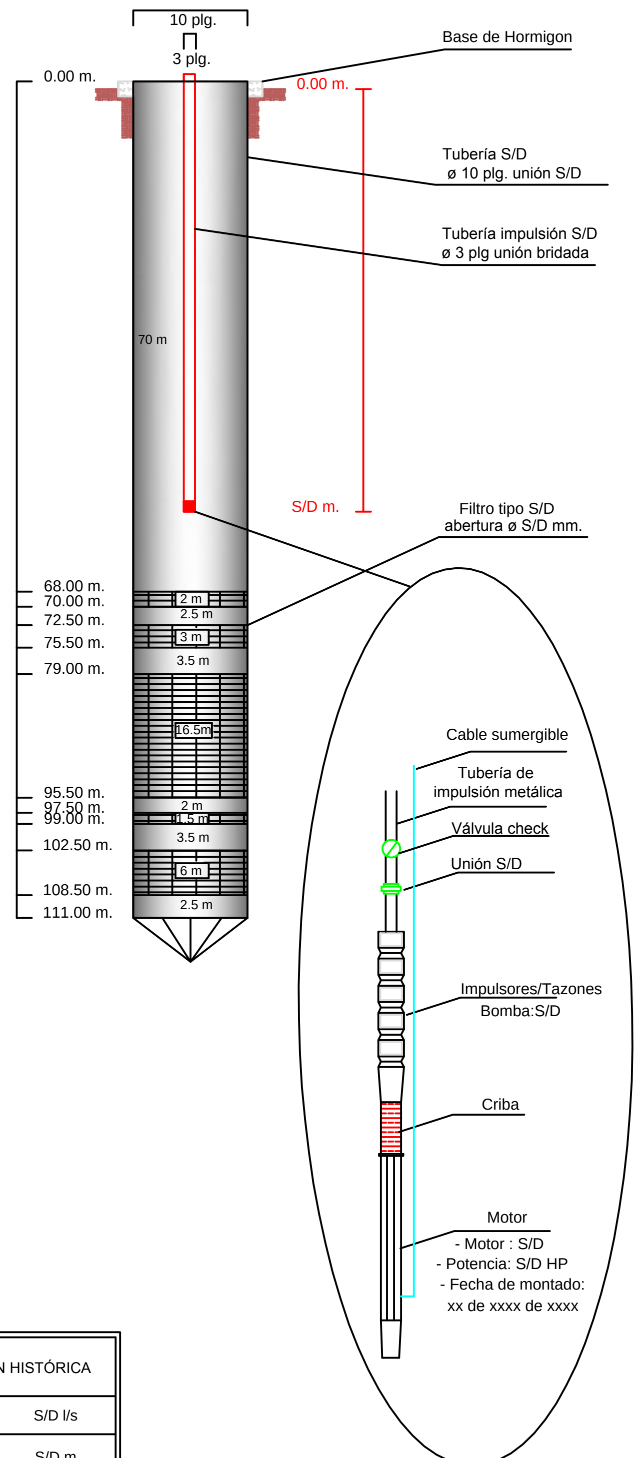

CAUDAL ACTUAL	
GESTIÓN JUNIO 2019	22.23 l/s
PROFUNDIDAD DE LA BOMBA	..........m
POTENCIA DE BOMBA	..........HP
DIÁMETRO IMPULSIÓN	...........Plg

INFORMACIÓN HISTÓRICA	
CAUDAL	S/D l/s
NIVEL ESTATICO	S/D m
NIVEL DINÁMICO	S/D m
LONG. DE FILTROS	29 m

COSAALT LTDA. TARIJA	COSAAL LTDA GESTION 2019	POZO : AVIT A	CÓDIGO TEC : P5-A	CÓDIGO NÚM.: 1051	REVISADO - APROBADO : MSc.ING.ALARCÓN R.GUALBERTO	FECHA DE PERFORACIÓN: 17 DE JUNIO DE 1980	LAMINA: 05/61
	GERENCIA DE OPERACIONES	DPTO. PROD. Y TRATAMIENTO UNIDAD SARH	ESC.V.: 1:100 ESC.H. : 1:10	FECHA ELAB. PLANO: ABR 2018 - EN 2019	ELABORADO - DIBUJANTE: EST. UNIV. ENCINAS M. LUIS A. EST. UNIV. TACACHO C. GUSTAVO	COORDENADAS: X:320844 Y:7620460 Z: 1914	